NOVEL REACTIONS OF NICKEL(II)-OLIGOPEPTIDE COMPLEXES WITH DIOXYGEN SPECIES

NOVEL REACTIONS OF NICKEL(II)-OLIGOPEPTIDE COMPLEXES WITH DIOXYGEN SPECIES

BY

RICKEY THOMAS TOM, B.Sc.

A Thesis

Submitted to the School of Graduate Studies

in Partial Fulfillment of the Requirements

for the Degree

Master of Science

McMaster University

April, 1987

MASTER OF SCIENCE (Biochemistry)

McMaster University
Hamilton, Ontario

TITLE: Novel Reactions of Nickel(II)-Oligopeptide Complexes with Dioxygen Species.

AUTHOR: Rickey Thomas Tom

SUPERVISOR: Dr. Evert Nieboer

NUMBER OF PAGES: XV, 132

ABSTRACT

The ability of simple oligopeptide complexes of nickel(II) to react with various dioxygen intermediates was investigated. Under physiological conditions, nickel(II)-histidine-containing oligopeptides were found to dismutate superoxide anions and disproportionate hydrogen peroxide. In the latter process, chemiluminescence was generated and a strongly oxidizing intermediate was detected capable of oxidizing uric acid, hydroxylating p-nitrophenol, and damaging 2-deoxy-D-ribose. The generation of this reactive intermediate likely occurs without the involvement of free hydroxyl radicals derived from Haber-Weiss or Fenton-type reactions. In addition, the Ni(II) complex of glycylglycyl-L-histidine (GGH) was found to react with molecular oxygen resulting in the oxidation of the ligand. An attempt was made to relate these reactions to the involvement of the nickel(III)/(II) redox couple which was shown to exist under physiological conditions. Similar reactivity was observed for non-histidine-containing oligopeptides but higher pH values were required.

The oligopeptides used not only represent biologically relevant ligands but the histidine containing oligopeptides mimics the specific copper(II)/nickel(II) binding and transport site of human serum albumin. The observations made in this study suggest some novel mechanism for the deleterious effects associated with excessive life-long exposure to nickel compounds, especially in relation to cancer of the respiratory tract.

ACKNOWLEDGEMENTS

I would very much like to thank Dr. E. Nieboer for the opportunity he has given me to do research under his supervision. I am grateful for the help provided by the lab members in room 3H43. I am especially indebted to Dr. D. W. Margerum (of Purdue University) for the use of his laboratory facilities and equipment, and to Robert James (McMaster University) for his cooperation.

LIST OF ABBREVIATIONS

abs	Absorbance
asp-ala-his-lys	L-Aspartyl-L-alanyl-L-histidyl-L-lysine
CAT	Catalase
CL	Chemiluminescence
Cyt c	Cytochrome c
CV	Cyclic Voltammetry
DDW	Double Distilled Deionized Water
DMSO	Dimethyl Sulphoxide
EDTA	Ethylene Diaminetetraacetic Acid (disodium salt)
EPR	Electron Paramagnetic Resonance
GGG	Triglycine (glycylglycylglycine)
GGGa	Triglycine Amide (glycylglycylglycine amide)
GGGG	Tetraglycine (glycylglycylglycylglycine)
GGH	Glycylglycyl-L-histidine
GGHG	Glycylglycyl-L-histidylglycine
H_2O_2	Hydrogen Peroxide
HEPES	N-2-Hydroxyethylpiperazine-N-2-ethanesulfonic Acid
HRP	Horse Radish Peroxidase
HSA	Human Serum Albumin
HX	Hypoxanthine
HXO	Xanthine
L	Ligand
NBT^{2+}	Nitro Blue Tetrazolium Ion
Ni	Nickel

$Ni(CO)_4$	Nickel Carbonyl
Ni_3S_2	Nickel Subsulfide
NMR	Nuclear Magnetic Resonance
O_2^-	Superoxide Radical
$^{\bullet}OH$	Hydroxyl Radical
PBS	Phosphate Buffered Saline
PMNs	Polymorphonuclear Leukocytes
SCE	Saturated Calomel Electrode
SHE	Standard Hydrogen Electrode
SOD	Superoxide Dismutase
TCA	Trichloroacetic Acid
TPA	12-O-Tetradecanoyl Phorbol 13-Acetate
UA, HXO_2	Uric Acid
UV/VIS	Ultraviolet/Visible

TABLE OF CONTENTS

LIST OF TABLES

LIST OF FIGURES

1.0. INTRODUCTION

1.1. Essentiality and Biochemistry of Nickel.

1.1.1. Essentiality.

Little is known about the biochemistry of nickel, but it has been established as an essential micronutrient in several prokaryotic organisms and in experimental animals (Thompson, 1982). The ubiquitous nature of nickel in food and water made early research into its deficiency difficult and results were often inconsistent. Later studies demonstrated adverse effects of nickel deprivation in several animals including chicks, cows, goats, minipigs, rats and sheep. These effects included alterations in the levels of metabolites (e.g., Ca^{2+}, Zn^{2+}, fat, glucose, ATP, etc.) and the activities of many enzymes (e.g., calcineurin, malate dehydrogenase), a decrease in the efficiency of iron absorption and homeostasis, and a reduction in growth rate and reproductive success (Kirchgessner and Schnegg, 1980; Anke et al., 1984; EPA, 1986; Spears et al., 1986).

The many changes brought about by nickel deficiency, together with reports that animals can store and regulate its absorption, suggest that nickel has a central role in metabolism. Hypothesized involvement ranges from participation in membrane metabolism, to structural or functional roles in RNA, DNA and proteins (EPA, 1986). Nickel is also the metal center of several metalloenzymes including ureases (Blakeley and Zerner, 1984), bacterial hydrogenase (Seefeldt and Arp, 1986) and acetogenic bacterial carbon-monoxide dehydrogenase (Drake, 1982).

Although it has been postulated that the dietary requirement of

nickel for humans is about 35 micrograms daily (Nielson and Flyvholm, 1984), essentiality in man has not been substantiated by demonstration of a nickel-deficient state (Anke et al., 1984).

1.1.2. Absorption, Distribution, and Excretion.

Absorption of nickel via the respiratory tract is perhaps the major route of exposure in man for both volatile and particulate nickel compounds. Workers at nickel refineries, at coal-fired power plants and those working with welding fumes are exposed to particulates containing nickel with a mass median aerodynamic diameter (MMAD) between 0.5 and 2 μM (Mushak, 1980). This size is believed to allow the particle to penetrate deepest into the respiratory system (Mushak, 1980; Bohning, 1983). If the inhaled compound is insoluble, it will likely be cleared by the mucociliary clearance system and/or by resident macrophages. If soluble, it will dissolve prior to absorption. By contrast, the volatile forms of nickel such as nickel tetracarbonyl, $Ni(CO)_4$, are very quickly and efficiently absorbed by the lungs (Mushak, 1980).

Dietary exposure to nickel ranges between 100 and 600 μg/day with up to 900 μg reported (Sunderman, 1977; Mushak, 1980, EPA, 1986). Fortunately, a healthy gastrointestinal tract will allow only 1-2 % to pass its walls. Percutaneous absorption is a minor route, although it does occur (Fullerton, 1986).

It has been shown that after parenteral administration of nickel salts in rodents, most of the nickel is rapidly excreted into the urine (Ho and Furst, 1973). The majority of this nickel was found to be associated in a nonspecific manner with the sulfated oligosaccharide fraction containing uronic acids and neutral sugars (Templeton and

Sarkar, 1985). The remaining nickel was found bound to a small acidic peptide with high affinity, and this complex appears to form only after glomerular filtration (Templeton and Sarkar, 1985). In addition, Oskarsson and Tjälve (1979a,b) have shown that immediately after intravenous injection (of $NiCl_2$), there is localization and retention of the metal in the kidney, in the parenchyma of the lungs and in the cartilage and connective tissues. By contrast, after inhalation or intravenous injection of $Ni(CO)_4$, there is significant accumulation in the respiratory tissues, the brain, the spinal cord, the heart muscle, the diaphragm, the adrenal cortex, the brown fat, the kidney and urinary bladder and in the corpora lutea of the ovaries (Oskarsson and Tjälve, 1979b,c). The different deposition patterns between the two forms of nickel may be related to the lipid solubility of $Ni(CO)_4$ (Oskarsson and Tjälve, 1979c). The accumulated nickel will be primarily excreted in the urine and to a smaller extent, via the bile (< 0.5%, Marzouk and Sunderman, 1985). Although most of the orally administered soluble forms of nickel remain unabsorbed and is excreted into the feces in animal studies, about 1-6 % is absorbed from the intestines and enters the plasma (Ho and Furst, 1973; Horak and Sunderman, 1973).

Blood is the main vehicle for transport of absorbed nickel and the level present is believed to represent blood burden and exposure status (Mushak, 1980). Human serum albumin (HSA) is the main transport protein, while α_2-macroglobulin (nickeloplasmin) and a 9.5 S α-glycoprotein are minor carrier proteins for nickel (Nomoto et al., 1971; Mushak, 1980; Nomoto, 1980; Glennon and Sarkar, 1982). The metal is also found associated with carbohydrates and several amino acids,

with L-histidine exhibiting the greatest affinity (Lucassen and Sarkar, 1979). The presence of so many binding constituents may have a modulating effect on the cellular uptake and cytotoxicity of the metal in living systems (Abbracchio et al., 1982a; Nieboer et al., 1984b). Early studies identified several nickel-binding constituents in the soluble cellular fraction of lung, liver and kidney (Oskarsson and Tjälve, 1979a). More recently, at least five different binding proteins have been found in the renal post-microsomal fraction of nickel chloride-exposed rats (by intravenous injection; Sunderman, 1981, 1983) and ten different binding proteins were found in both the lung and liver (by intraperitoneal injection; Herlant-Peers et al., 1983). The identity and/or function of these nickel binding constituents have not yet been determined, but their predominance in these organs may explain target organ specificity (Templeton and Sarkar, 1985).

1.1.3. Nickel Levels in Man.

The normal levels of nickel in serum are 0.46±0.26 µg/L with the urine concentrations in the range of 2.0±1.5 µg/L (Sunderman et al., 1984b, 1986); and the total body burden is estimated as 140 µg/kg (EPA, 1986). These body fluid levels increase in individuals with stainless steel prothesis, those who recieve nickel contaminated intravenous fluids, or who are suffering from myocardial infarction, angina pectoris, cerebral stroke, or thermal burns. Specifically, studies have shown that dissolution of stainless-steel implants results in the release of 260-300 pg/cm^2/day. Although this level is easily cleared, development of tumors around these implants have been reported in isolated cases. However, the role of nickel in this tumourigenic

process remains obscure since elevated levels of chromium and cobalt around these implants are also observed (Linden et al., 1985). High serum-nickel concentrations have also been documented in patients who have kidney dysfunctions (Sunderman, 1983).

Acceptable airborne nickel levels in the work place set by the US Occupational Safety & Health Administration are usually between 0.1-1 mg/m^3, which is 10^5-10^6 times greater than the natural concentration in the air (Grandjean, 1984; EPA, 1986). During an 8-h shift, when approximately 5 m^3 of air is inhaled, an estimated retention factor of 30 % in an environment containing 0.1 mg/m^3 of nickel will result in significant deposition in the respiratory tract (Grandjean, 1984). However, deposition in the respiratory tract is dependent on particle size and retention on mucociliary clearance and solubility (Grandjean, 1986). High urinary levels of nickel may be observed following exposure and the total concentration excreted is an index of not only the solubility of the compound, but also of the degree of retention. Hence, a negative balance between exposure and clearance over many years can lead to a significant accumulation of nickel in the lungs, especially in individuals exposed to particles containing nickel (Nieboer et. al., 1984b).

1.2. Toxic Effects of Nickel Compounds Other than Cancer.

Nickel exists mainly in the divalent form and hence is expected to bind to nucleophilic sites on nucleic acids and proteins and other biologically important molecules. The toxic effects of exposure to high concentrations of nickel and its compounds have been extensively

studied in animals and toxicity has been induced in the kidney, lungs, heart, endocrine glands, fetus and liver (Donskoy et al., 1986). Different nickel compounds were found to have different effects on the respiratory system in animal experiments. Ni_3S_2, $NiCl_2$ and $NiSO_4$ have been shown to induce inflammation in the lungs as well as alterations in the activity of alveolar macrophages (Benson et al., 1986). Exposure to the less soluble forms of nickel (e.g., Ni_3S_2 and crystalline NiS) resulted in respiratory tract irritations and the development of lesions and malignant tumours. Although the soluble forms of nickel (e.g., $NiCl_2$ and $NiSO_4$) do not appear to be tumourogenic, its inhalation leads to the suppression of the immunological response of the respiratory system and the release of ethene and ethane gas which has been attributed to the induction of lipid peroxidation (Gardner, 1980; Knight et al., 1986). Various nickel compounds have been shown in vivo and in vitro to alter the levels of various metabolites (e.g., ATP and triglycerides), and the activities of several enzymes (e.g., RNA polymerase and ATPase; Mushak, 1980). Furthermore, nickel compounds have been shown to produce alterations in heme metabolism and to compromise the fidelity of DNA synthesis (Maines, 1980). Morphological alterations include nuclear segregation, dilation of the rough endoplasmic reticulum and the appearance of cytoplasmic inclusion bodies.

Nickel carbonyl is the most acutely toxic form of nickel in man. It induces severe chemical pneumonitis which has often been fatal. Exposures can also lead to the development of asthma and/or Loffler's syndrome (Mushak, 1980; Dolovich et al., 1984). Similarly, soluble

salts such as nickel sulfate have also been associated with adverse respiratory effects, and these include asthma and mucosal tissue injury (EPA, 1986). Nickel is recognized as the most common inducer of contact dermatitis. Sensitization in women not occupationally exposed to this metal or its compounds may be as high as 9 % (EPA, 1986). Inadvertent exposure from jewelry, coins, detergents, make-up preparations, etc., have been documented sources of nickel.

The geno- and embryotoxicity of nickel compounds in experimental animals have been reported; however, relatively high levels of nickel were invariably used and it is believed that pregnant (human) females are unlikely to encounter the amounts necessary to induce toxic effects (Léonard and Jacquet, 1984).

1.3. Nickel Carcinogenesis.

1.3.1. Carcinogenesis.

Based on epidemiological studies, several nickel compounds have been identified as human carcinogens and many of the same compounds are able to induce tumours in experimental animals (EPA, 1986). Specific reports have demonstrated the occupationally-exposed workers display an increased tumour incidence in the upper (e.g., nasal) and lower (e.g., lungs) respiratory tract, which is directly correlated with the type of work, duration of work and perhaps smoking status (EPA, 1986; Kaldor et al., 1986). Specifically, those involved in the refining process (e.g., roasting, smelting and perhaps electrolysis) which involves exposure to the insoluble forms of nickel (e.g., Ni_3S_2, NiS or NiO) are at greatest risk (Cecutti and Nieboer, 1981; EPA, 1986). Kreyberg et al. (1978)

found that in these workers, the mean time for the development of various types of respiratory cancers varied from 20 to 35 years. More recently, Roberts et al. (1984) observed substantially increased incidence of lung and nasal cancer in workers 15-20 years after initial exposure (see also EPA, 1986).

Certain nickel compounds are potent experimental metallic carcinogens, while others are non-carcinogenic (Berry et al., 1984; Sen and Costa 1986). Nevertheless, ionic nickel (Ni^{2+}) is thought to be the ultimate carcinogen as defined in the somatic mutation model of cancer induction (Reith and Brogger, 1984). Ni^{2+} ions are believed to affect the genetic material by inducing mutations through direct chemical reaction with DNA or indirectly by interference with DNA repair, replication or folding. Possible molecular mechanisms contributing to nickel carcinogenesis may include: potentiation of direct DNA damage (e.g., sister chromatid exchanges, strand breaks and protein and DNA crosslinks), induction of B- to Z-DNA conformational changes and modification of chromatin structure potentially affecting gene expression, and non-isomorphous replacement of endogenous metal ions in enzymes required to maintain the integrity of genetic material (Sunderman, 1984b; Patierno and Costa, 1985; Biggart and Costa, 1986; Nieboer et al., 1987). Although reports on direct mutagenic effects of nickel compounds have been varied, increased numbers of chromosomal gaps and breaks have been observed in peripheral lymphocytes of retired nickel workers (Boysen et al., 1980; Waksvik et al., 1984).

The cytotoxic or carcinogenic potential of any nickel compound is likely related to their bioavailability (Hansen and Stern, 1984;

Patierno and Costa, 1985; Nieboer et al., 1987). Hence water soluble nickel compounds are generally not carcinogenic since they are not easily taken up by cells, are bound to specific amino acid and serum components in extracellular fluids, and are quickly eliminated in vivo (Abbracchio, 1982a; Nieboer et al., 1987). By contrast, a number of water-insoluble nickel compounds which are crystalline and less easily eliminated are able to produce tumours in laboratory animals at almost any site of implantation (Sunderman, 1984a,b).

Studies indicate that the tumourogenic potential of various nickel compounds might be related to its ability to be taken up by cells and to the availability of nickel(II) ions within cancer-target cells (Costa and Mollenhauer, 1980; Hansen and Stern, 1983). Factors affecting phagocytosis include size, surface charge and solubility (Abbracchio, 1982b). Once internalized, particulate nickel compounds are contained within vacuoles which ultimately aggregate near the nucleus (Costa et al., 1982). During this migration, repeated interactions with lysosomes are believed to acidify the foreign body facilitating the dissolution of these compounds and the release of large amounts of nickel (Berry et al., 1984; Costa and Heck, 1984). Studies using labelled nickel compounds showed that dissolution of such particles do not correlate with clearance from the cell, suggesting that potentially large quantities of nickel have been liberated and redistributed intracellularly (Abbracchio et al., 1982b). These studies collectively demonstrate one mechanism by which large amounts of Ni^{2+}, the presumed primary carcinogen, can accumulate and be compartmentalized within a cell. High extracellular pools of

particulates (e.g., in the lungs) may also assure a chronic influx of nickel(II) into cells. Subsequent interactions of nickel(II) with cellular ligands, cytosolic components and/or DNA itself somehow yields the cytotoxic and carcinogenic effects by mechanisms that remains to be elucidated.

1.3.2. Nickel Compounds as Tumour Promoters.

There is growing evidence that nickel has properties of being a complete carcinogen, affecting both the initiation and promotion stages of carcinogenesis. A number of studies have shown that nickel has the ability to potentiate mutagenic effects in mammalian systems and may therefore be involved in the first stage of cancer induction (Reith and Brogger, 1984; Nieboer et al., 1987). However, only a few studies have tested its ability to promote carcinogenesis. Specifically, Rivedel and Sanner (1980) and Kurokawa et al. (1985) reported that nickel was the only metal to promote rat renal tumourigenesis initiated with N-ethyl-N-hydroxyethylnitrosamines and transformation in hamster embryo cells initiated with benzo(a)pyrene. Recently, Uziel et al. (1986) reported that low concentrations of nickel salts (e.g., 10 μM) are toxic and act synergistically in a nucleoside excretion assay (using hamster embryo cells) with the well-known carcinogen, benzo(a)pyrene.

Epidemiological studies have also shown that nickel has a role in the initiation and in the promotion of cancer. Development of cancer in the lungs or in nasal tissues in occupationally-exposed workers appears to be dependent on whether the nickel is acting at an early stage or at a late stage of carcinogenesis (Doll et al.,1970; Day and Brown, 1980). Specifically, a positive relationship between excess mortality ratio

and/or the standardized mortality ratio and the time since exposure ceased to nickel-refining intermediates was observed for nasal sinus cancer; whereas this relationship was absent for lung cancer. This observation suggests that nickel-containing substances in the work place are affecting these cancers at different stages; namely they act as early-stage or late-stage carcinogens, respectively, as defined in the multistage model of cancer (Day and Brown, 1980; Kaldor et al., 1986).

1.4. Nickel Peptide Complexes.

Human serum albumin possesses a specific binding site for Ni^{2+} and Cu^{2+} characterized by a square-planar chelate formed by the N-terminus alpha-amino nitrogen, the deprotonated form of the first two peptide nitrogens and the 3-nitrogen of the imidazole ring of the third amino acid (Fig. 1.1.; Glennon and Sarkar, 1982; Dolovich et al., 1984). The binding of nickel to human serum albumin results in the formation of a very unique complex such that antibodies recognizing this binding have developed in some patients with respiratory hypersensitivity to nickel (Dolovich et al., 1984; Nieboer et al., 1984a). Histidine in the third position appears to be very important to the formation of this stable complex and only nonspecific binding occurs in dog serum albumin which has a tyrosine at residue number 3 (Glennon et al., 1983). Earlier investigations have shown that simple tripeptides can be used to mimic this binding site. It appears that nickel can catalyze the deprotonation of almost any small peptide (Eqn. 1.1), forming a square-planar complex involving a minimum of three amino acids (possibly excluding proline, cysteine and methionine); and if histidine is in the

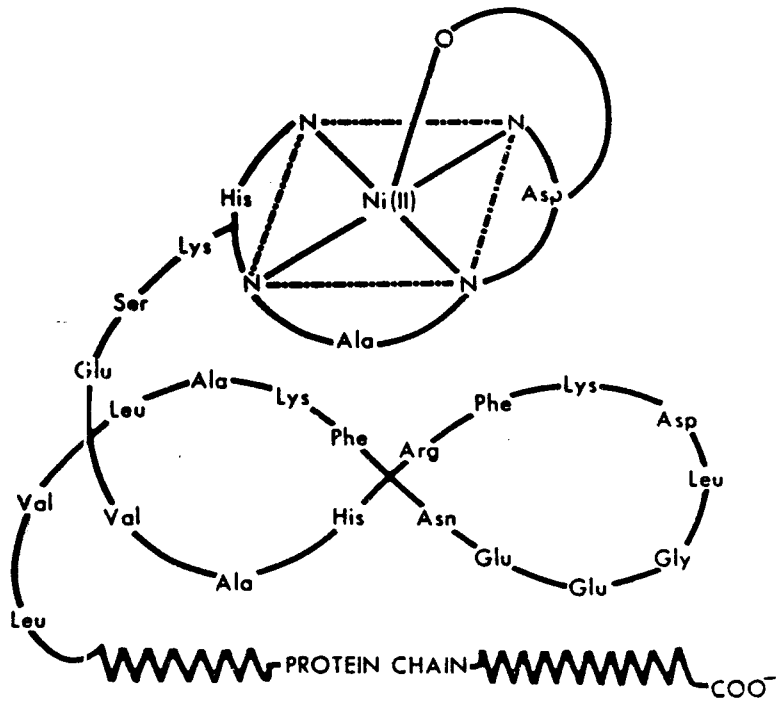

Figure 1.1: Proposed structure based upon NMR and UV/VIS absorption spectrometric evidence of the Ni(II)- and Cu(II)-binding site of human serum albumin. Adopted from Laussac and Sarkar (1984).

third position, the reaction will occur at physiological pH (Bryce et al., 1966; Bossu and Margerum, 1977; Laussac and Sarkar, 1984).

$$Ni^{2+} + HL \rightleftharpoons Ni(H_{-n}L)^{2-(n-1)} + (n+1)\ H^{+} \qquad (1.1)$$

(Values of n are limited to 1 or 2.) Other biological ligands with the ability to chelate nickel include proteins like transferrin (Harris, 1986), haemoglobin (Shelnutt et al., 1986) and porphyrins (Shelnutt, 1987); hormones like gonadotropic releasing factor (Dr Jarrell, private communication) and thyrotropin releasing factor (Formicka-Kozlowska et al., 1983); and short peptides like glutathione.

1.5. Oxygen Toxicity.

The survival of an aerobic organism in an oxygen environment involves a complicated interplay between the biological generation of highly reactive free radicals and the ability of the organism to control it. Molecular oxygen is itself actually a radical, containing two unpaired electrons with parallel spin in the two outer π^{*}-antibonding orbitals (Halliwell and Gutteridge, 1984). This parallel electron spin arrangement prevents the direct addition of a spin-paired set of electrons, since few atoms or molecules have electrons with parallel spins in their valence orbitals (Del Maestro, 1980). Specifically, by the rules of quantum mechanics reactions between molecules with different spin states (multiplicity) are forbidden. As a result, reactivity between oxygen and nonradical-species are slow, but are very fast in the presence of transition metals which are themselves radicals and have the ability to donate and accept single electrons.

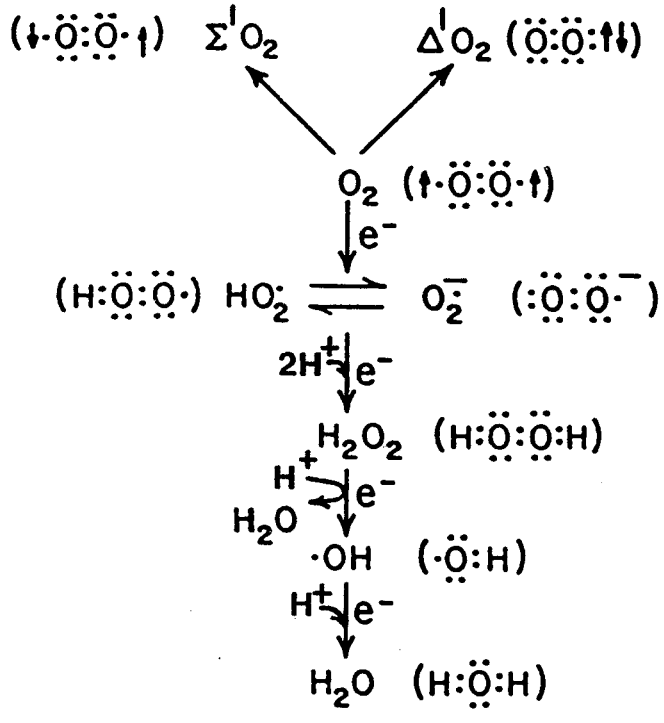

Figure 1.2: Univalent reduction and excitation schemes for molecular oxygen. Adopted from Klebanoff (1980).

Addition of one electron to molecular oxygen generates the superoxide anion and the addition of a second electron forms hydrogen peroxide. Both species are formed during enzymatic and nonenzymatic reactions. (Halliwell and Gutteridge, 1986). Scavenging enzymes such as superoxide dismutase (SOD), catalase (CAT) and peroxidase and water soluble scavengers like glutathione, ascorbic acid and possibly uric acid exist to minimize and consume these reactive oxygen intermediates (Del Maestro, 1980; Frank and Massaro, 1980; Ames et al., 1981). However, the respiratory burst of activated white blood cells and hyperbaric conditions have been shown to potentiate damaging effects on exposed tissues (e.g., lungs) and hemolysis of red blood cells (Vercellotti et al., 1985). This demonstrates that oxygen itself can have a direct role in toxicity (Frank and Massaro, 1980; Witschi and Hakkinen, 1984; Fantone and Ward, 1985; Dorinsky and Davis, 1986). The levels of superoxide and hydrogen peroxide likely increase under hyperbaric conditions and a further basis for oxygen toxicity has been attributed to the generation of highly reactive hydroxyl radicals (Frank and Massaro, 1980; Halliwell and Gutteridge, 1986). This reaction is much faster in the presence of certain metals (e.g., iron and copper) in what is known as the Fenton-type reaction (Fridovich, 1986; Halliwell and Gutteridge, 1984, 1986).

$$Fe^{2+} + H_2O_2 \longrightarrow Fe^{3+} + {}^{\bullet}OH + OH^- \qquad (1.2)$$

The Fe^{3+} can react with O_2^- or H_2O_2 to regenerate Fe^{2+}:

$$Fe^{3+} + H_2O_2 \longrightarrow Fe^{2+} + O_2^- + 2H^+ \qquad (1.3)$$

$$Fe^{3+} + O_2^- \longrightarrow Fe^{2+} + O_2 \qquad (1.4)$$

The hydroxyl radical is an extremely reactive species capable of reacting with almost every type of molecule, probably at the site of production. It is capable of hydrogen abstraction, addition (e.g., onto aromatic ring structures such as the purine and pyrimidine bases of DNA), and electron transfer (Halliwell and Gutteridge, 1984). The ability of hydroxyl radicals to react with DNA suggests that it has mutagenic potential. Exposure of DNA to oxygen-radical generating systems or to stimulated human leukocytes results in extensive strand breakage and deoxyribose degradation (Klebanoff, 1980; Birnboim, 1982; Brawn and Fridovich, 1980; Weitberg et al., 1983). Hence alterations in iron or copper metabolism along with abnormalities in the handling of various reduced oxygen species can result in the potential release of damaging oxidative intermediates manifested as a development of a diseased state (Del Maestro, 1980; Monteiro et al., 1986). The role of oxygen radicals in biology is further complicated by observations that oxygen scavengers and protease inhibitors have modulating effects on the process of tumour promotion (Troll and Wiesner, 1985). Specifically, Marx (1983) argued that tumour promoters such as the phorbol esters contribute to the development of cancer by generating activated oxygen intermediates that damage DNA. This non-specific chromosomal damage has the potential to affect gene expression and presumably cell growth and differentiation.

Singlet oxygen is a highly reactive molecule and its generation requires the input of energy. Delta singlet oxygen is the more biologically relevant species ($^1\Delta_g$ O_2) and it dissipates its energy (102 kJ mol^{-1}) by thermal decay, light emission or chemical reaction

(Klebanoff, 1980). There are many potential sources of singlet oxygen and its presence allows for some very damaging reactions to occur due to its electrophilic nature.

1.6. Objective of this Thesis.

The main objective of this study was to determine if simple oligopeptide complexes of nickel(II) can participate in reactions with and in the activation of molecular oxygen, superoxide anions and hydrogen peroxide under physiological conditions. In addition, the formation of potentially damaging intermediates generated in these pathways and capable of mediating the destruction of biologically relevant molecules is examined. Both these approaches were successful and nickel(II) bound to human serum albumin was also active. Subsequently, an attempt was made to link these activities to the involvement of the Nickel(III)/(II) redox couple, which was characterized spectrometrically and electrochemically. The observations made in this study may serve to identify a novel mechanism for some toxic and/or carcinogenic consequences from excessive exposure to nickel compounds. Hydrogen peroxide, the respiratory burst of polymorphonuclear leukocytes and the hypoxanthine/xanthine oxidase system are employed in characterizing the catalytic effects of nickel(II) complexes formed with oligopeptide and protein ligands. The ligands used in this study include glycylglycylhistidine (GGH), glycylglycylhystidylglycine (GGHG), aspartylalanylhistidyllysine (asp-ala-his-lys), triglycine (GGG), triglycineamide (GGGa), tetraglycine(GGGG) and human serum albumin (HSA).

2. MATERIALS AND METHODS

2.1. Materials.

2.1.1. Chemical Reagents and Ligands.

Table 2.1 lists all the routine chemical reagents and their sources, and Table 2.2 lists the corresponding information for the ligands used in this study.

2.1.2. Preparation of the Chelex-100 Column.

Fifty g of Chelex-100 resin (100-200 mesh, sodium form, Bio Rad) were swollen in 400 mL of DDW for one h. After decantation, the resin was resuspended in 300 mL of 1 N NaOH and then in 300 mL of 1 N HCI; this washing cycle was repeated twice more. After rinsing the resin two times with ample amounts of DDW, it was resuspended twice in 0.01 M. Na_2EDTA and was subsequently stored in a fresh EDTA aliquot overnight. The resin was subsequently packed to form a 2.6 x 23 cm column bed and then washed with 2 L of DDW. The ability of this column to remove metal impurities was confirmed by electrothermal atomic absorption spectrometry (A. Nguyen, private communication).

2.1.3. Buffers.

0.1 M Potassium Phosphate Buffer, pH=7.4. In 400 mL of DDW, 22.0 g of K_2HPO_4 and 5.18 g KH_2PO_4 were dissolved and then adjusted to the required pH with 1 N KOH or 1 N HCI as required. After diluting to 2.0 L, the buffer was passed through the Chelex-100 column.

Phosphate Buffered Saline (PBS), pH=7.4. In 400 mL of DDW, 8 g NaCI (137mM), 0.020 g KCI (2.7 mM), 0.12 g KH_2PO_4 (0.88 mM) and 0.91 g

Table 2.1: Chemical Reagents

Chemical Reagents	Source	Comments
Acetaldehyde	J.T. Baker	
Allantoin (5-Ureidohydantoin)	SIGMA	
Azide (Sodium Salt)	SIGMA	
Bovine Albumin, Fraction V	SIGMA	
Catalase	SIGMA	From Bovine Liver
$Cd(NO_3)_2 \cdot 4H_2O$	BDH	AnalaR*
$CuSO_4$	J.T. Baker	"Baker Analyzed" Reagent
Cytochrome c, Type VI	SIGMA	From Horse Heart
2-Deoxy-D-Ribose	SIGMA	
Diethyl Ether (anhydrous)	BDH	A.C.S. assured
2-5-Dimethylfuran	SIGMA	
Dimethyl Sulphoxide	Caledon Lab.	A.C.S. assured
$Na_2EDTA \cdot 2H_2O$	BDH	A.C.S. assured
$FeSO_4 \cdot 7H_2O$	BDH	A.C.S. assured
Glutathione (Reduced Form)	SIGMA	
Glutathione (Oxidized Form)	SIGMA	
Glyoxylic Acid	SIGMA	
HCl (37 % w/w)	Fisher	A.C.S. specification
$HClO_4$ (70 % w/w)	Fisher	A.C.S. assured
HEPES (Free Acid, Crystalline)	SIGMA	

Table 2.1: Continued

Chemical Reagents	Source	Comments
Hydrogen Peroxide (30 % w/w)	BDH	Concentration of stock solution monitored frequently. Stored at 4 °C.
Hypoxanthine (6-hydroxypurine)	SIGMA	A.C.S. assured
Imidazole (White, Crystalline)	SIGMA	
KCl	BDH	Aristar Grade
KH_2PO_4	BDH	A.C.S. assured
K_2HPO_4	BDH	A.C.S. assured
D-Mannitol (Mannite)	SIGMA	
$MnSO_4 \cdot H_2O$	J.T. Baker	"Baker Analyzed" Reagent
NaCl	BDH	Analytical Reagent
NaH_2PO_4	BDH	A.C.S. assured
Na_2CO_3	BDH	A.C.S. assured
$NaHCO_3$	BDH	A.C.S. assured
NaOH	SIGMA	
$(NH_4)_2HPO_4$	BDH	AnalaR*
$NiCL_2 \cdot 6H_2O$	BDH	AnalaR*
Nitro Blue Tetrazolium (Grade III)	SIGMA	
p-Nitrophenol	SIGMA	Spectrotometric grade
o-Dianisidine Dihydrochloride (3,3'-Dimethoxy Benzidine)	SIGMA	
Peroxidase	SIGMA	From Horse Radish

Table 2.1: Continued

Chemical Reagents	Source	Comments
12-o-Tetradecanoyl Phorbol 13-Acetate Phorbol 12-Myristate 13-Acetate	SIGMA	A 2mg/mL stock solution was prepared by dissolving the purchased sample in DMSO and stored at -20 °C. (Markert et al., 1984).
Superoxide Dismutase	SIGMA	From Bovine Liver
$TiOSO_4$	A.D. Mackay Inc.	Gift from Dr. Rachubinski (McMaster University)
Trichloroacetic Acid	J.T. Baker	A.C.S. assured
Trypan Blue, 0.4 % (w/v) in ethanol	Gibco	Purchased as a Solution.
Urea	SIGMA	
Uric Acid	Aldrich	Gold Label
Xanthine Oxidase	Boehringer Mannheim	From Cow Milk
Xanthine	SIGMA	
$ZnSO_4 \cdot 7H_2O$	J.T. Baker	"Baker Analyzed" Reagent

Table 2.2: Ligands Used

Ligand (abbreviation)	Source	Comment
L-Aspartyl-L-alanyl-L-histidyl -lysine (asp-ala-his-lys)	Biosynthetica	Gift from Dr. Margerum (Purdue University)
L-Cysteine	BDH	Biochemical Grade
L-Histidine	Aldrich	
Human serum albumin (HSA)	SIGMA	Fraction IV
Glycylglycine (GG)	SIGMA	
Glycylglycyl-L-histidine (GGH)	Peninsula	
Glycylglycyl-L-histidyl-glycine	Biosynthetica	Gift from Dr. Margerum (Purdue University)
1-10 Phenanthroline hydrate (o-Phenathroline Hydrate)	BDH	AnalaR*
Tetraglycine (GGGG)	SIGMA	
Triglycine (GGG)	Vega	
Triglycine amide (GGGa)	Vega	

$Na_2(HPO_4)$ (6.4 mM) were dissolved. After adjusting the pH to 7.4 with 0.1 N KOH or 0.1 N HCl, the volume was adjusted to 1.0 L. No further purification of this buffer was carried out.

0.1 M HEPES, pH=7.4. In 200 mL of DDW, 11.92 g HEPES were dissolved and the pH was adjusted to 7.4 with 1 N NaOH or 1 N HCI as required. This solution was then adjusted to 500 mL with DDW.

0.1 M $NaClO_4$. To a 90 mL solution containing 1.06 g Na_2CO_3, 1.43 mL of $HClO_4$ were added slowly with stirring. The pH was adjusted with 1 N NaOH or 1 N $HClO_4$ and then diluted to 1.0 L with DDW.

2.1.4. Miscellaneous Solution.

Ficoll-Hypaque, Stock Ficoll-Hypaque was obtained from Dr. D. Singal (McMaster University). It had been prepared by dissolving 75.5 g of Ficoll (Pharmacia, Sweden) in 7 L of DDW; 950 mL of sodium hypaque (Winthrop, Aurora, Ontario) was then added to 440 mL of this Ficoll solution to give a final density of 1.075 g/L.

Buffered Ammonium Chloride Lytic Solution, pH=7.4. To 80 mL DDW, 0.83 g NH_4CI (0.83 % w/v), 3.7 mg Na_2EDTA (10^{-4}) and 84.69 mg $NaHCO_3$ (0.01 M) were added. The pH was adjusted with 1 N NaOH or 1 N HCI and the final volume was adjusted to 100 mL with DDW.

2.2. Experimental Techniques

2.2.1. Synthesis and Characterization of Nickel(II)/(III) Peptide Complexes.

2.2.1.1. Preparation.

Solutions of Nickel(II) peptides were prepared by adding $NiCl_2 \cdot 6H_2O$

to the peptide dissolved in either 0.1 M KH_2PO_4, in 0.1 M HEPES buffer at pH=7.4 or in 0.1 M $NaClO_4$ (pH=9.6). In all cases, the peptide was in slight excess (10 %) to ensure that all the nickel was complexed. Freshly prepared nickel(II) peptide solutions were used in each experiment.

Solutions of bis(dipeptide)nickelate(II) complexes (Ni(II)(glygly)$_2$) were prepared as described by Jacobs and Margerum (1984). Specifically, three equivalents of glycylglycine were added to one equivalent of $NiCl_2$. 1.0 M NaOH was then added very slowly to prevent formation of the insoluble nickel hydroxide. A very light-blue solution appeared at pH=11, signaling the formation of the fully deprotonated biscomplex.

2.2.1.2. Electrochemical Synthesis.

Solutions of Nickel(III) peptide complexes were prepared by controlled electrode-potential electrolysis employing a flow-through bulk electrolysis column based upon the design of Lappin et al. (1978) and Clark and Evans (1976). It consists of a graphite-powder working electrode packed in a porous-Vycor glass column externally wrapped with a platinum wire, which constitutes the auxiliary electrode (Fig 2.1). A second platinum coil that makes internal contact with the entire length of the graphite column provides a convenient lead to the working electrode. A model 363 potentiostat/galvanostat (EG & G Princeton Applied Research) supplies a constant voltage source for the working electrode, measured relative to the calomel reference electrode. In general, the column was cleaned prior to use by passing a minimum of 25

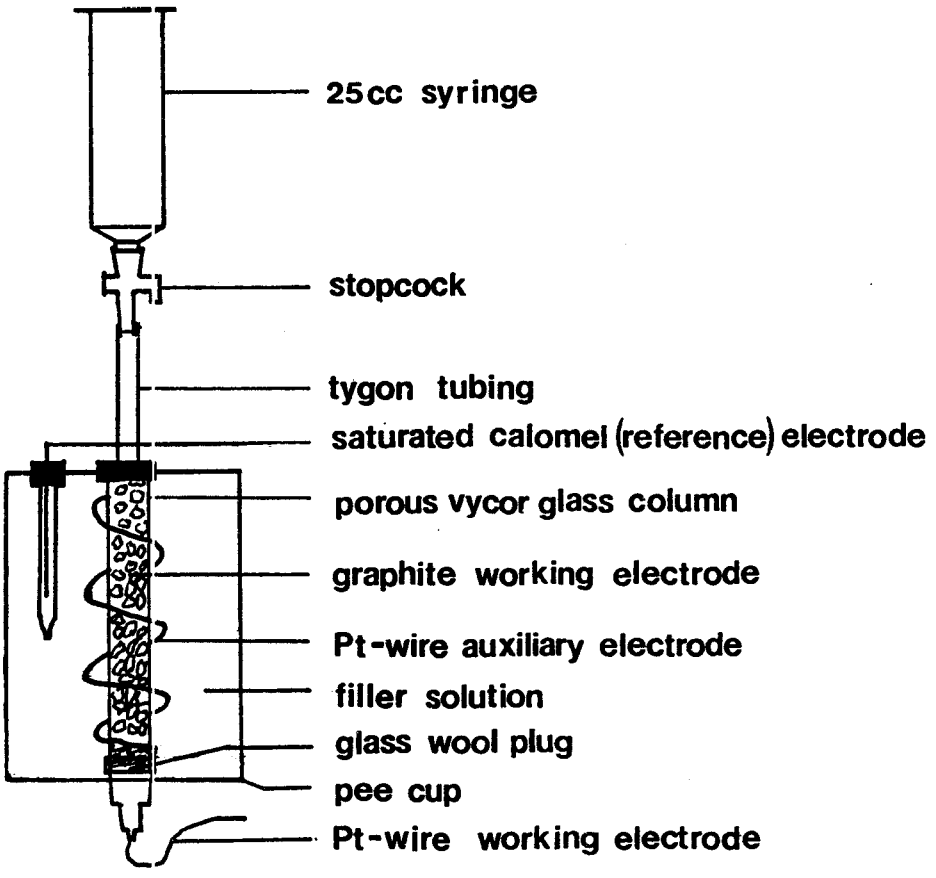

Figure 2.1: Diagram of the controlled electrode-potential electrolysis column used to oxidize the nickel(II)-oligopeptide complexes.

mL of the working buffer through the column while manually cycling between +1.5 V and -1.5 V by employing the polarity switch. Solutions of nickel(II) complexes (10^{-3} M or 10^{-4} M) were oxidized at a potential 200 mV above the E° values reported by Bossu and Margerum (1976). The flow rate through the column was gravity controlled and was approximately 1 mL/min.

2.2.1.3. Autoxidation of Ni(II)GGH.

Fresh solutions of Ni(II)GGH, prepared as described in Section 2.2.1.1., were allowed to incubate overnight in loosely capped plastic 20-mL scintillation vials. Spectral scans (600-190 nm) of this sample were taken before use to determine the degree of oxidation.

2.2.1.4. Characterization of Nickel(III)/(II) Complexes.

UV/VIS Absorption Spectrometry. Ultraviolet-visible spectra of freshly prepared nickel(II) and some nickel(III) peptide complexes were recorded using a Perkin Elmer UV/VIS Lambda 3B spectrometer equipped with a Perkin Elmer R100A recorder.

Electron Paramagnetic (Spin) Resonance (EPR). Nickel(III) peptide samples (10^{-3} M) prepared by bulk electrolysis were immediately transferred to magnetically dilute aqueous EPR tubes and were quenched in liquid nitrogen. The EPR spectra were measured at -150 °C using a Varian E-109 X-band EPR spectrometer modulated at 100 kHz.

Cyclic Voltammetry (CV). CV voltammograms were recorded with a three-electrode system consisting of a saturated Ag/AgCl reference electrode, a platinum wire auxiliary electrode, and a carbon-paste working electrode. Voltammograms were generated with a Bioanalytical

Systems, Inc., Bas-100 Electrochemical Analyzer and were recorded on a standard dot-matrix printer. Preconditioning of the carbon-paste working electrode was achieved by applying a new carbon-paste layer on the working electrode for each sample and by cycling (linear sweep) between +1.5 V and -1.5 V versus Ag/AgCl. This procedure gives contamination free, "quasi-reversible" cyclic voltammograms (Bossu and Margerum, 1977).

2.2.2. Generation and Detection of Oxygen Radicals.

2.2.2.1. Isolation of Human Polymorphonuclear Leukocytes.

PMNs were isolated as described by Boyum (1968). In general, 10 mL of venous blood was drawn from healthy volunteers on the day of the experiment by venipuncture into heparinized tubes. The plasma layer that forms after centrifugation at 1500 rpm for 10 min. was removed to about 4 mm above the (white) buffy-coat layer. The remaining cell suspension (consisting of WBCs and RBCs) was transferred to 50-mL Falcon tubes and diluted to 40 mL with PBS. This mixture was then layered over 10 mL of Ficoll-Hypaque and centrifuged at 1500 rpm for 30 min. The plasma, platelet, lymphocyte and Ficoll-Hypaque containing supernatant was aspirated off. Erythrocytes present in the red pellet were lysed using the buffered ammonium chloride lytic solution in a 1:8 ratio. The reddish mixture turned deep purple after shaking slowly for about 5 min. signalling RBC lysis. Centrifugation at 1500 rpm for 10 min. and subsequent aspiration of the supernatant left a pellet consisting of about 95 % PMNs. The lytic step was repeated when erythrocyte contamination was substantial. Otherwise, the cell pellet was washed

twice with PBS and adjusted to 10^7 PMNs mL^{-1}.

2.2.2.2. Generation and Measurement of Superoxide Anions.

Enzymatic Generation. A modified method based on the work of McCord and Fridovich (1968) was used for the determination of the superoxide anion. It employs SOD-inhibited reduction of cytochrome c as a way of monitoring the flux of superoxide anions. In general, 10^{-7} M xanthine oxidase was added to a sample containing 50 µg/mL catalase, 50 µM cytochrome c and 100 µM acetaldehyde or 10 µM hypoxanthine or xanthine. In addition to these constituents, the reference sample also contained 25 µg/mL SOD. The superoxide anions generated during xanthine-oxidase catalyzed oxidation of the substrates reduce ferricytochrome c, causing a UV/VIS spectral change that was continuously monitored at 550 nm (Margoliash and Frohwrit, 1959; Fridovich, 1985b). All reactions with nickel(II) peptides were done in 0.1 M KH_2PO_4 (pH=7.4) or in 0.1 M HEPES (pH=7.4) when the hydrated Ni^{2+} ions were tested.

The activity of xanthine oxidase itself in the presence of the different nickel(II)-peptide complexes was monitored by following the conversion of hypoxanthine to uric acid. The absorbance increase at 292 nm which accompanies this oxidation is characterized by ε=11,000 M^{-1} cm^{-1} (Fridovich, 1985a) under the conditions used in the experiment.

Cellular Generation. A continuous assay was used to monitor the flux of superoxide anions after TPA stimulation of the respiratory burst in PMNs (Markert et al., 1984). In general, 20 µg/mL TPA were added to a sample containing 20 µM cytochrome c, 50 µg/mL catalase, and 10^6 PMNs mL^{-1}. The reference sample also contained 25 µg/mL SOD. The reduction

of cytochrome c was followed at 550 nm. All experiments were done in duplicate and in 0.1 M KH_2PO_4 (pH=7.4).

2.2.2.3. Detection of Superoxide Anions with Nitro Blue Tetrazolium.

In experiments with high concentrations of hydrogen peroxide (10^{-1}-10^{-4} M), NBT^{2+} was used to quantify superoxide anion production. In some cases, NBT^{2+} was prepared in 0.1 M KH_2PO_4 (pH=7.4) in the presence of 0.15 % BSA (Kimura et al., 1981). When H_2O_2 was used to initiate a reaction, it was added last to samples containing 10^{-5} M NBT^{2+} and varying concentrations of nickel(III)/(II) peptide complexes and to control samples which in addition contained 10 µg/mL SOD. The absorbance at 550 nm was then recorded relative to this control sample (i.e., the reference sample) at regular intervals. Although there are reports that H_2O_2 inactivates SOD (Heikkila, 1985; Markland, 1985), control experiments confirmed that enough SOD remained active to completely inhibit NBT^{2+} reduction by superoxide anions under the conditions used in the experiment described. An absorptivity of 15,000 M^{-1} cm^{-1} at 550 nm for the initial reduction product of NBT^{2+} in neutral buffered aqueous solutions was used to quantify superoxide anion generation (Auclair and Voisin, 1985).

2.2.2.4. Quantification of Hydrogen Peroxide with Peroxidase-o-Dianisidine.

The generation of H_2O_2 from the hypoxanthine/xanthine oxidase system was quantified using a peroxidase reaction to yield a stoichiometric quantity of chromophore. In the assay, 50 µg/mL xanthine oxidase (final concentration) were added to a solution containing varying concentrations of Ni(II)GGH, 0.2 mM o-dianisidine, 40 µM

hypoxanthine, and 0.6 mg/mL peroxidase; and to a reference sample which also contained 0.3 mg/mL catalase. The absorbance at 460 nm was monitored continuously for 10 min. All reactions were carried out in duplicate and in 0.1 M KH_2PO_4 (pH=7.4), unless otherwise specified. In reaction mixtures containing catalase, the amount of chromophore formed was below the detection limit, indicating that o-dianisidine oxidation was specifically caused by the hydrogen peroxide present.

2.2.2.5. Quantification of Hydrogen Peroxide with $TiOSO_4$.

$TiOSO_4$ was used to quantify H_2O_2 in the 10^{-1}-10^{-4} M range (Sellers, 1980). A saturated stock solution of $TiOSO_4$ had been prepared by boiling 41 g $TiSO_4$ in 6 L 2 N H_2SO_4. The mixture was cooled and filtered through two sheets of Whatman filter paper #1. The filtrate was then diluted by adding 3 L of 2 N H_2SO_4. Experiments in which the consumption of H_2O_2 was monitored, 200 µL of the reaction mixture (which initially contained 10^{-3} or 10^{-4} M Nickel(II)GGH and 10 mM H_2O_2) was added to 1 mL of $TiOSO_4$ reagent. The solution was allowed to stand for 10 min. at room temperature, and the absorbance at 410 nm was read relative to a reference sample containing a corresponding aliquot of 0.1 M KH_2PO_4 (pH=7.4). The quantity of H_2O_2 present in the samples was extrapolated from a standard curve relating the amount of chromophoric product formed (absorbance at λ max of 460 nm) to known concentrations of H_2O_2 added.

2.2.2.6. Measurement of Oxygen Production.

Continuous monitoring of oxygen levels during a reaction was made with a Rank Oxygen Electrode (Rank Bros., Bottisham Cambridge. U. K.)

connected to a flat bed (Johns Scientific, Kipp & Zonen) recorder. Only assessments of relative rates of oxygen release were made since repeated attempts to quantify oxygen concentrations were unsuccessful. In general, a specific volume of H_2O_2 was added last and with stirring to a mixture containing the nickel complex in 0.1 M KH_2PO_4 (pH=7.4), or in 0.1 M $NaClO_4$ (pH=9.6). The increase in oxygen tension was recorded for 10 min. or until the slope of the curve was zero. The electrode was vigorously rinsed with DDW between each run and dried thoroughly with paper tissues (Kimwipes). Data was tabulated in units of divisions/min and was estimated as the number of divisions on the recorder paper (total of 100 divisions) the curve crossed in one minute. This was evaluated for the linear segment of the curve at the beginning of the reaction, and thus represents the initial rate of the reaction.

2.2.2.7. Hydroxylation of p-Nitrophenol.

Hydroxylation of p-nitrophenol during nickel(II)-complex catalyzed decomposition of H_2O_2 was measured by a modification of the hydroxyl radical assay reported by Florence (1984). (The product of this reaction is p-nitrocatechol.) Varying concentrations of H_2O_2 were added to samples containing 1 mM p-nitrophenol, and 10^{-3} or 10^{-4} M catalyst (nickel(II) or copper(II) complex) in 0.1 M KH_2PO_4 (pH=7.4). Except in time-dependent assays, reactions were stopped after 45 min. or 60 min. by adding 25 µL 6 N HCl. These solutions were then extracted three times with fresh aliquots of (1 mL) diethyl ether. The combined ether extracts were vortexed in 0.5 mL of 0.1 M NaOH and the ether evaporated off by incubating the samples in a 37 °C waterbath. A sample containing the same constituents except the catalyst provided a convenient blank.

The absorbance of each sample was then measured at 522 nm relative to this blank. If the absorbance was greater that 1.0, the sample was diluted 1:1 with 0.1 M NaOH.

2.2.3. Effects of Hydrogen Peroxide and Nickel(II) Peptide Complexes on Uric Acid and 2-Deoxy-D-Ribose.

2.2.3.1. Decomposition of Uric Acid.

Nickel(II)-peptide catalyzed degradation of uric acid was followed spectrometrically at a λ max (uric acid) of 292 nm (Fridovich, 1985a). In general, 10 mM H_2O_2 was added last to samples containing 10^{-4} M nickel(II) peptide catalyst and 2 x 10^{-4} M uric acid in phosphate buffer (pH=7.4). When triglycine, triglycineamide or tetraglycine was used, the identical reactions were carried out in 0.1 M $NaClO_4$ (pH=9.6). The absorbance at 292 nm (ε=11,000 M^{-1} cm^{-1}; Fridovich, 1985a) was measured relative to the appropriate buffer alone, employing 0.4 mL aliquots.

2.2.3.2. Quantification of Glyoxylic Acid.

The main product of uric acid oxidation is thought to be allantoin. Chemical conversion of allantoin to a measurable chromophore of glyoxylic acid was used to assess the quantity of allantoin originally present (Borchers, 1977). In general, varying concentrations of H_2O_2 were added to samples containing final concentrations of 2.4 x 10^{-4} M uric acid and 10^{-4} M Ni(II)GGH in phosphate buffer (pH=7.4). At 30 min and after measuring the absorbance at 292 nm (relative to a blank containing 10^{-4} M Ni(II)GGH alone), 500 µL of each sample was transferred to a test tube containing 50 µL (0.43 mg/mL) of catalase and was vortexed. Subsequently, 100 µL of 0.6 N NaOH was added and the

sample was placed in a boiling waterbath for 20 min to hydrolyze any allantoin to allantoic acid. While heating, 200 µL of 0.1 % 2,4-dinitrophenylhydrazine in 2 N HCl were added; the heating continued for 5 min. In this step, the allantoic acid is hydrolyzed to glyoxylic acid which then forms a characteristic hydrazone complex. After cooling, 1 mL of 2.5 N NaOH was added and after 10 min of equilibration, the absorbance was read at 520 nm. A sample containing only uric acid and Ni(II)GGH (in phosphate buffer) and carried through all colour development stages was used as the reference sample. Pure glyoxylic acid yielded a product with $\varepsilon = 8276\ M^{-1}\ cm^{-1}$. This value was used to assess the concentration of glyoxylic acid present in the samples. Spectral scans (650-390 nm) were then recorded for some of the same samples and of the glyoxylic acid positive control sample to ensure that the same products were measured.

2.2.3.3. Determination of 2-Deoxy-D-Ribose Damage.

Nickel(II)-peptide complex catalyzed degradation of 2-deoxy-D-ribose in the presence of hydrogen peroxide was quantified with thiobarbituric acid as described by Halliwell and Gutteridge (1981). In general, varying concentrations of H_2O_2 (50 mM to 50 µM) were added to samples containing 70 mM KCl, 1 mM 2-deoxy-D-ribose, and a copper or nickel(II)-complex catalyst in phosphate buffer (pH=7.4). After incubating at 37 °C for 25 min 1.0 mL of 2.8 % (w/v) TCA was added, and the whole sample was heated at 100 °C for 10 min. The samples were cooled and the absorbance read at 535 nm against a reference sample which lacked H_2O_2 and the metal catalyst but treated as described above.

2.2.4. Dioxygen Chemiluminescence in the Presence of Ni(II) Peptide Complexes.

Chemiluminescence was detected using a Thorn-EMI-Gencom photon counter with instrumental support as described by Goddard et al. (1986). Reactions were performed at 37 °C in a six-well culture dish (Linbro Plastics, No. FB6) containing teflon stirring paddles. A shutter is placed between the reaction vessel and the photomultiplier tube to minimize exposure to background light. In general, reagents were added while the shutter was closed and then opened to determine background chemiluminescence. The increase in chemiluminescence was measured after addition of hypoxanthine, xanthine oxidase or hydrogen peroxide and recorded using a standard strip chart recorder.

3. RESULTS.

3.1. Characterization of Nickel(II) and Some Nickel(III) Peptide Complexes.

3.1.1. Characterization by UV/VIS Absorption Spectrometry.

Nickel(II) ions form square-planar or square-pyramidal complexes with ligands providing molecular cavities containing a minimum of four nitrogen atoms (Glennon and Sarkar, 1982). Figure 3.1 illustrates a UV/VIS absorption spectrum for Ni(II)GGH and is characterized by a low-intensity d-d absorption band centered near 420 nm, which is typical of these yellow-coloured complexes (Bossu and Margerum, 1976). All nickel(II) complexes, except Ni(II)GGH, exhibit another poorly defined shoulder on the long wavelength side (approximately 480 nm) of this peak. The spectrum of the autoxidized product of Ni(II)GGH, oxNi(II)GGH, is further characterized by an additional intense absorption band at 305 nm. The intensity of this peak is dependent on the buffer, the oxygen concentration and the pH, and reaches maximal intensity after about 23 h of exposure to air.

All histidine-containing complexes are capable of complexing nickel(II) ions at pH=7.4 (Table 3.1), whereas the multiglycine peptides require more alkaline conditions (pH=9.6). The former have dissociable nitrogen-bound protons with lower pK_a values (near 6.5; Bryce *et al.*, 1966), which facilitates complex formation at pH=7.4. The association constant for GGH is very high (log K_{ML}=8.6 and log β_2=15.6; Glennon and Sarkar, 1982) and is strong enough for this ligand to compete for nickel(II) ions with phosphate, thus preventing precipitation in

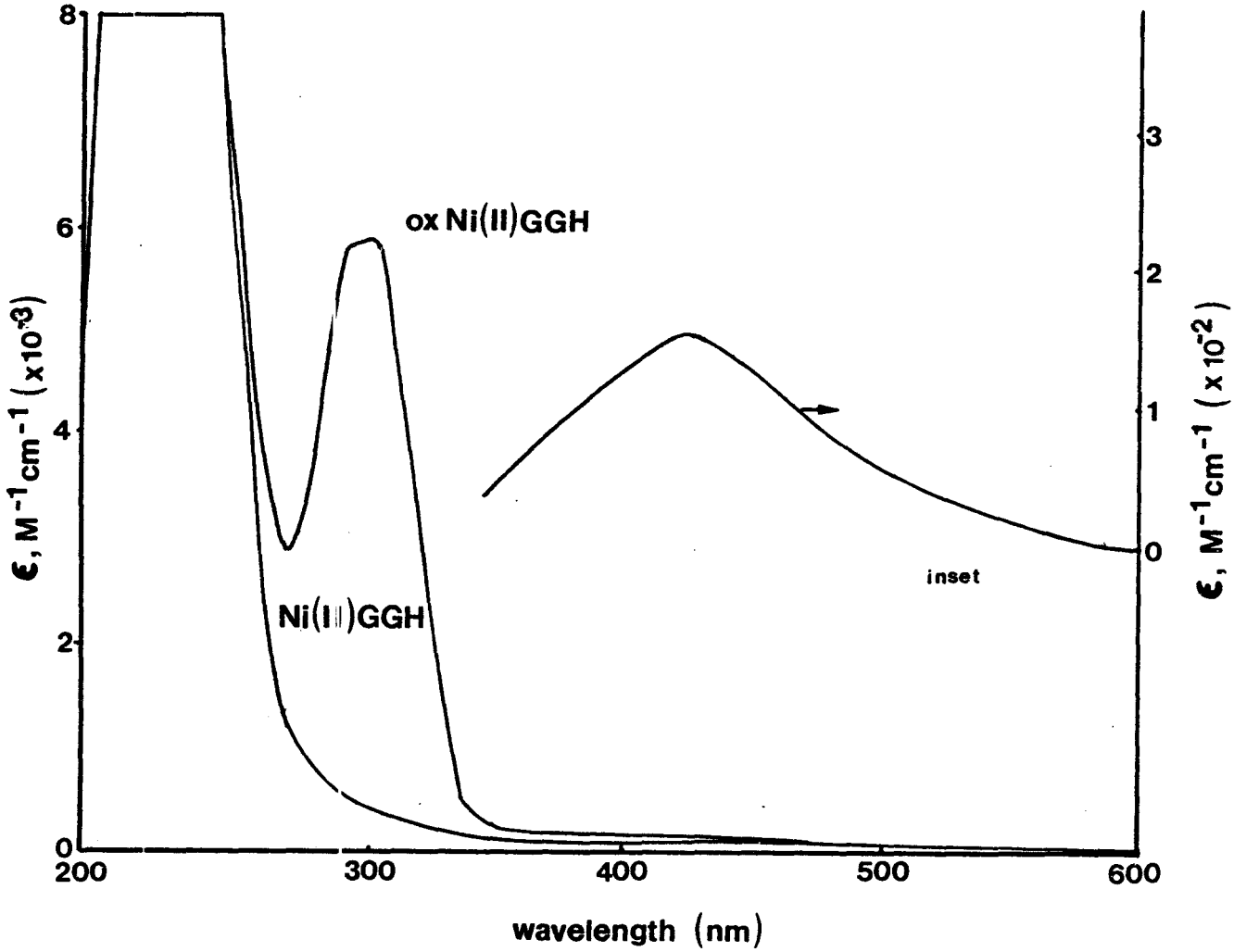

Figure 3.1: Visible absorption spectra of Ni(II)GGH and its air-oxidized product (oxNi(II)GGH) in 0.1 M KH_2PO_4 (pH=7.4). Air oxidation at room temperature (25 °C) occurred for 22-24 h. In the inset, the 350-600 nm region is shown on an expanded molar absorptivity scale.

Table 3.1: UV/VIS Spectral Properties of the Nickel(III)/(II)-Peptide Complexes Used.

Nickel Complex	λ max (absorptivity) Ni(II)L, nm (ε, $M^{-1}cm^{-1}$)	λ max (absorptivity) "Ni(III)L", nm (ε, M^{-1}, cm^{-1})[a]
Complexes Prepared in 0.1 M KH_2PO_4 (pH=7.4)		
L-Cysteine[b]	453(150), 271(13,490)	nd
Glutathione[b]	389(20)	nd
GGH[d]	425(160), 305(50±20)	425(160±25), 305[c]
GGHG[d]	425(160), 380(50) 275(400)	425(170±20), 380s(350±10) 275(810±10)
asp-ala-his-lys[d]	420(130), 365(31) 270(80)	420(140±10), 365s(320±20) 270(614±14)
oxNi(II)GGH[d]	425(130), 305(5930±200)	425(140±25), 305(300±100)
Complexes Prepared in 0.1 M $NaClO_4$ (pH=9.6)		
GG	none	560(230±10), 355(264±102) 255(7530±300)
GGG	431(250)	
GGGa	410(220), 315(20)	410(230±10), 315(1000±130)
GGGG	420(250)	
Complex Prepared in 0.1 M HEPES (pH=7.4)		
HSA	425(100)	

a: Assuming 100 % conversion to Ni(III) for freshly prepared solutions; nd, not determined.
b: Nickel complexes were reddish in colour.
c: Absorbance at 305 nm continues to increase with standing immediately after electrochemical oxidation.
d: Solutions are brownish immediately after electrochemical synthesis, and their UV/VIS spectra are very unstable.
s: Appears as a shoulder.

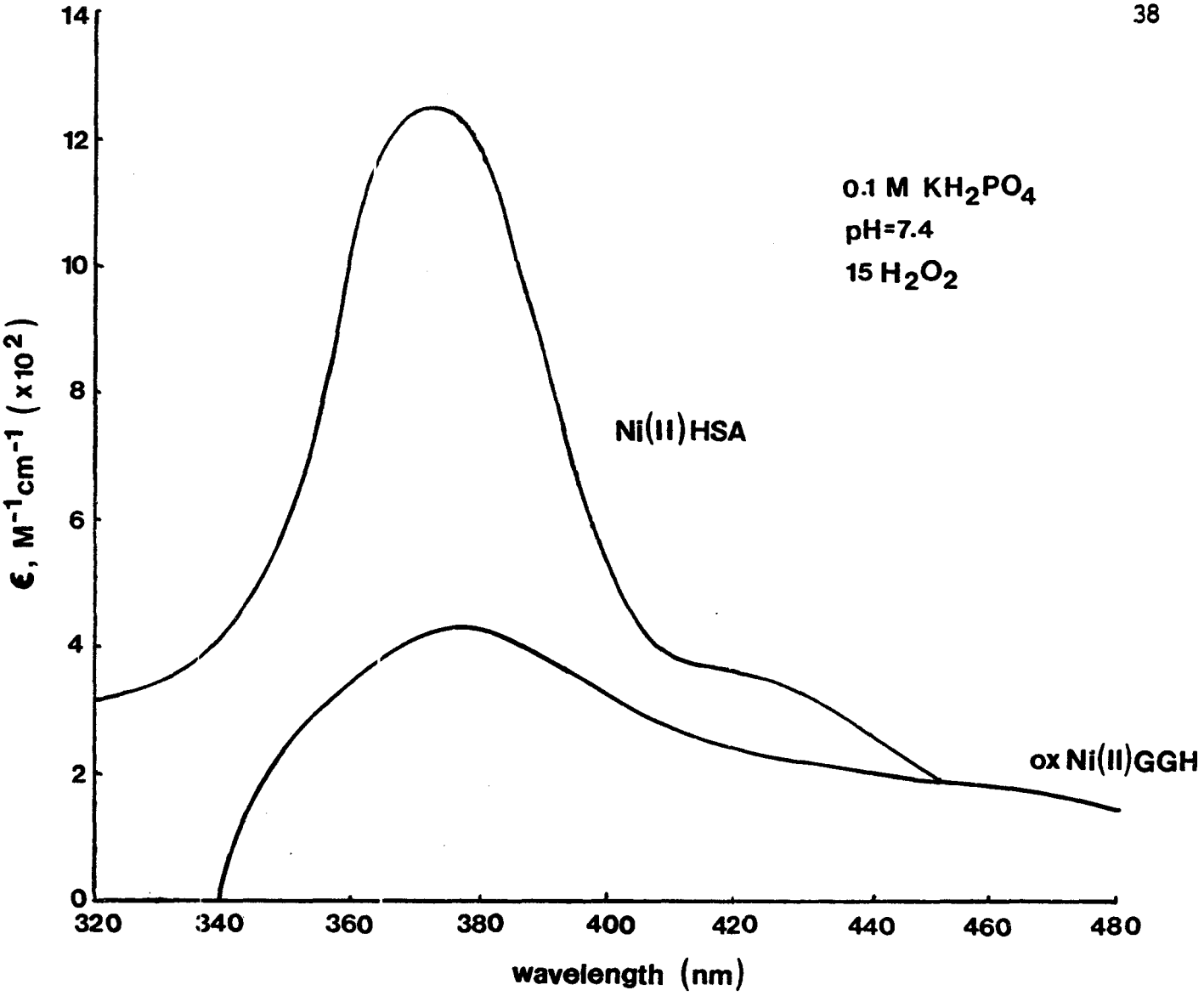

Figure 3.2: UV/VIS-difference spectra of Ni(II)HSA and oxNi(II)GGH treated with 15 mM H_2O_2. Ni(II)HSA (10^{-3} M) and oxNi(II)GGH (10^{-3} M) were treated with H_2O_2 for 20 min., and an absorption spectrum was recorded relative to the corresponding untreated complexes.

phosphate buffer.

Addition of hydrogen peroxide to nickel(II)HSA or oxnickel(II)GGH resulted in the formation of a distinct peak centered near 378 nm. In both cases, the samples darkened upon the addition of H_2O_2. Spectrometrically, this activity corresponded to an increase in the intensity of this peak to about 1300 M^{-1} cm^{-1} for nickel(II)HSA and 425 M^{-1} cm^{-1} for oxnickel(II)GGH. With observation times exceeding approximately 45 min, the intensity of this peak begins to decrease. No comparable spectral changes were observed when H_2O_2 was added to the other nickel(II)-oligopeptide complexes used in the study.

Electrochemical oxidation of Ni(II)GGHG, or Ni(II)asp-ala-his-lys results in the formation of new, extremely unstable compounds with unique UV/VIS spectra. In addition, the yellow colour of the nickel(II) complex turns to a brown colour immediately following oxidation. The intensity of this colour quickly dissipates making it difficult to obtain a UV/VIS spectrum of the immediate product (of electrochemical oxidation) within the time frame required. Electrolysis of Ni(II)GGH results in the development of a new band centered at 305nm, which ultimately on standing converts to the same spectral product as that previously described for oxNi(II)GGH (c.f., Figs. 3.1 and 3.3). The rate at which the 305 nm peak forms is shown in Figure 3.3. Although similar spectral changes were not observed for Ni(II)GGHG and Ni(II)asp-ala-his-lys, there was an overall increase in absorbance on electrolysis between 600-190 nm with a discernable shoulder centered near 365 nm for both complexes (Fig. 3.4). The molar absorptivities reported in Table 3.1 for all nickel(III)-peptide

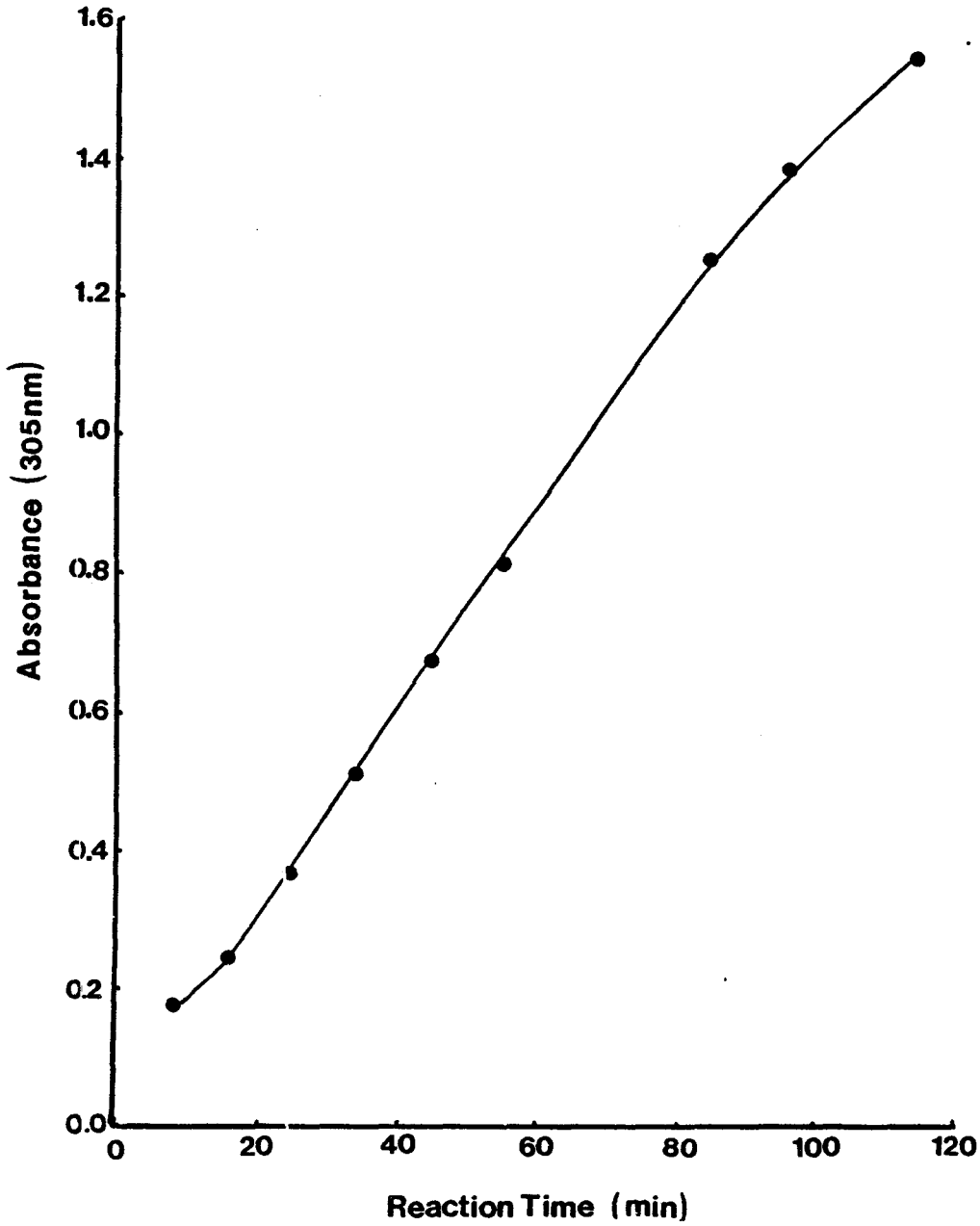

Figure 3.3: Time-dependent change in the absorbance at 305 nm immediately after controlled-electrode-potential electrolysis of 1 mM Ni(II)GGH at 0.96 V versus SCE. The absorbance at 305 nm was measured at various times against a reference that contained fresh (unoxidized) Ni(II)GGH.

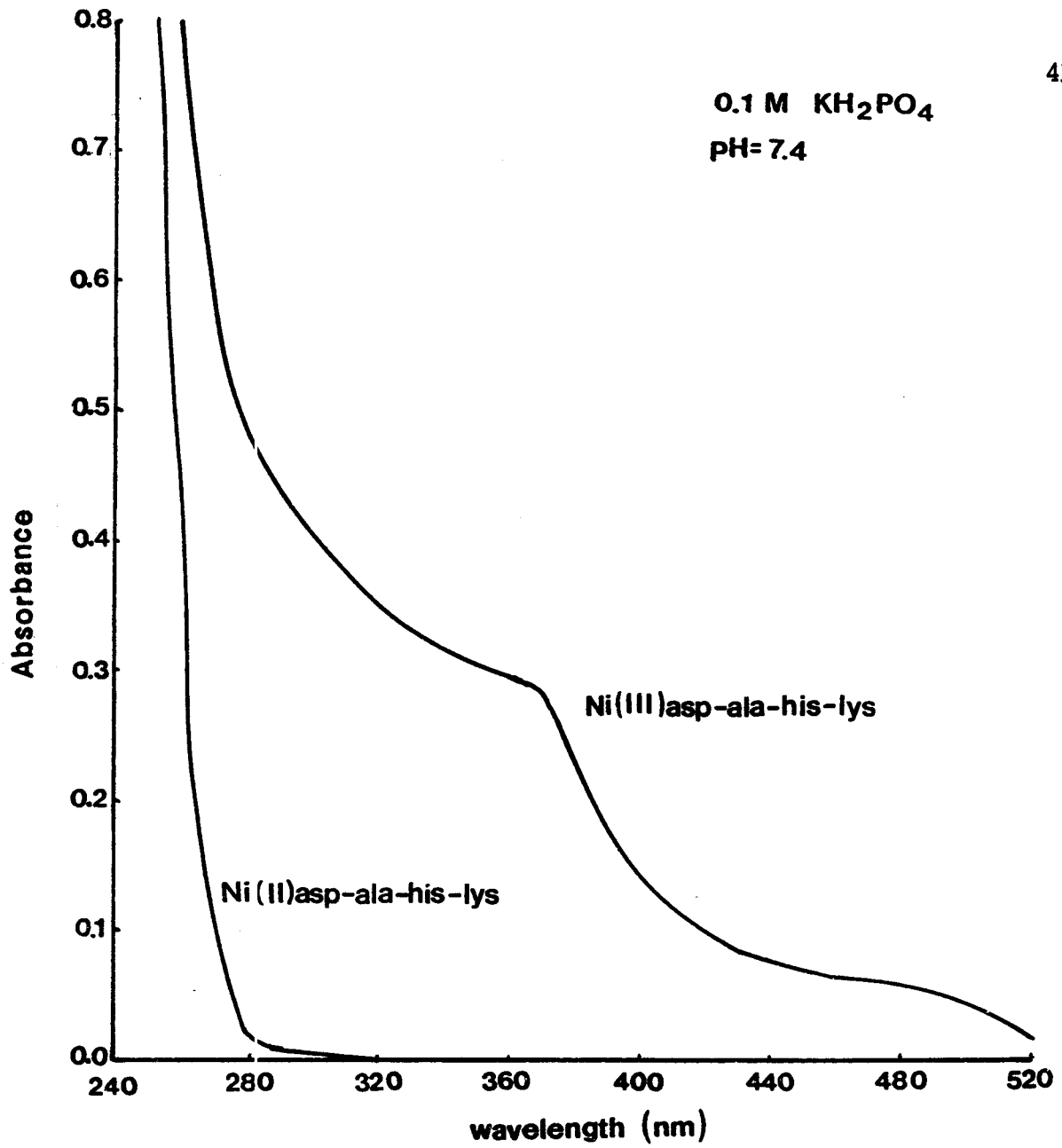

Figure 3.4: Visible absorption spectra of freshly-prepared Ni(II)asp-ala-his-lys (10^{-3} M) and its electrochemically oxidized product. UV/VIS scans were obtained relative to a reference that contained buffer alone.

complexes are only approximate, since the exact number of oxidizing equivalents (ie. nickel(III)) present were not determined.

By contrast to the square-planar complexes, the geometry of Ni(II)$(GlyGly)_2$ is thought to be a tetragonally compressed octahedron (Jacobs and Margerum, 1984). The electrochemical oxidation of this complex results in the formation of violet-black solutions containing a series of new spectral peaks (Table 3.1). Although the Ni(III)$(GlyGly)_2$ is stable for several days, the molar absorptivities of these peaks were only 60 % of those given by Jacobs and Margerum (1984) suggesting incomplete oxidation.

3.1.2. Detection of Nickel(III).

The detection of EPR signals for the nickel peptide complexes (Figs. 3.5-3.7) confirms that the immediate products of controlled electrode-potential electrochemical oxidation in phosphate buffer at pH=7.4 are nickel(III) complexes. These complexes are relatively unstable and must be frozen (in liquid nitrogen) within minutes, or the EPR signal will be lost (i.e., reversion or decomposition of nickel(III) to nickel(II)). Ni(III)GGH and Ni(III)GGHG have EPR signals with multiple peaks of uneven intensity at $g_{//}$ suggesting that at least 2 different nickel(III) peptide complexes are present. It was found that the formation of the minor species can be circumvented by lowering the pH to 6.5 (Fig. 3.8). Conversion to a tetragonally distorted octahedral structure accompanies the oxidation to nickel(III) state. Hence, the nature of the axial species can be identified since the presence of an oxygen donor atom axially coordinated to the plane results in one band at $g_{//}$ (Figs. 3.6 and 3.8); while a nitrogen

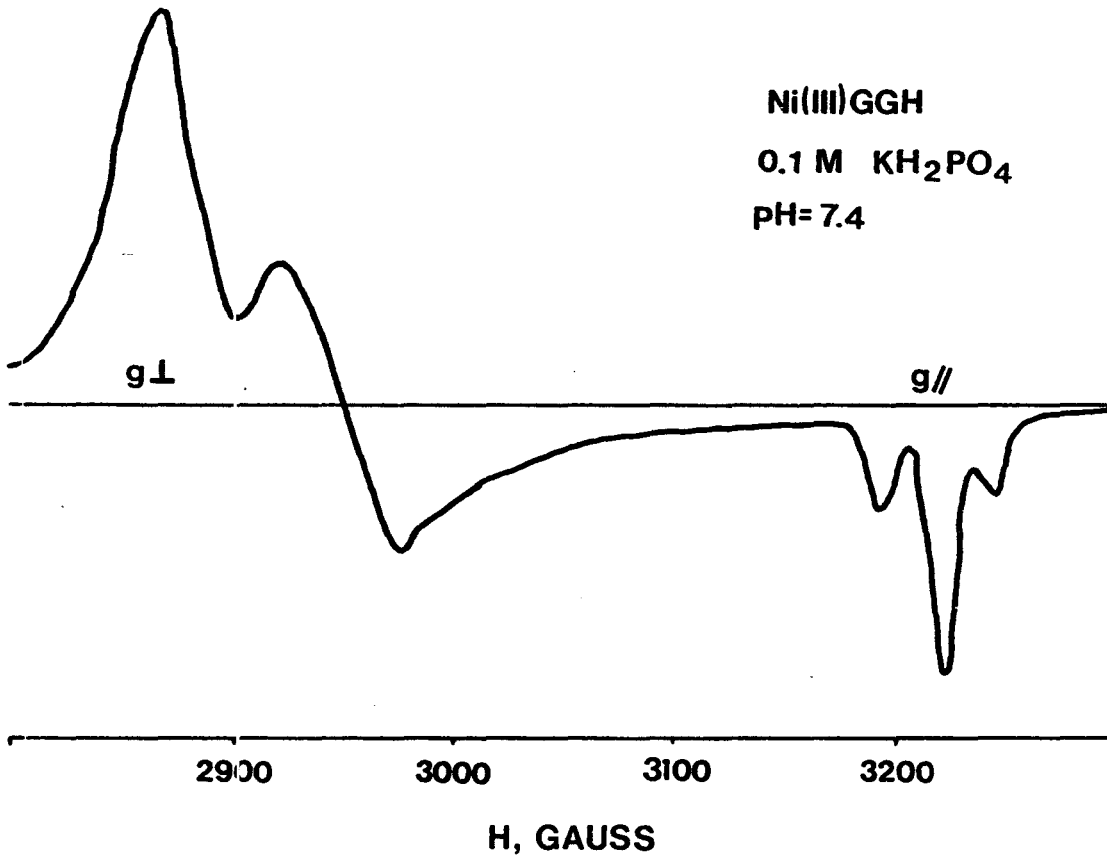

Figure 3.5: EPR spectrum of Ni(III)GGH prepared from 10^{-3} M Ni(II)GGH in 0.1 M KH_2PO_4 (pH=7.4) by controlled-potential electrolysis at 0.96 V (versus SCE). The spectrum was obtained at -150 °C and 9.081 GHz.

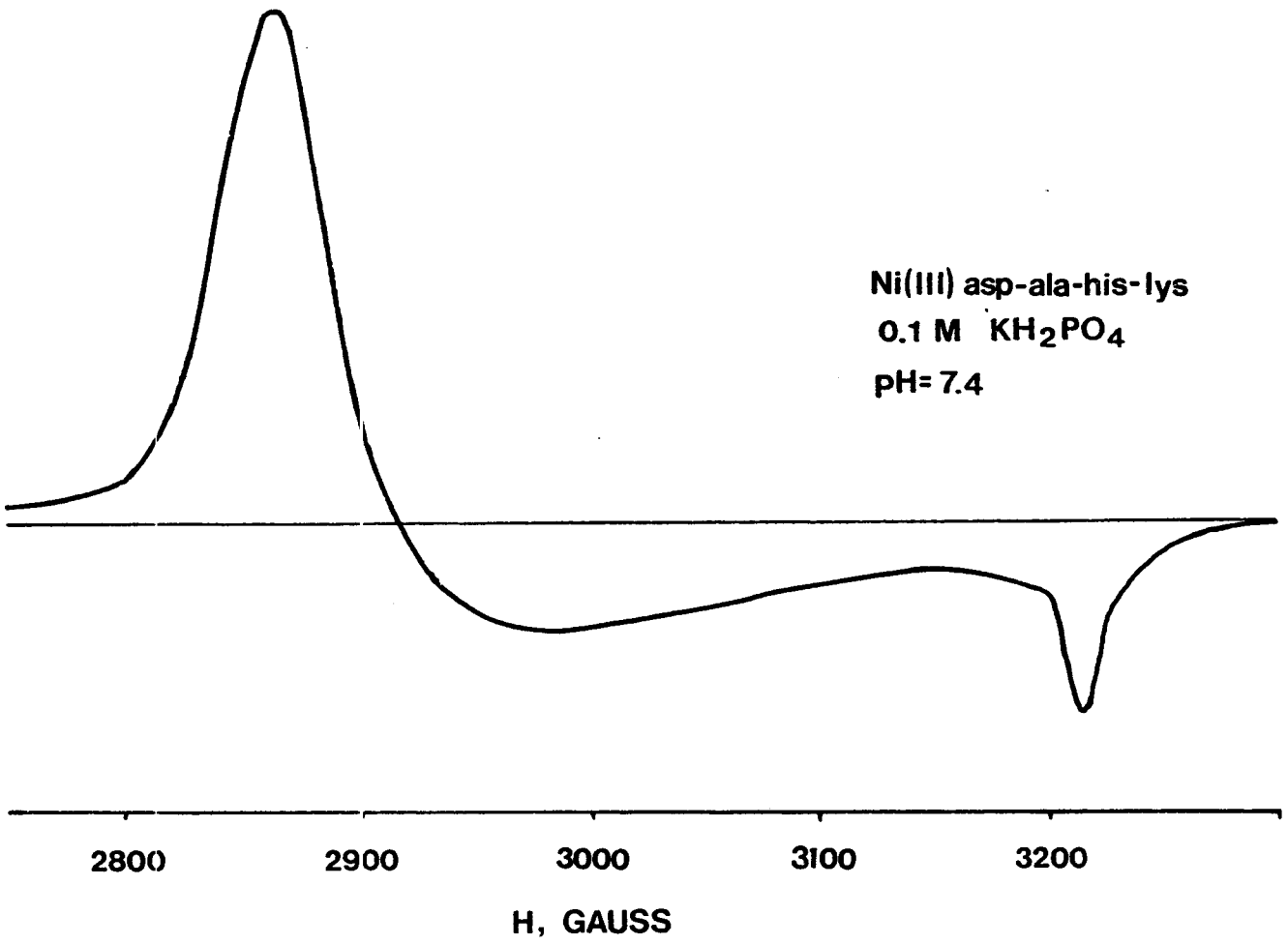

Figure 3.6: EPR spectrum of Ni(III)asp-ala-his-lys prepared from 10^{-3} M Ni(II)asp-ala-his-lys in 0.1 M KH_2PO_4 (pH=7.4) by controlled-potential electrolysis at 0.96 V (versus SCE). The spectrum was obtained at -150 °C and 9.081 GHz.

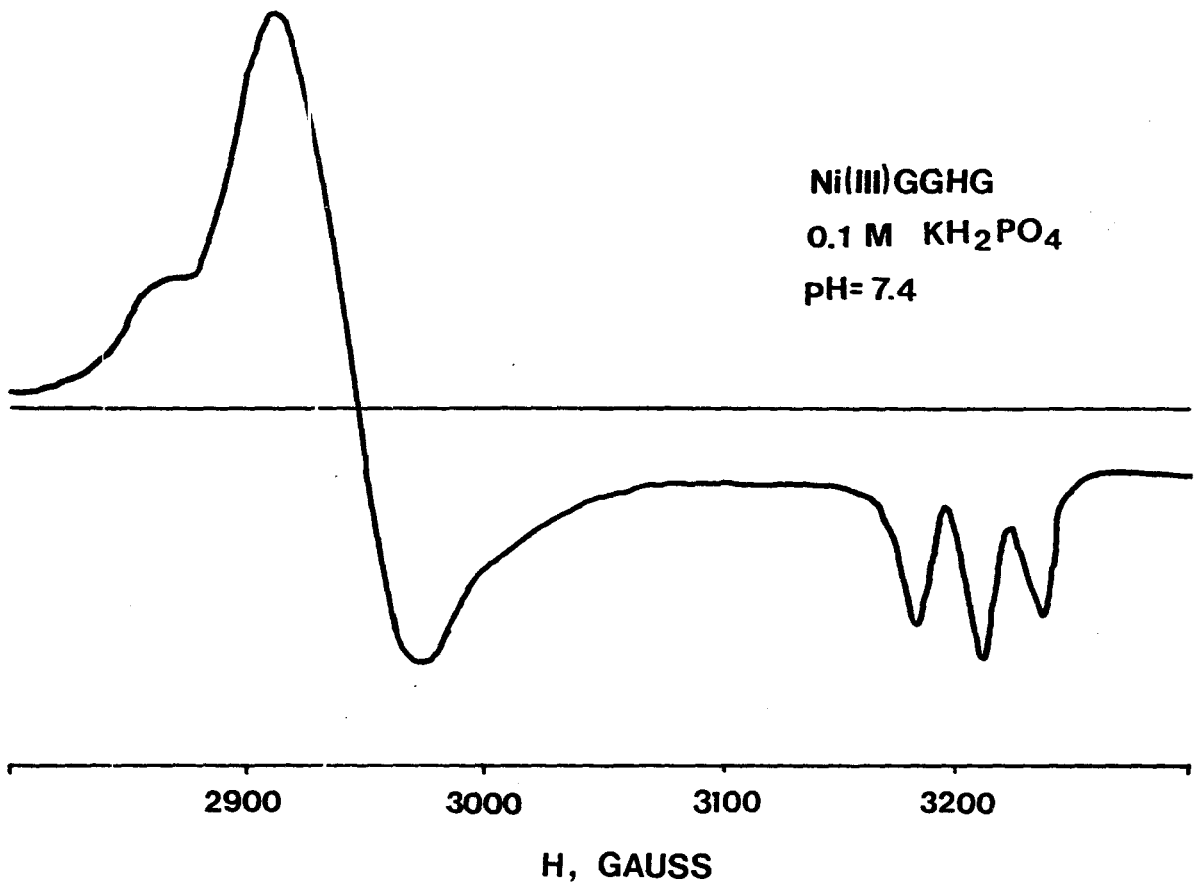

Figure 3.7: EPR spectrum of Ni(III)GGHG prepared from 10^{-3} M Ni(II)GGHG in 0.1 M KH_2PO_4 (pH=7.4) by controlled-potential electrolysis at 0.96 V (versus SCE). The spectrum was obtained at -150 °C and 9.081 GHz.

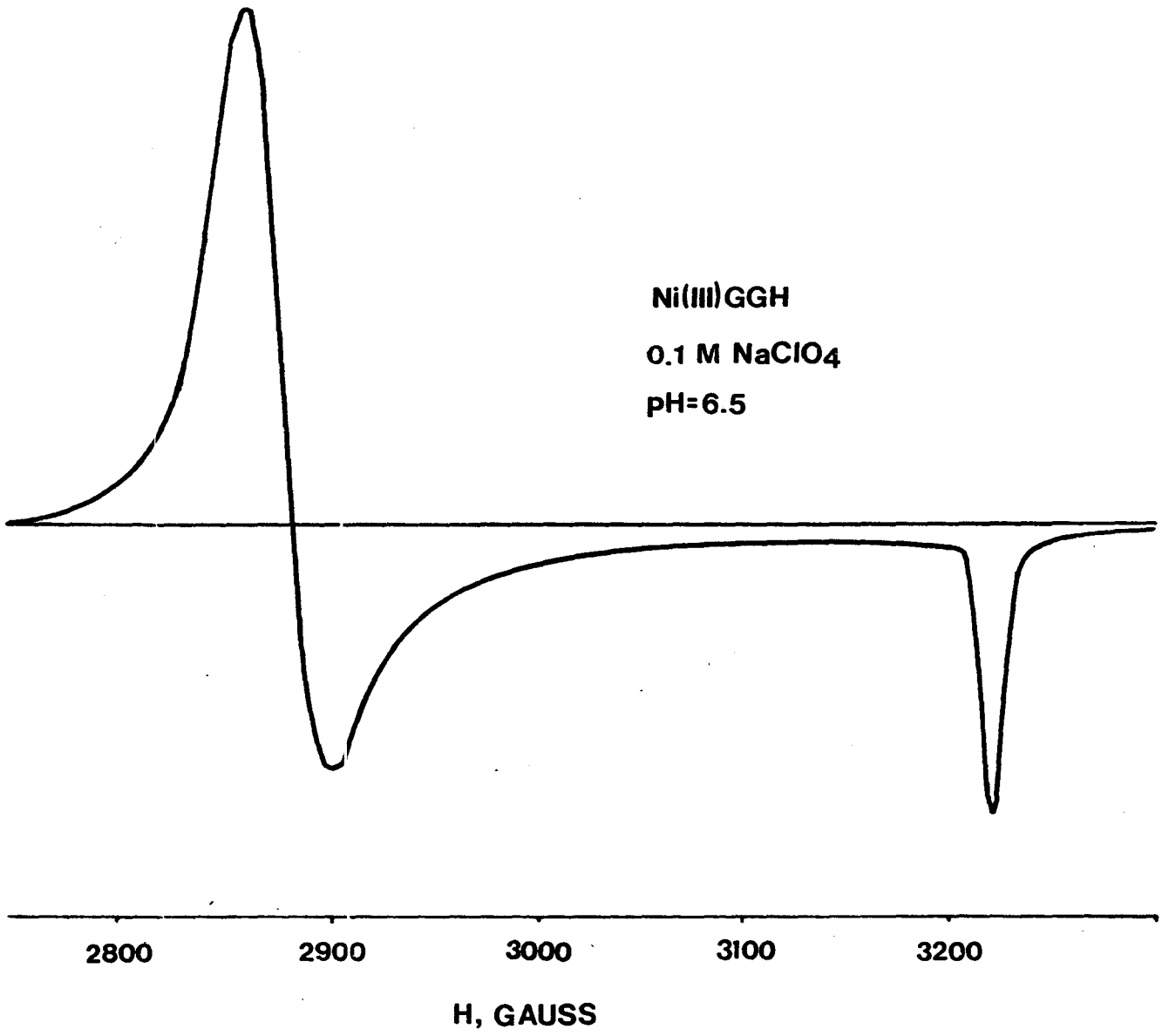

Figure 3.8: EPR spectrum of Ni(III)GGH prepared from 10^{-3} M Ni(II)GGH in 0.1 M $NaClO_4$ (pH=6.5) by controlled-potential electrolysis at 0.96 V (versus SCE). The spectrum was obtained at -150 °C and 9.081 GHz.

linkage in the same position would result in the presence of three bands (Fig. 3.7). The nitrogen linkage in the axial position results in further splitting due to the hyperfine coupling between the unpaired electron on the nickel(III) species and the ^{14}N nucleus (multiplicity of 2I + 1; with nuclear spin I=1 for ^{14}N).

3.1.3. Reversibility of the Ni(III)/(II) Redox Couple.

The reversibility of the Ni(III)/(II) redox couple was studied using cyclic voltammetry. A typical current-voltage response curve in unsupplemented 0.1 M KH_2PO_4 buffer (i.e., no $NaClO_4$ added to adjust the ionic strength) is shown for Ni(II)GGHG in Figure 3.9. The initial solution contains only the divalent nickel complex which generates the oxidation wave (negative current) when scanning from 0 to 1.0 V; while the trivalent complex that forms generates the reduction wave (positive current) when scanning in the reverse direction from 1.0 to 0 V. The voltammogram for Ni(II)GGH was similar, while only anodic peaks (oxidation waves) could be obtained for Ni(II)HSA. Attempts to get comparable data for the HSA-binding site analog, Ni(II)asp-ala-his-lys, were not pursued.

The midpoint between the anodic and cathodic peaks were used to estimate the electrode potentials of the Ni(III)/(II) redox couple.

$$\text{Ni(III)GGHG} + e^- \longrightarrow \text{Ni(II)GGHG} \qquad E=0.73\ V \quad (3.1)$$

$$\text{Ni(III)GGH} + e^- \longrightarrow \text{Ni(II)GGH} \qquad E=0.73\ V \quad (3.2)$$

$$\text{Ni(III)asp-ala-his-lys} + e^- \longrightarrow \text{Ni(II)asp-ala-his-lys} \qquad E=0.74\ V \quad (3.3)$$

The redox potential for the couple depicted in Equation 3.3 was estimated using square-wave voltammetry (a feature of the Bas-100

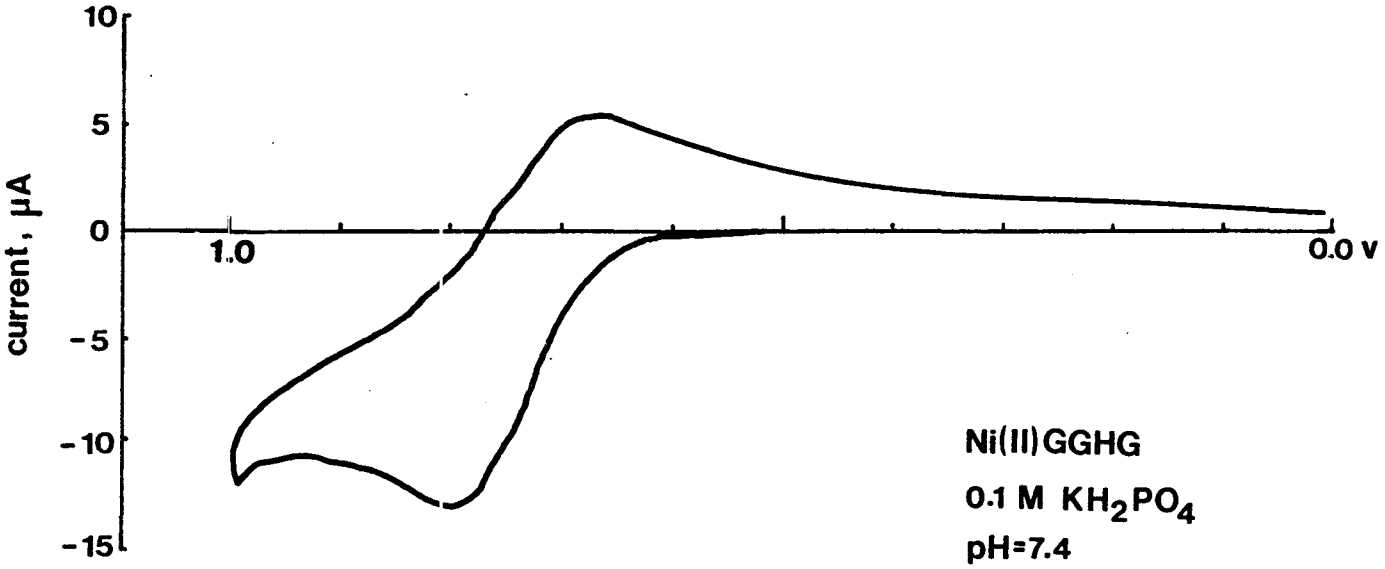

Figure 3.9: Cyclic voltammogram of 10^{-3} M Ni(II)GGHG in 0.1 M KH_2PO_4 using a carbon-paste electrode at a scan rate of 100 mV s^{-1}; E=0.732 V versus Ag/AgCl.

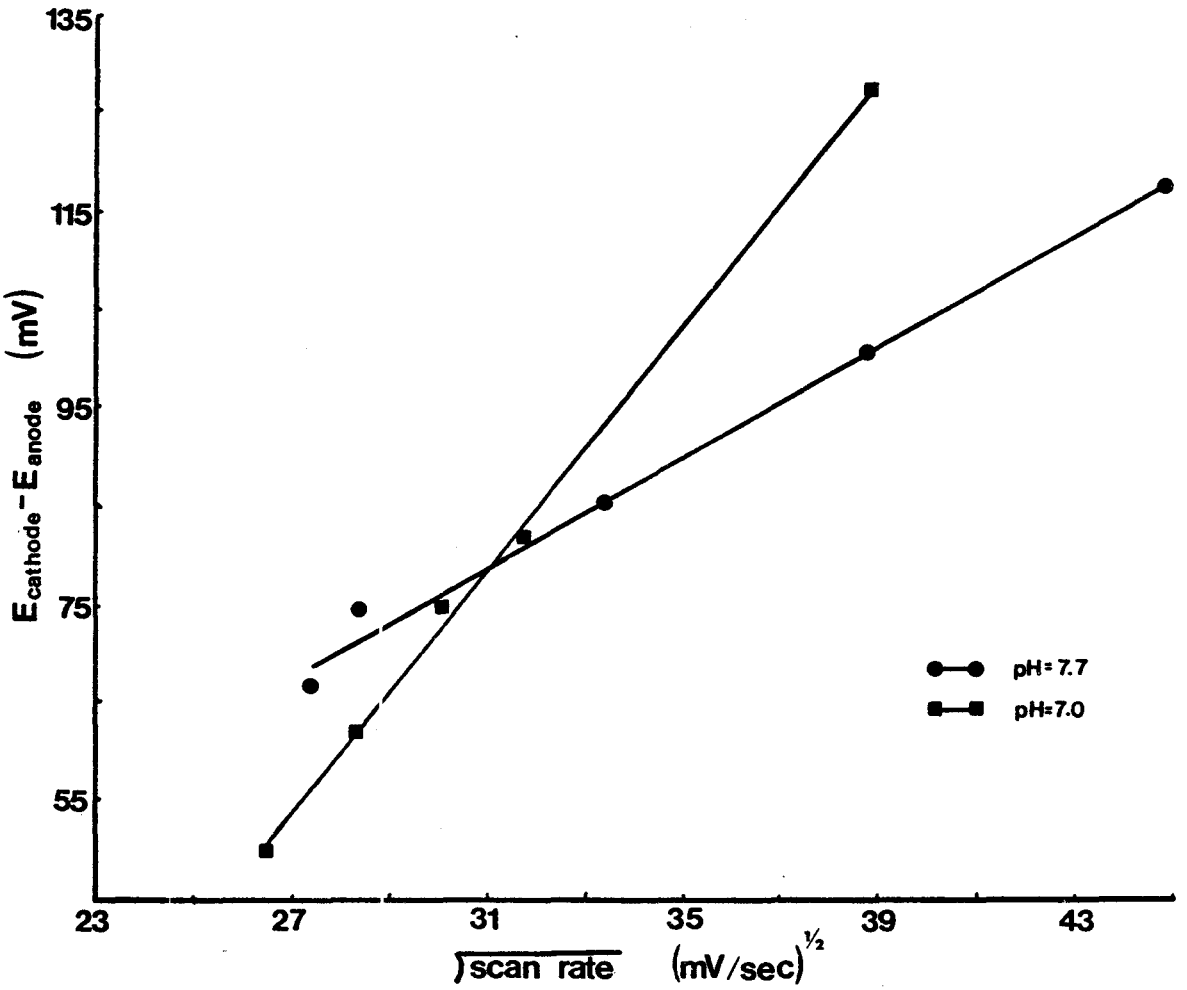

Figure 3.10: Linear Relationship between ($E_{cathode}-E_{anode}$) and the square root of the scan rate for 10^{-3} M Ni(II)GGH in 0.1 M NaH_2PO_4 containing 1.0 M $NaClO_4$. Cyclic voltammograms were obtained at various scan rates and the ($E_{cathode}-E_{anode}$) values were determined from the peak potentials.

electrochemical analyzer). All values are expressed relative to the SCE. The linearity of the plots in Figure 3.10 attest to the reversibility of the redox couple for millimolar levels of Ni(II)GGH.

3.2. Dismutase-Type Activity of Nickel(II) Peptide Complexes in Superoxide Anion Generating Systems.

3.2.1. Concentration-Dependent Scavenging of Superoxide Anions.

As illustrated in Figure 3.11, freshly prepared Ni(II)GGH and 24 h air-oxidized Ni(II)GGH (oxNi(II)GGH) clearly diminished the flux of superoxide anions generated during xanthine-oxidase oxidation of hypoxanthine detected by cytochrome c reduction. Furthermore, dose-dependent inhibition can be observed with Ni(II)GGH (Fig. 3.12), Ni(II)GGHG (Fig. 3.13) and Ni(II)asp-ala-his-lys (Fig. 3.14). The relative ability of each nickel complex to diminish the superoxide radical flux is summarized in Table 3.2. The data in this table also demonstrate that Ni(II)HSA, but not Ni(II)GGGa nor Ni(II)histidine, has this scavenging ability. The following reactivity sequence is observed based upon the percent inhibition determined under the same experimental conditions.

$$\text{Ni(II)GGH} > \text{Ni(II)GGHG} > \text{Ni(II)asp-ala-his-lys} > \text{Ni(II)HSA} \qquad (3.4)$$

As demonstrated in Figure 3.11, Ni^{2+} enhances the reduction of cytochrome c (over the control), and this effect was maximal at 10^{-4} M. Hence, it can be seen that the decrease in the superoxide anion flux is clearly dependent on the nickel(II)-complex concentration and this effect is observable at concentrations as low as 10^{-6} M (for Ni(II)GGH; Table 3.2). The data in Figure 3.15 show that Ni(II)GGH and Ni(II)asp-

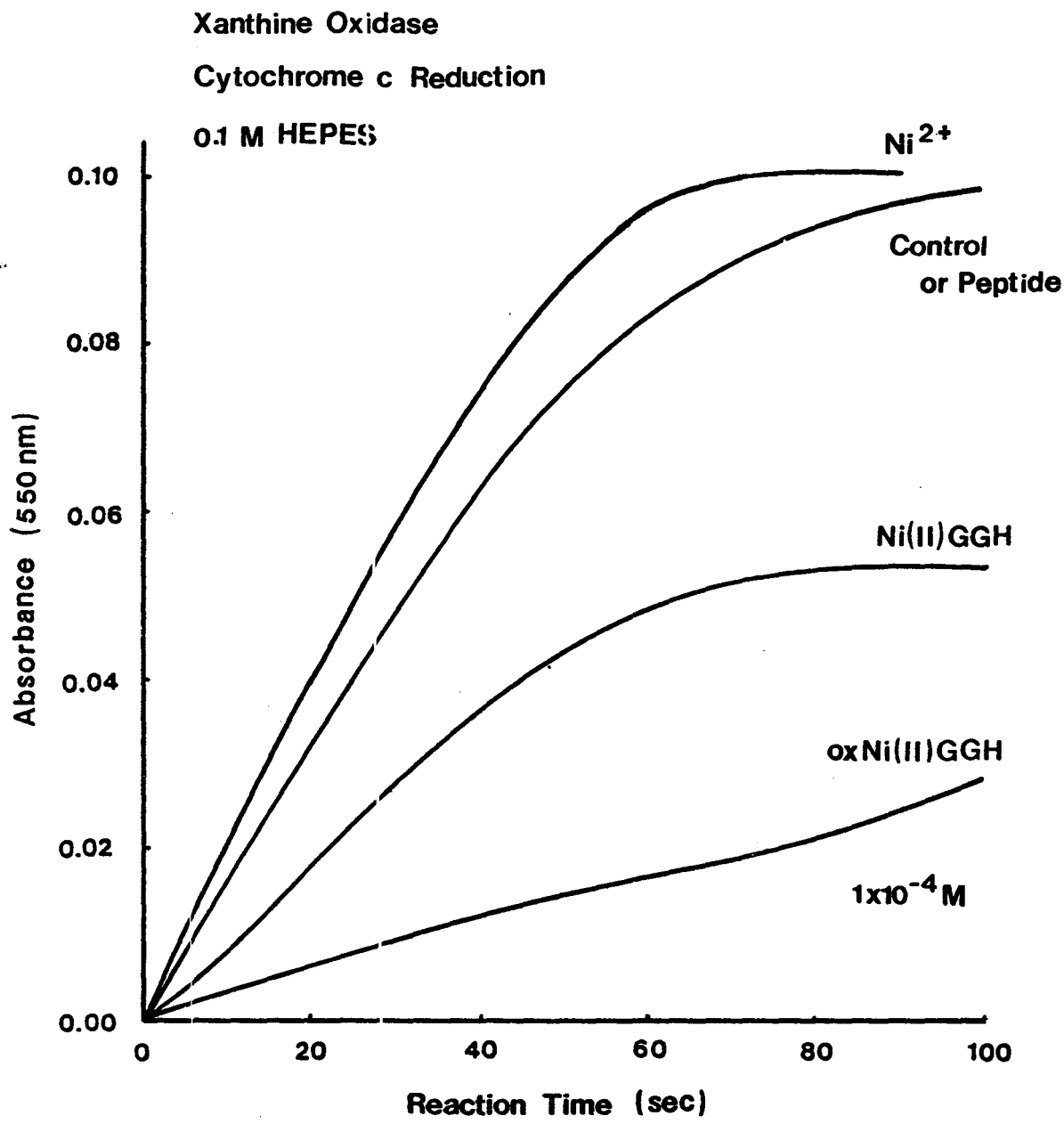

Figure 3.11: Effect of 10^{-4} M Ni^{2+}, GGH, freshly prepared Ni(II)GGH or air-oxidized Ni(II)GGH on the superoxide anion flux generated during xanthine oxidase oxidation of hypoxanthine. Reaction medium (control) contained: 10^{-5} M hypoxanthine, 10^{-7} M xanthine oxidase, 11 µM ferricytochrome c and 43 µg/mL catalase in HEPES buffer (pH=7.4). Reference samples also contained 25 µM/mL SOD.

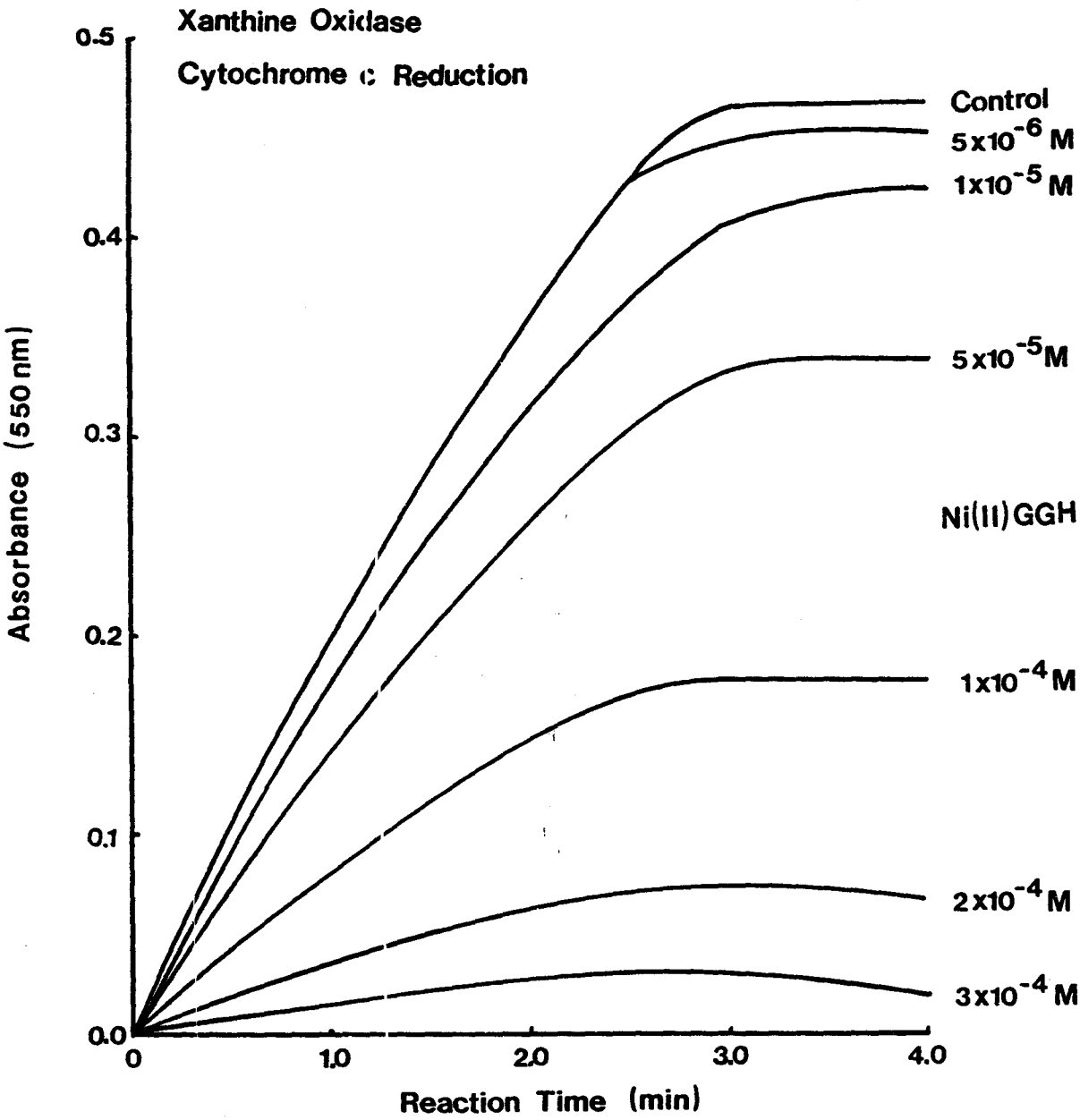

Figure 3.12: Dose-dependent inhibition of cytochrome c reduction by the hypoxanthine/xanthine oxidase superoxide anion generating system with increasing Ni(II)GGH concentration. Reaction medium contained: 33 µM hypoxanthine, 10^{-7} M xanthine oxidase, 58 µM ferricytochrome c and 43 µg/mL catalase in 0.1 M KH_2PO_4 (pH=7.4). Ni(II)GGH was added at the concentrations indicated. The control sample contained 500 µM GGH and 25 µg/mL of SOD was added to all reference samples.

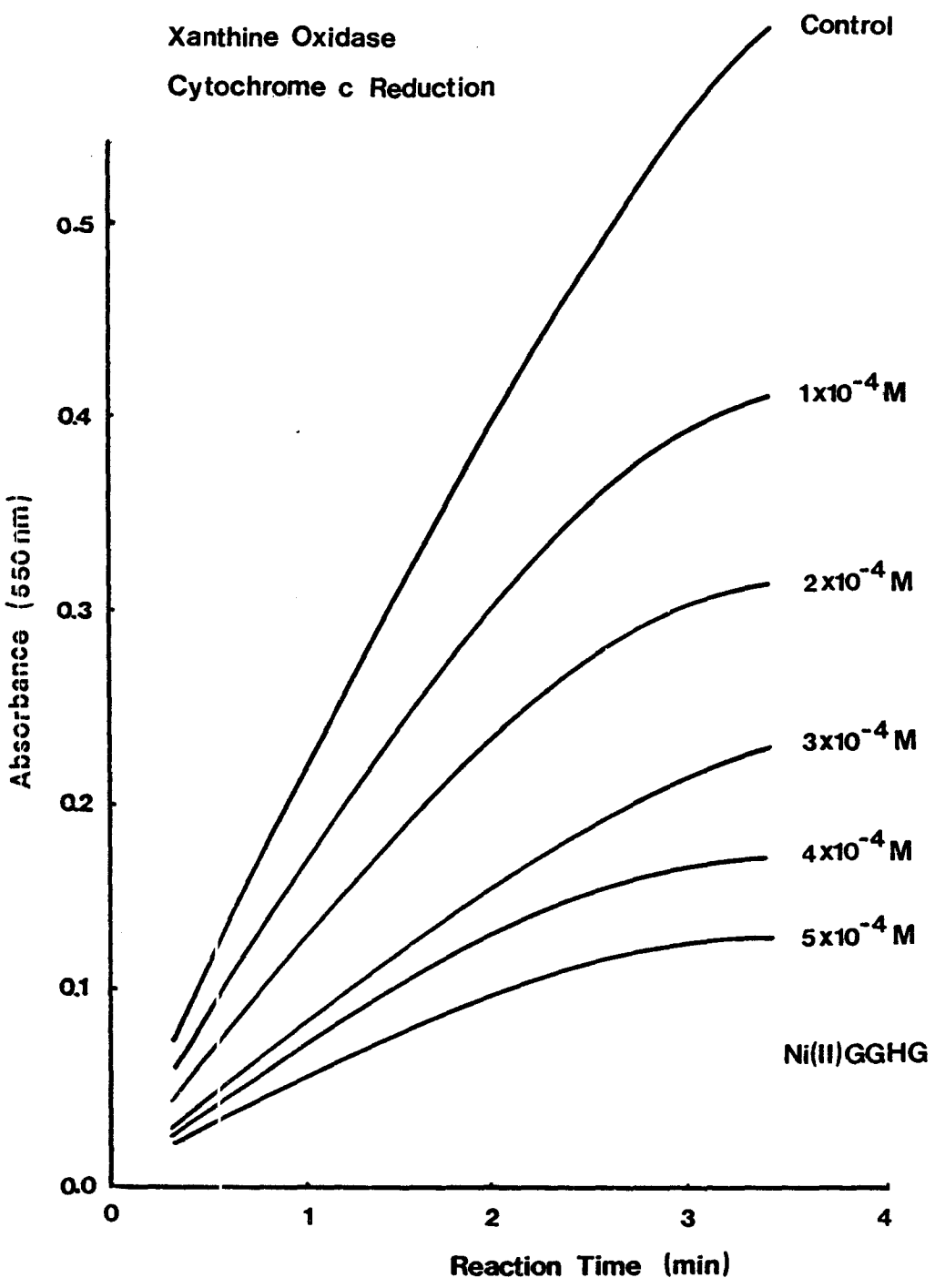

Figure 3.13: Dose-dependent inhibition of cytochrome c reduction by the hypoxanthine/xanthine oxidase superoxide anion generating system with increasing Ni(II)GGHG concentration. Reaction medium contained: 42 μM hypoxanthine, 10^{-7}M xanthine oxidase, 50 μM ferricytochrome c and 42 μg/mL catalase in 0.1 M KH_2PO_4 (pH=7.4). Ni(II)GGHG was added at the concentrations indicated, 500 μM GGHG was present in the control sample and 25 μg/mL of SOD was added to all reference samples.

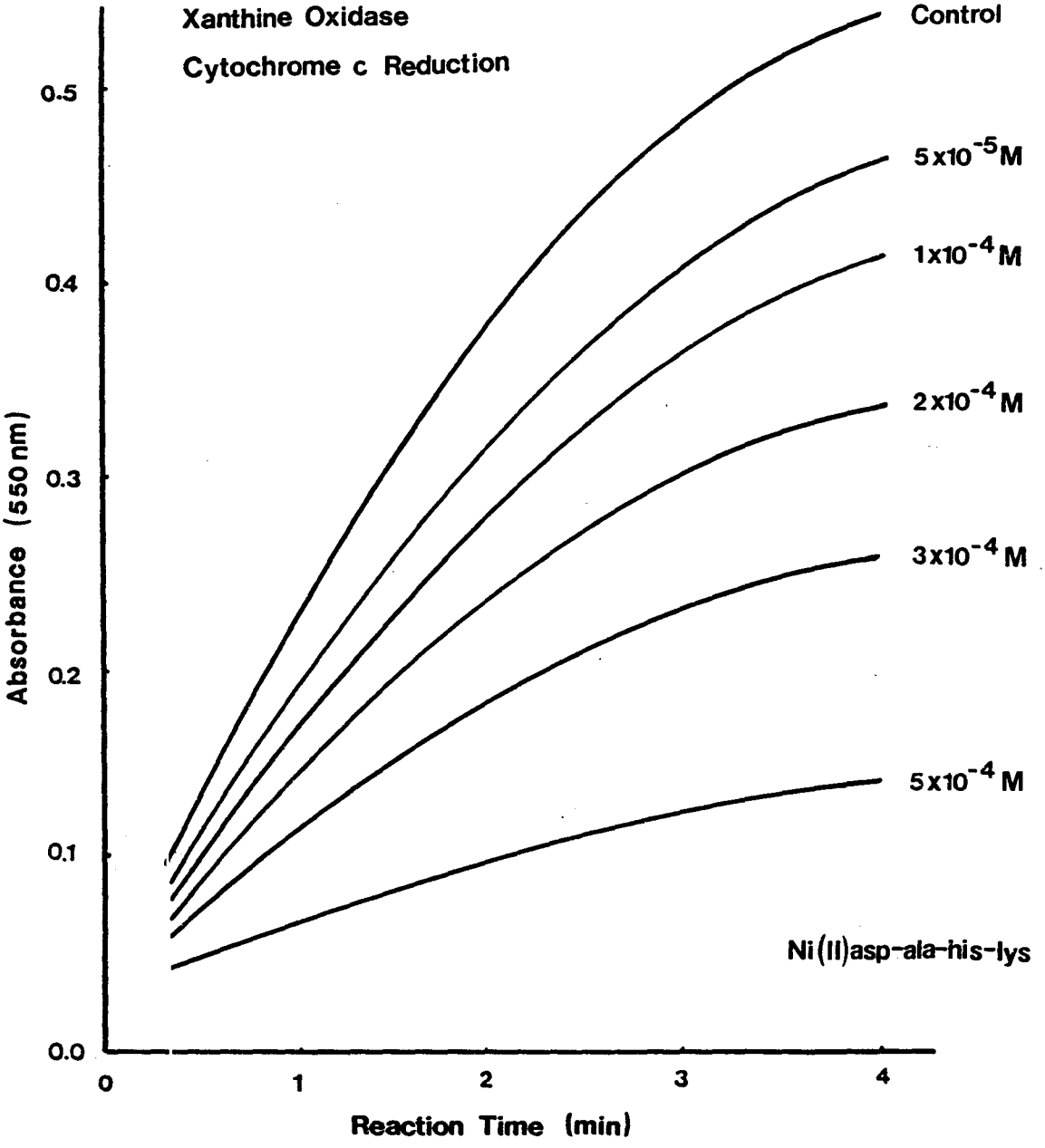

Figure 3.14: Dose-dependent inhibition of cytochrome c reduction by the hypoxanthine/xanthine oxidase superoxide anion generating system with increasing concentrations of Ni(II)asp-ala-his-lys. Reaction medium contained: 44 μM hypoxanthine, 10^{-7} M xanthine oxidase, 88 μM ferricytochrome c and 43 μg/mL catalase in 0.1 M KH_2PO_4 (pH=7.4). Ni(II)asp-ala-his-lys was added at the concentrations indicated. The control sample contained 500 μM asp-ala-his-lys and 25 μg/mL SOD was added to all reference samples.

Table 3.2: Dose-Dependent Inhibition of Cytochrome c Reduction by the Superoxide Anion Flux Generated by the Hypoxanthine/Xanthine Oxidase System in the Presence of Some Nickel-Peptide Complexes.

Additions to Reaction Mixture[a]	Absorbance (550 nm)	% Inhibition[b]
no addition	0.469	----
1 μM Ni(II)GGH	0.463	1.1 %
5 μM Ni(II)GGH	0.450	4.1 %
10 μM Ni(II)GGH	0.421	10.0 %
50 μM Ni(II)GGH	0.365	22.0 %
100 μM Ni(II)GGH	0.174	62.8 %
300 μM Ni(II)GGH	0.018	97.9 %
no addition[c]	0.505	----
50 μM Ni(II)asp-ala-his-lys	0.427	15.4 %
100 μM Ni(II)asp-ala-his-lys	0.382	24.4 %
300 μM Ni(II)asp-ala-his-lys	0.241	52.3 %
500 μM Ni(II)asp-ala-his-lys	0.131	74.1 %
500 μM Ni(II)GGH	0.000	100. %
no addition[d]	0.593	----
100 μM Ni(II)GGHG	0.406	31.6 %
300 μM Ni(II)GGHG	0.223	62.5 %
500 μM Ni(II)GGHG	0.126	78.7 %
100 μM Ni(II)asp-ala-his-lys	0.448	23.3 %
100 μM Ni(II)GGH	0.219	62.5 %
100 μM Ni(II)Histidine	0.576	2.7 %
100 μM Ni(II)GGGa	0.576	2.7 %
minus catalase	0.593	0.0 %
no addition[e]	0.128	----
100 μM Ni^{2+} alone	0.133	< 0.0 %
100 μM HSA	0.118	7.8 %
100 μM Ni(II)HSA	0.082	35.9 %

a: Reaction mixture contained: 32.5 μM hypoxanthine, 0.1 μM xanthine oxidase, 50 μM cytochrome c in 0.1 M KH_2PO_4 buffer containing 36.6 μg/mL catalase (pH=7.2). Reference samples also contained 25 μg/mL SOD.

b: % inhibition is defined as the decrease in the reduction of cytochrome c relative to the sample with no addition; results are expressed as the mean value of duplicate runs. The SD did not exceed ± 0.1 %.

c: Same as in a, but 43.4 μM hypoxanthine was used (Fig. 3.14).

d: Same as in a, but 46.8 μM hypoxanthine was used (Fig. 3.13).

e: Reaction mixture contained: 11 μM hypoxanthine, 17 μM cytochrome c and 0.1 μM xanthine oxidase in 0.1 M HEPES (pH=7.4).

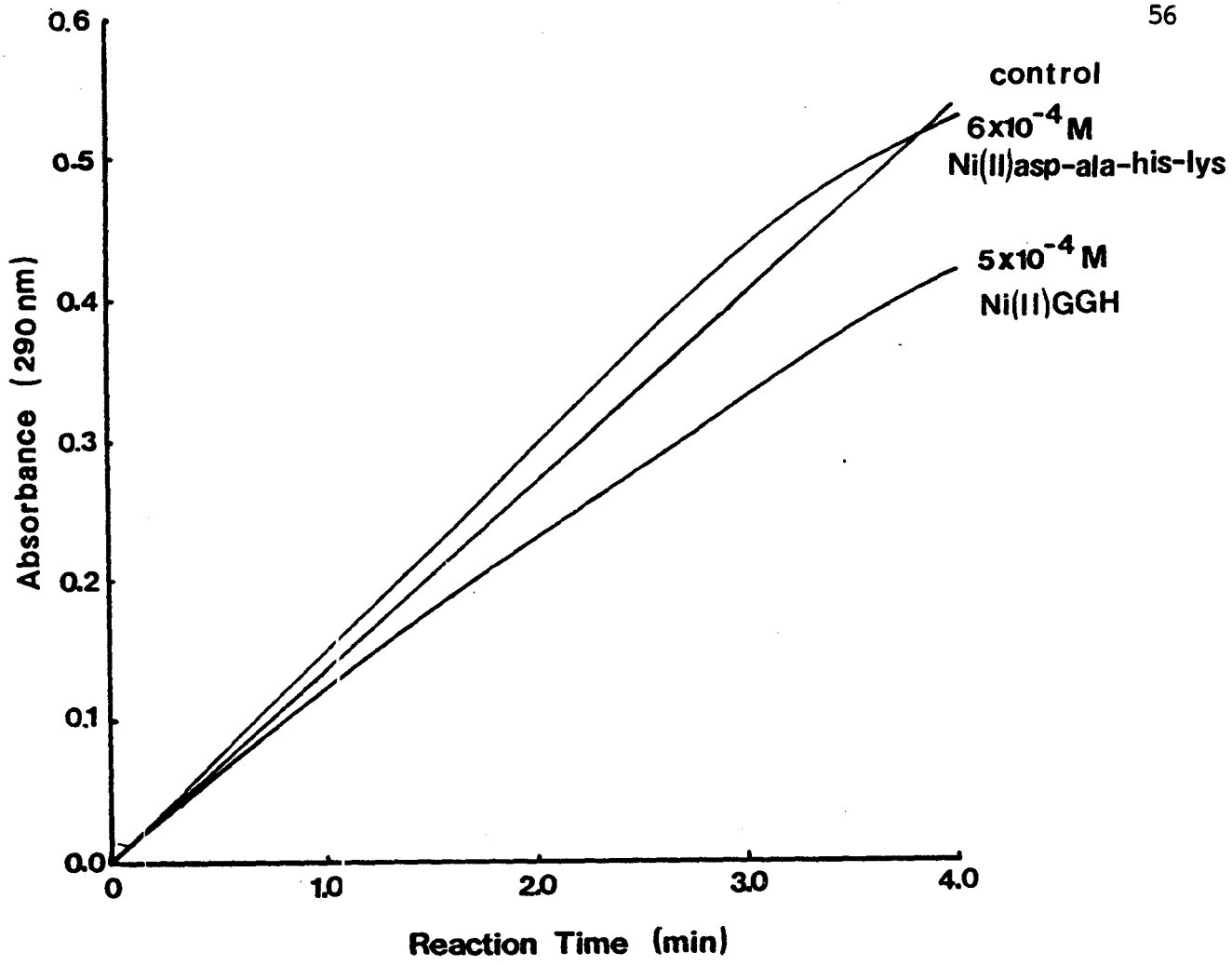

Figure 3.15: Uric acid production in the xanthine-oxidase system in the presence of Ni(II)GGH and Ni(II)asp-ala-his-lys at concentrations for which nearly 100 % inhibition of cytochrome c reduction was observed (See Figs. 3.12 and 3.14). Control sample contained: 44 μM hypoxanthine, 10^{-7} M xanthine oxidase and 43 μg/mL catalase in 0.1 M KH_2PO_4 (pH=7.4)

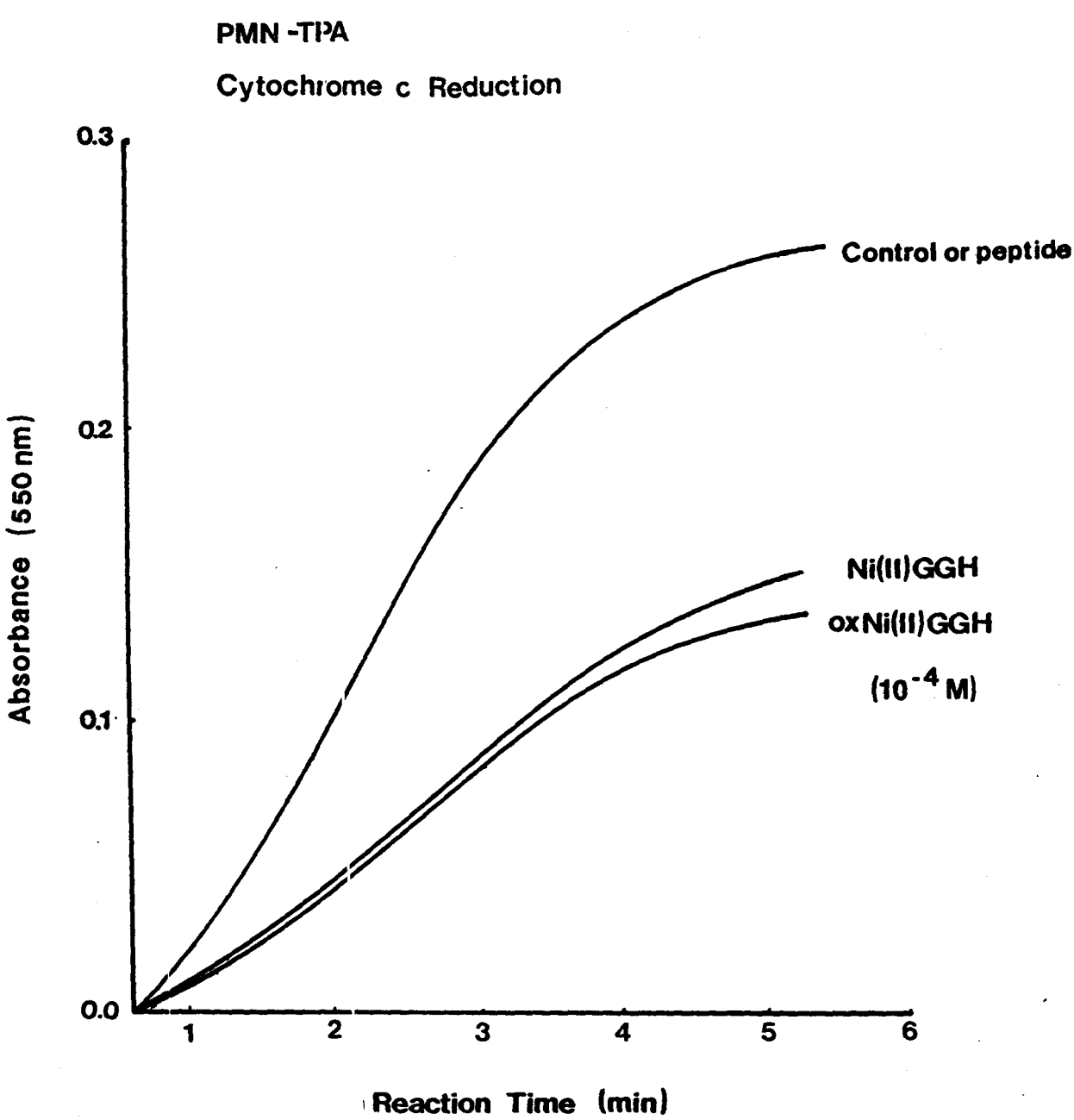

Figure 3.16: Inhibition of ferricytochrome c reduction by freshly prepared and 24-h oxidized Ni(II)GGH in the TPA-induced superoxide anion burst by human PMNs. Reaction mixture contained: 32 μM TPA, 10^6 PMNs/mL and 20 μM cytochrome c in 0.1 M KH_2PO_4 (pH=7.4).

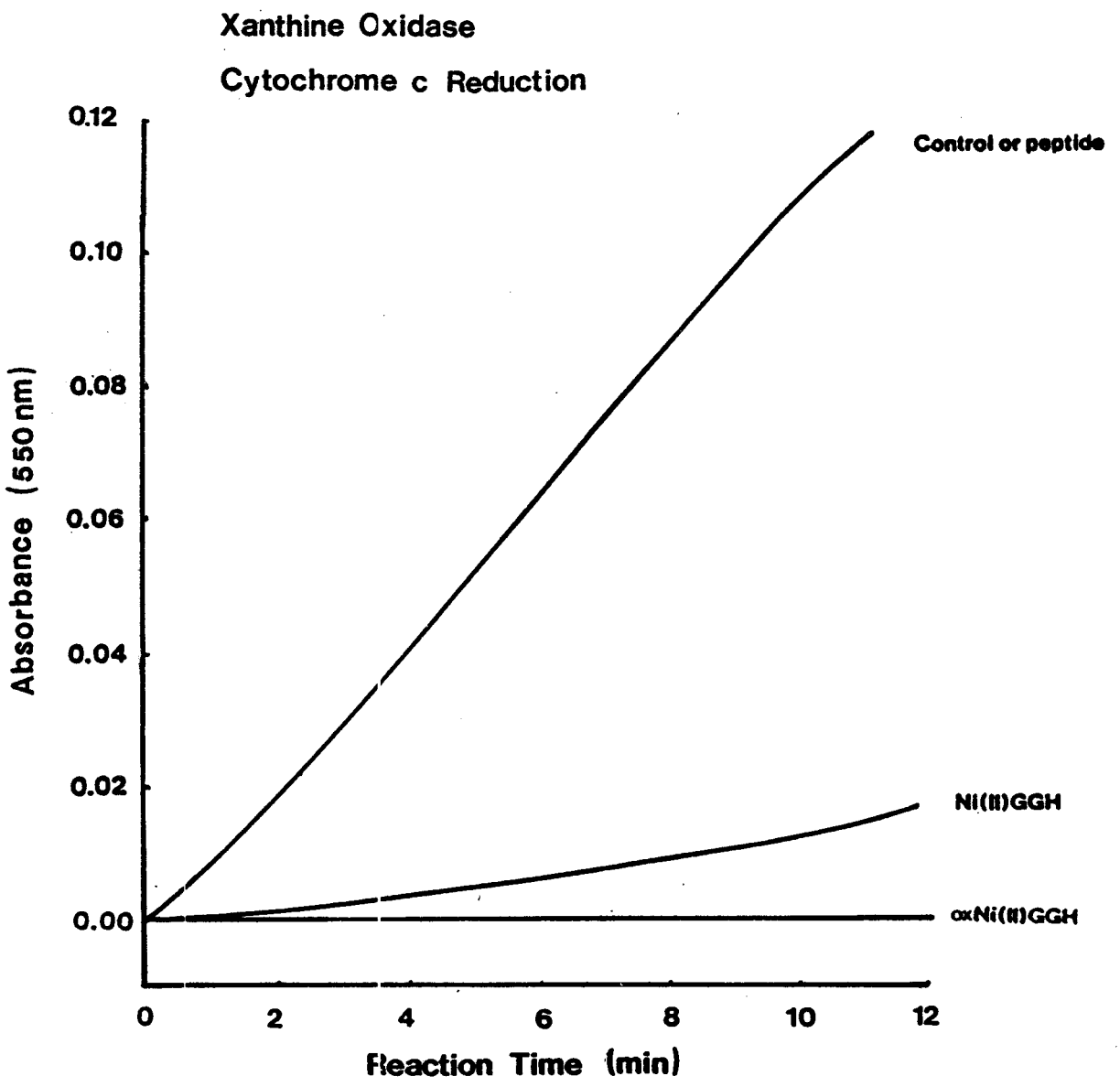

Figure 3.17: Inhibition of cytochrome c reduction in the acetaldehyde/xanthine oxidase superoxide generating system by freshly prepared and 24-h oxidized Ni(II)GGH. All additions were made at 10^{-4} M. Reaction mixture contained: 90 μM acetaldehyde and 0.1 μM xanthine oxidase in 0.1 M KH_2PO_4 (pH=7.4).

Table 3.3: Effect of other Metals in the Presence and Absence of GGH on the Superoxide Anion Flux Generated in the Hypoxanthine/Xanthine Oxidase System.

Additions to Reaction Mixture[a]	Absorbance[b] (550 nm)	% Inhibition[c]
GlyGlyHis	0.176	-----
Zn^{2+}	0.175	0.0 %
Cd^{2+}	0.183	< 0.0 %
Ni^{2+}	0.177	0.0 %
Cu^{2+}	-0.011	> 100 %
Mn^{2+}	-0.021	> 100 %
GlyGlyHis alone[d]	0.180	-----
Zn^{2+} GGH	0.177	0.0 %
Cd^{2+} GGH	0.195	0.0 %
Ni(II)GGH	0.046	74.4 %
Cu(II)GGH	0.088	51.1 %
Mn^{2+} GGH	-0.049	> 100 %

a: Additions of metal or ligand were made at 0.3 μM final concentration to the reaction mixture containing: 30.8 μM hypoxanthine, 0.1 μM xanthine oxidase, and 28.9 μM cytochrome c in 0.1 M HEPES (pH=7.4). Reference samples contained 25 μg/mL SOD.

b: Values represent the average of duplicate runs with a maximum range of ±0.005 in all cases.

c: Inhibition is defined as a decrease in the superoxide-anion flux detected as a diminished degree of cytochrone c reduction assessed relative to GlyGlyHis alone.

d: Metal-ion complexes were prepared prior to their addition to the reaction mixture; all additions made at 0.3 mM; the use of the symbols Zn^{2+}, Cd^{2+} and Mn^{2+} implies that complexes involving the deprotonated amide centers do not form (see text).

ala-his-lys have little effect on the production of uric acid from hypoxanthine at concentration observed to inhibit completely cytochrome c reduction.

The ability of Ni(II)GGH and oxNi(II)GGH to consume superoxide anions was further investigated using alternative sources of these radicals. Both nickel peptides will diminish the flux of superoxide anions generated by the TPA-induced respiratory burst in PMNs by about 50 % (Fig. 3.16). By contrast, inhibition of cytochrome c reduction was almost complete when acetaldehyde was used as the substrate instead of hypoxanthine in the xanthine-oxidase assay (Fig. 3.17).

The effect of other first-row transition metals on the superoxide anion flux in the presence and absence of GGH is shown in Table 3.3. Cu^{2+} and Mn^{2+} alone but not Zn^{2+}, Cd^{2+}, or Ni^{2+} can catalyze the dismutation of superoxide anions (to hydrogen peroxide and presumably molecular oxygen as well) as shown by the negative absorbance values which indicate oxidation of partially reduced cytochrome c in the sample. The effect of Zn^{2+}, Cd^{2+} or Mn^{2+} on cytochrome c reduction was not significantly different in the presence of GGH. Nickel displays the expected inhibitory effect, whereas the copper ion's inherent superoxide dismutase activity was diminished in the presence of the tripeptide.

3.3.2. Generation of Hydrogen Peroxide.

Hydrogen Peroxide production can be monitored since o-dianisidine forms a chromophoric product in the presence of horse radish peroxidase (HRP; Eqn. 3.5)

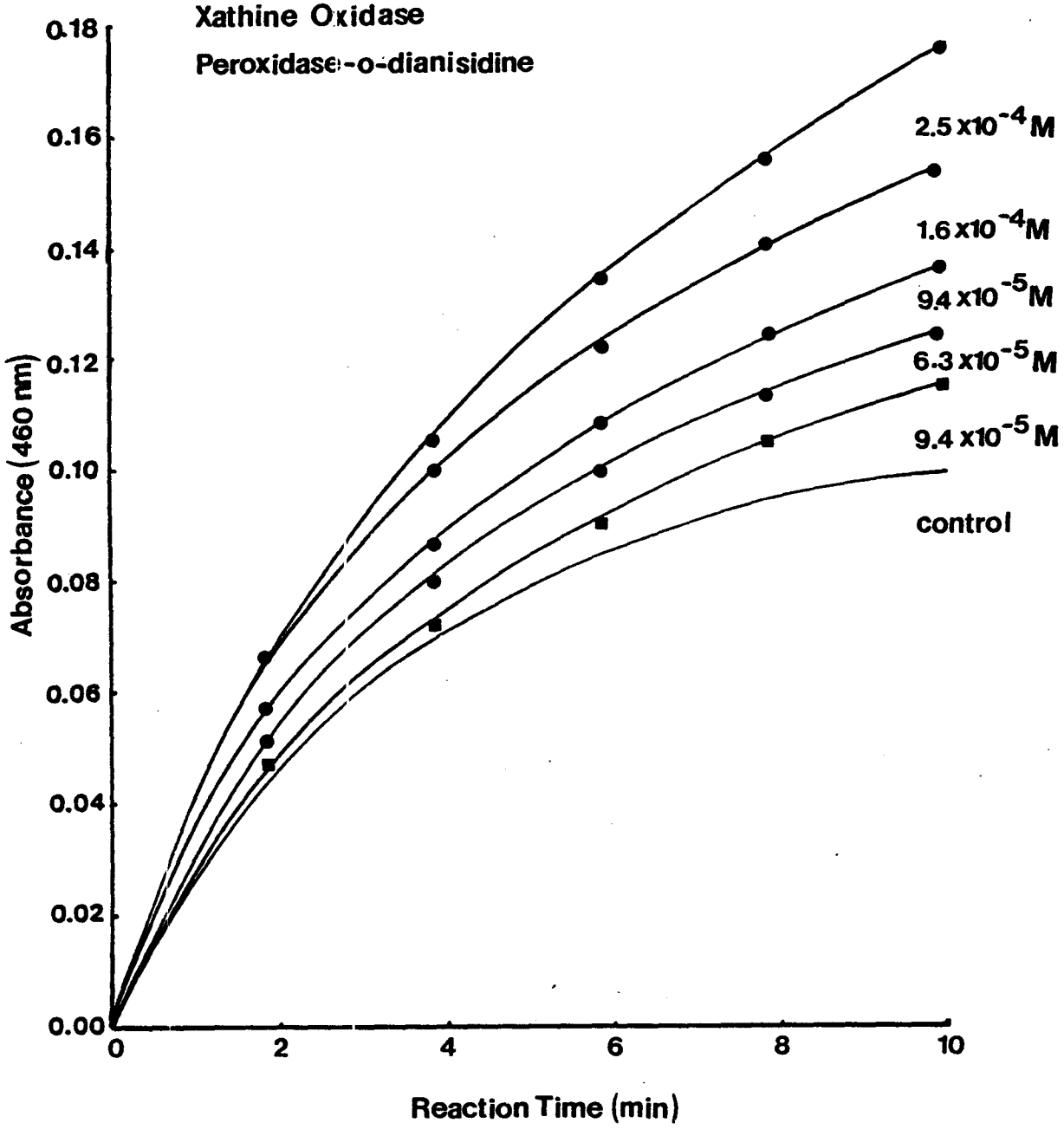

Figure 3.18: Dose-dependent oxidation of o-dianisidine with varying concentration of Ni(II)GGH in the hypoxanthine/xanthine oxidase system. Reaction mixture consisted of: 37.5 µM hypoxanthine, 45 nM xanthine oxidase, 85 µg/mL horse radish peroxidase, and 0.2 mM o-dianisidine in 0.1 M KH_2PO_4 (pH=7.4). Additions: none (▲—▲), Ni^{2+} only (■—■), or Ni(II)GGH (●—●). 42 µg/mL Catalase was added to all reference samples.

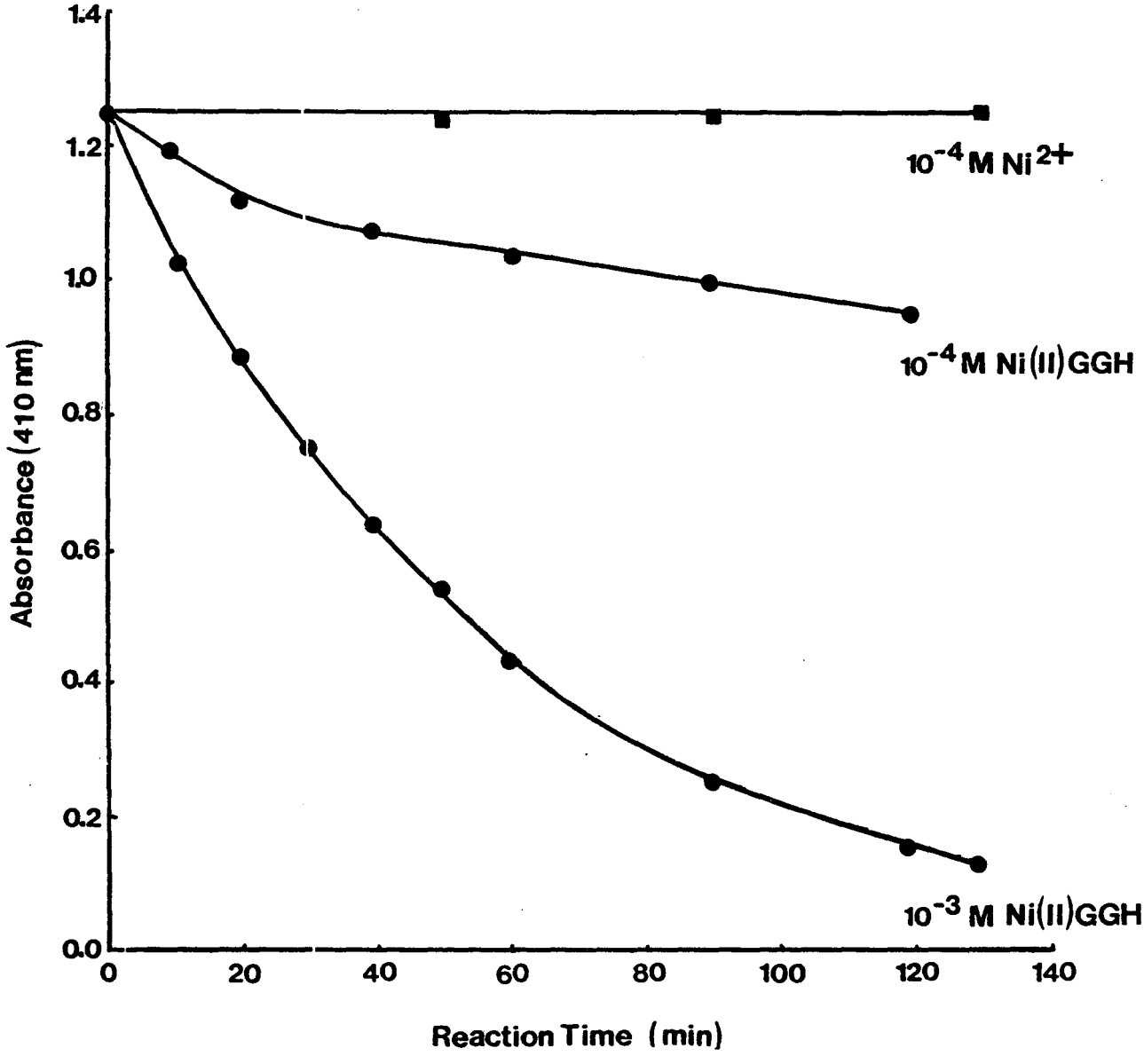

Figure 3.19: Decomposition of H_2O_2 in the presence of Ni(II)GGH. The concentration of H_2O_2 was measured with $TiOSO_4$; samples initially contained 10 mM H_2O_2 and all reactions were performed in 0.1 M KH_2PO_4 (pH=7.4).

$$H_2O_2 + \text{o-dianisidine} \xrightarrow{\text{HRP}} \text{chromophoric product } (\lambda \text{ max}=460 \text{ nm}) \quad (3.5)$$

Dose-dependent increase in o-dianisidine oxidation occurs in the presence of Ni(II)GGH during xanthine oxidase catalyzed oxidation of hypoxanthine (Fig. 3.18). Similar results were obtained when acetaldehyde was used as the substrate (data not shown). Higher concentrations of Ni(II)GGH resulted in a nonlinear increase in o-dianisidine oxidation, presumably due to the reaction of increasing hydrogen peroxide product with Ni(II)GGH and H_2O_2 (see below).

3.3. Hydrogen Peroxide Disproportionation Activity of Nickel(III)/(II) Peptide Complexes.

3.3.1. Decomposition of Hydrogen Peroxide.

Ni(II)GGH, but not Ni^{2+} alone, will catalyze the decomposition of hydrogen peroxide as shown in Figure 3.19. $TiOSO_4$-detectable levels of hydrogen peroxide clearly decreases with time and the rate of breakdown is dependent on the concentration of Ni(II)GGH.

3.3.2. Oxygen Production.

Disproportionation of H_2O_2 activity is defined as the production of molecular oxygen concurrent with a decrease in H_2O_2 concentration. Figure 3.20 illustrates that increased oxygen production from H_2O_2 occurs in the presence of Ni(II)GGH. Disproportionation activity can be observed at concentrations as low as 5×10^{-6} M for Ni(II)GGH in the presence of very high concentrations of hydrogen peroxide (eg. 50 mM). Ni(II)GGH is far more active in breaking down H_2O_2 than any of the

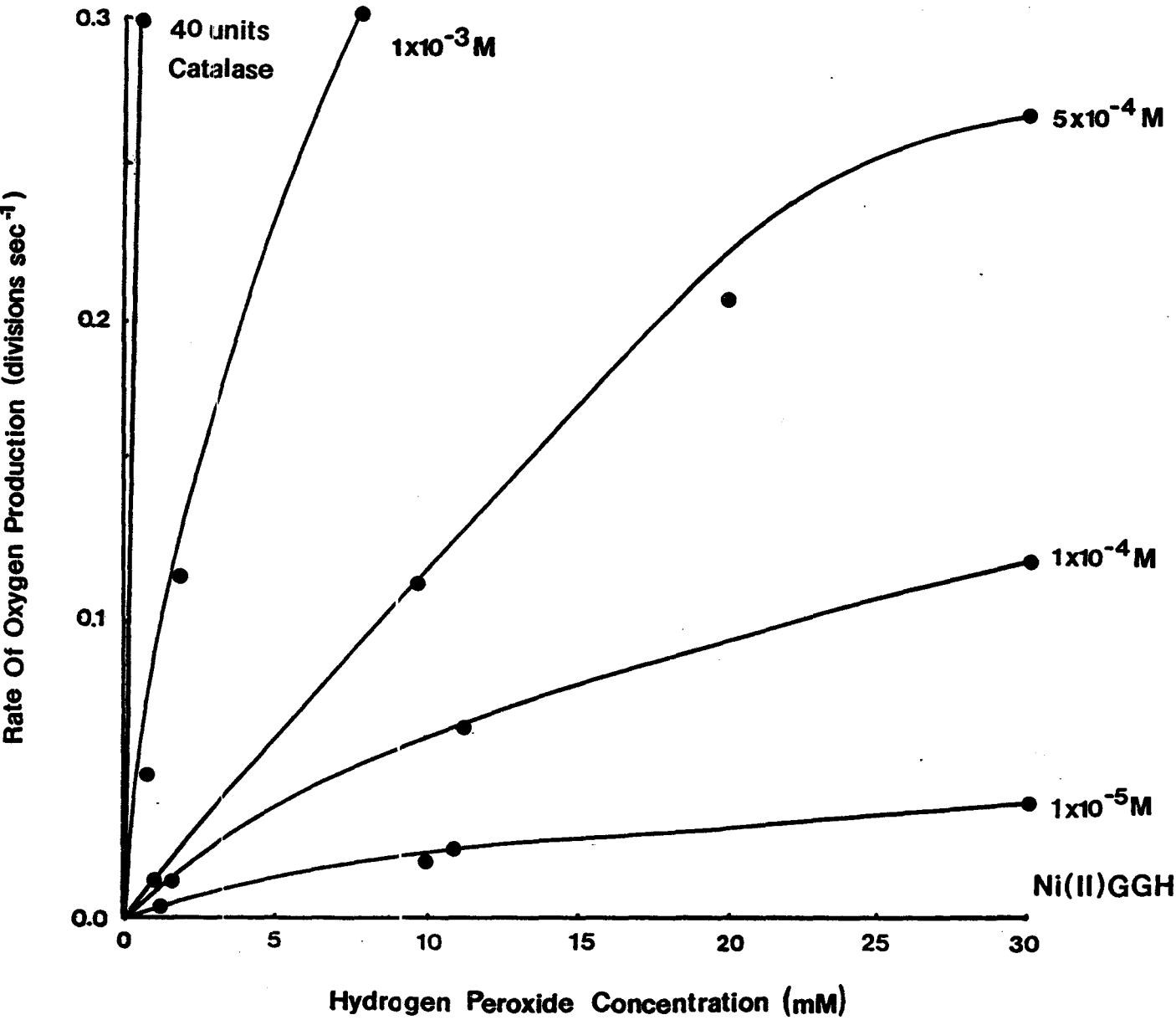

Figure 3.20: Dose-dependent rate of molecular oxygen production with increasing Ni(II)GGH and H_2O_2 concentrations. Additional details are provided in Table 3.4.

Table 3.4: Hydrogen Peroxide Disproportionation Activity of Some Nickel-Peptide Complexes.

Additions to Reaction Mixture[a]	Rate of Oxygen Production (divisions/sec) Hydrogen Peroxide Concentration[d] 10^{-2} M	10^{-3} M	10^{-4} M
1 mM Ni(II)GGH	0.335 ±0.018	0.035 ±0.001	0.026 ±0.005
500 µM Ni(II)GGH	0.110 ±0.001	0.012 ±0.001	0.000 ±0.001
100 µM Ni(II)GGH	0.063 ±0.001	0.013 ±0.001	0.000 ±0.001
10 µM Ni(II)GGH	0.020 ±0.001	0.007 ±0.001	0.000 ±0.000
100 µM GGH (alone)	0.000	0.000	nd
1 mM Ni^{2+} (alone)	0.000	nd	nd
1 mM Ni(III)GGH	0.131 ±0.020	nd	nd
1 mM Cu^{2+}, Mn^{2+}, Cd^{2+}, or Zn^{2+} GGH	0.000	nd	nd
40 units catalase	nd	1.158	0.102
1 mM Ni(II)GGHG	0.142 ±0.008	0.011 ±0.001	0.001 ±0.001
500 µM Ni(II)GGHG	0.081 ±0.003	0.012 ±0.001	0.003 ±0.001
100 µM Ni(II)GGHG	0.016 ±0.002	0.009 ±0.001	0.007 ±0.001
1 mM Ni(II)GGH	0.307	nd	nd
1 mM oxNi(II)GGH[b]	0.125 ±0.006	0.023 ±0.003	0.000 ±0.002
500 µM oxNi(II)GGH	0.055 ±0.055	0.008 ±0.001	0.000 ±0.001
100 µM oxNi(II)GGH	0.022 ±0.010	0.002 ±0.002	0.000 ±0.001
1 mM Ni(II)HGGH	0.315	nd	nd
1 mM Ni(II)asp-ala-his-lys	0.015 ±0.001	0.006 ±0.001	nd
100 µM Ni(II)asp-ala-his-lys	0.000	0.000	nd
1 mM Ni(II)GGH	0.302	nd	nd
100 µM Ni(II)Cysteine	0.023	nd	nd
100 µM Ni(II)GGGa	0.000	nd	nd
100 µM Ni(II)GGG	0.000	0.000	0.000
100 µM Ni(II)Histidine	0.000	nd	nd
100 µM Ni(II)HSA	0.000	nd	nd
100 µM Ni(II)EDTA	0.000	0.000	nd
0.1 M $NaClO_4$ (pH=9.6)	0.012	0.000	nd
1 mM Ni(II)GGG[c]	0.089 ±0.030	0.078 ±0.020	0.039 ±0.009
100 µM Ni(II)GGH[c]	0.861 ±0.149		

a: All experiments were done in 0.1 M KH_2PO_4 (pH=7.4) unless otherwise specified.
b: oxNi(II)GGH is a air-oxidized sample (24 h) of Ni(II)GGH.
c: Reactions were performed in 0.1 M $NaClO_4$, pH=9.6.
d: nd, not determined.
Values are expressed as the mean ± SD of two replicates.

other nickel complexes tested (Table 3.4), but it is obviously not as effective as catalase. The catalytic activity of Ni(II)GGH is more potent when reactions were carried out in 0.1 M $NaClO_4$ (pH=9.6).

3.3.3. Detection of Superoxide Anions.

Both Ni(II)GGH and Ni(II)HSA will catalyze the reduction of NBT^{2+} in the presence of H_2O_2. This reduction does not occur in the absence of the metal (i.e., ligand alone), in the absence of the ligand (i.e., metal alone), and is clearly dependent on the concentration of H_2O_2 present (Fig. 3.21). The spectrum of the initial reduction product of NBT^{2+}, namely NBT^{+} (monoformazan), is shown in Figure 3.22 and is identical to that reported in the literature (Auclair and Voisin, 1985). Thus NBT^{2+} reduction is confirmed. Furthermore, addition of various inhibitors attest to the fact that NBT^{2+} reduction is mediated by superoxide anions (Table 3.5). Specifically, SOD and catalase completely inhibit NBT^{2+} reduction, whereas heat-treated SOD is less effective and mannitol does not. The 15-min heat treatment (in a boiling waterbath) of SOD was later found not adequate for its complete inactivation, and this provides an explanation of the partial inhibition observed.

3.3.4. Hydroxylation of p-Nitrophenol.

Hydroxylation of p-nitrophenol was observed during nickel(II) complex disproportionation of hydrogen peroxide (Fig. 3.23). This reaction is dependent on the concentration of both H_2O_2 and the nickel(II)-complex catalyst concentration (Fig. 3.24). Hydroxylation of p-nitrophenol was observed at levels as low as 10^{-5} M H_2O_2 in the

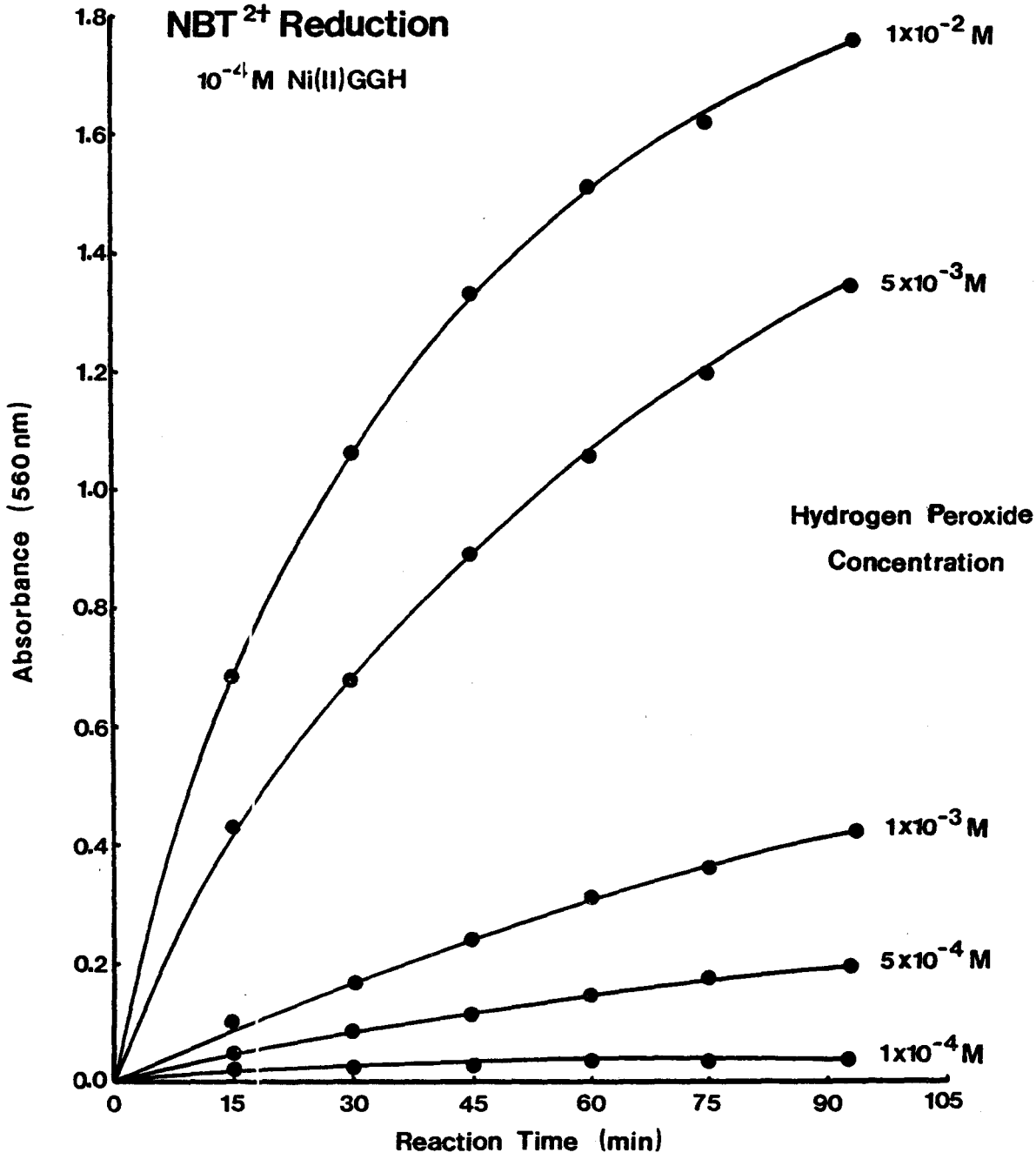

Figure 3.21: Dose-dependent reduction of NBT^{2+} with increasing H_2O_2 concentration in the presence of Ni(II)GGH. The reaction medium consisted of 2 x 10^{-4} M NBT^{2+} and 1 x 10^{-4} M Ni(II)GGH in 0.1 M KH_2PO_4 (pH=7.4).

Table 3.5: Nitroblue Tetrazolium Reduction During Ni(II)GGH-Catalyzed Disproportionation of Hydrogen Peroxide[a]

Additions to Reaction Mixture	Absorbance (560 nm) at time 15 min.	30 min.	45 min.
System 1			
none	0.865		
82 µg/mL Catalase	0.006		
10 mM Mannitol	0.861		
20 mM Mannitol	0.868		
System 2			
none	0.000	0.001	0.001
Ni^{2+} alone	0.006	0.006	0.010
GGH alone	0.010	0.010	0.008
Ni(II)GGH	0.678	1.057	1.327
Ni(II)GGHG	0.297	0.447	0.610
Ni(II)asp-ala-his-lys	0.022	0.037	0.050
oxNi(II)GGH	0.191	0.380	0.537
Ni(II)GGH + 11 µg/mL SOD	0.019	0.019	0.019
Ni(II)GGH + 11 µg/mL heat-treated SOD	0.244	0.528	0.773
HSA	0.016	0.014	0.016
Ni(II)HSA	0.035	0.057	0.074
Ni(II)HSA + 11 µg/mL SOD	0.001	0.000	0.001
Ni(III)GGH	0.209	0.370	0.496
Ni(II)GGHG	0.097	0.229	0.346
Ni(II)asp-ala-his-lys	0.042	0.071	0.083
Ni(III)GGH minus H_2O_2	0.009	0.012	0.012

a: Experimental Details: Reduction of NBT^{2+} is detected as an increase in the absorbance at 560 nm. Reference contains NBT^{2+} only. All additions were made at 1×10^{-4} M unless otherwise specified.

System 1: Reaction mixture contained: 7.8×10^{-5} M NBT^{2+}, 1×10^{-4} M Ni(II)GGH, and 17 mM H_2O_2 in 0.1 M KH_2PO_4 (pH=7.4).

System 2: Reaction mixture mixture contained: 2.0×10^{-4} M NBT^{2+}, 10 mM H_2O_2 in 0.1 M KH_2PO_4 (pH=7.4).

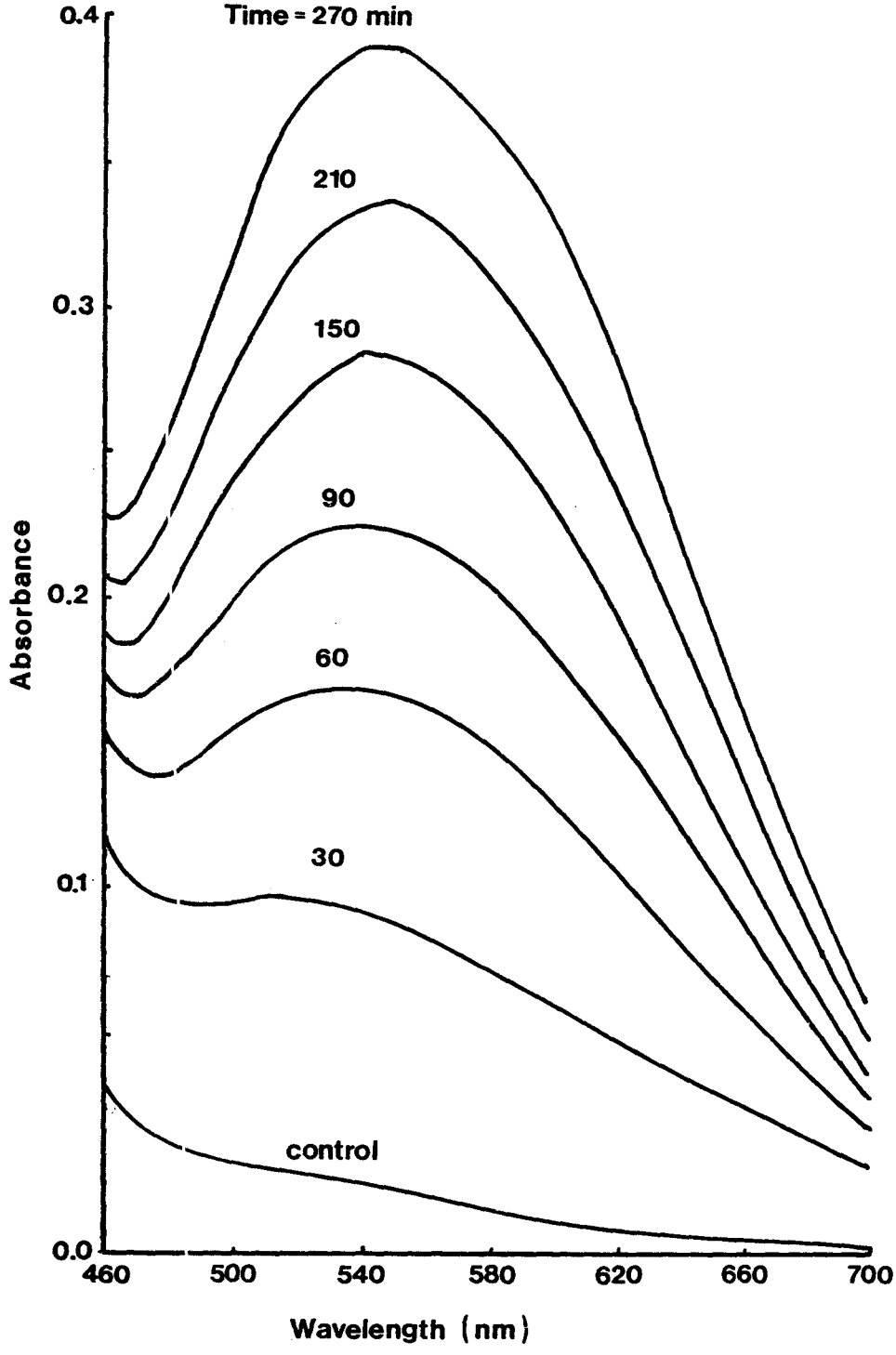

Figure 3.22: Time-dependent reduction of NBT^{2+} in the presence of Ni(II)HSA and H_2O_2. The reaction medium consisted of: 2.0 x 10^{-4} M NBT^{2+}, 1 x 10^{-4} M Ni(II)HSA and 10 mM H_2O_2 in 0.1 M KH_2PO_4 (pH=7.4).

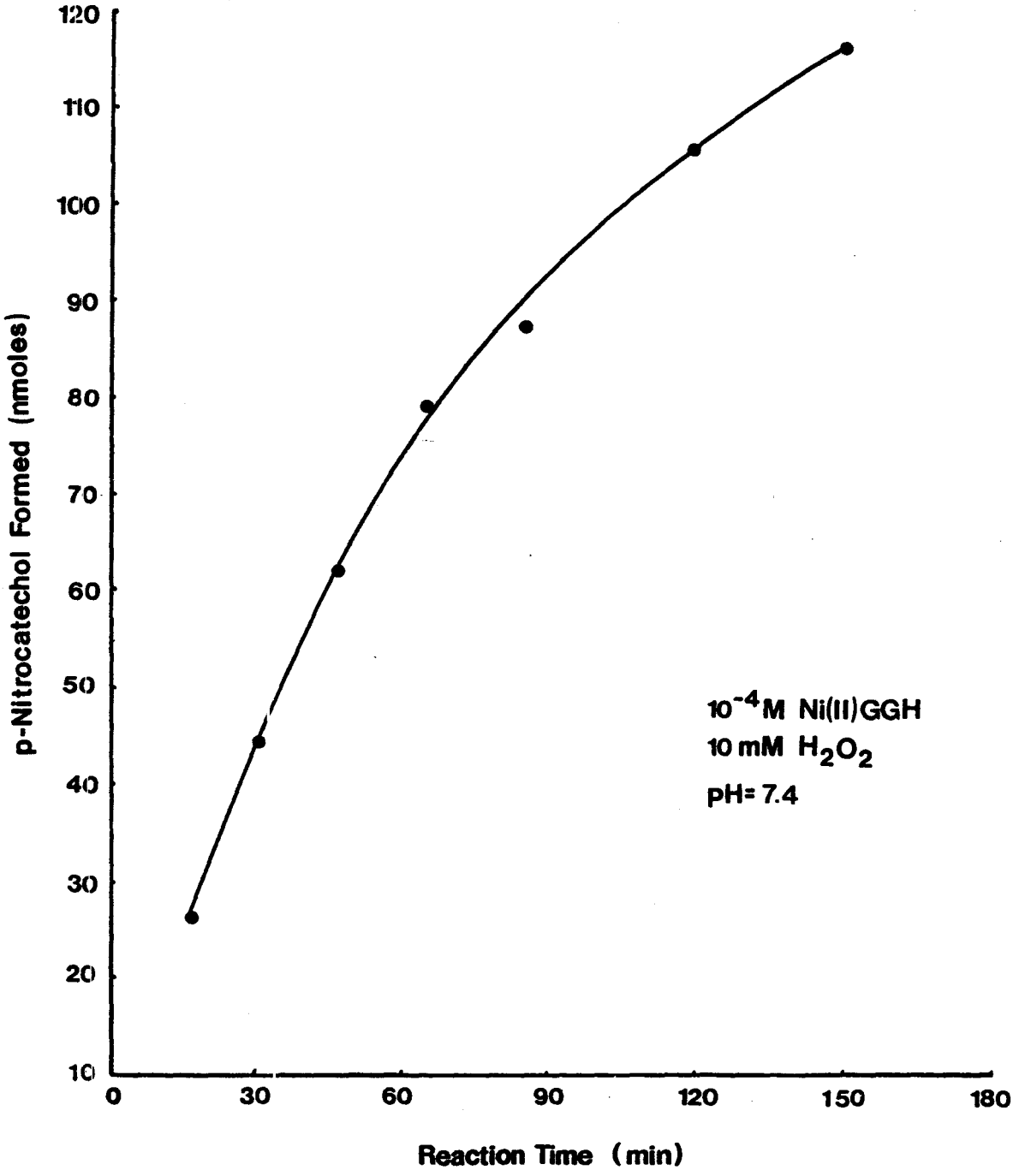

Figure 3.23: Hydroxylation of p-nitrophenol during Ni(II)GGH-catalyzed disproportionation of H_2O_2. The reaction mixture consisted of 1.5 mM p-nitrophenol in 0.1 M KH_2PO_4 (pH=7.4).

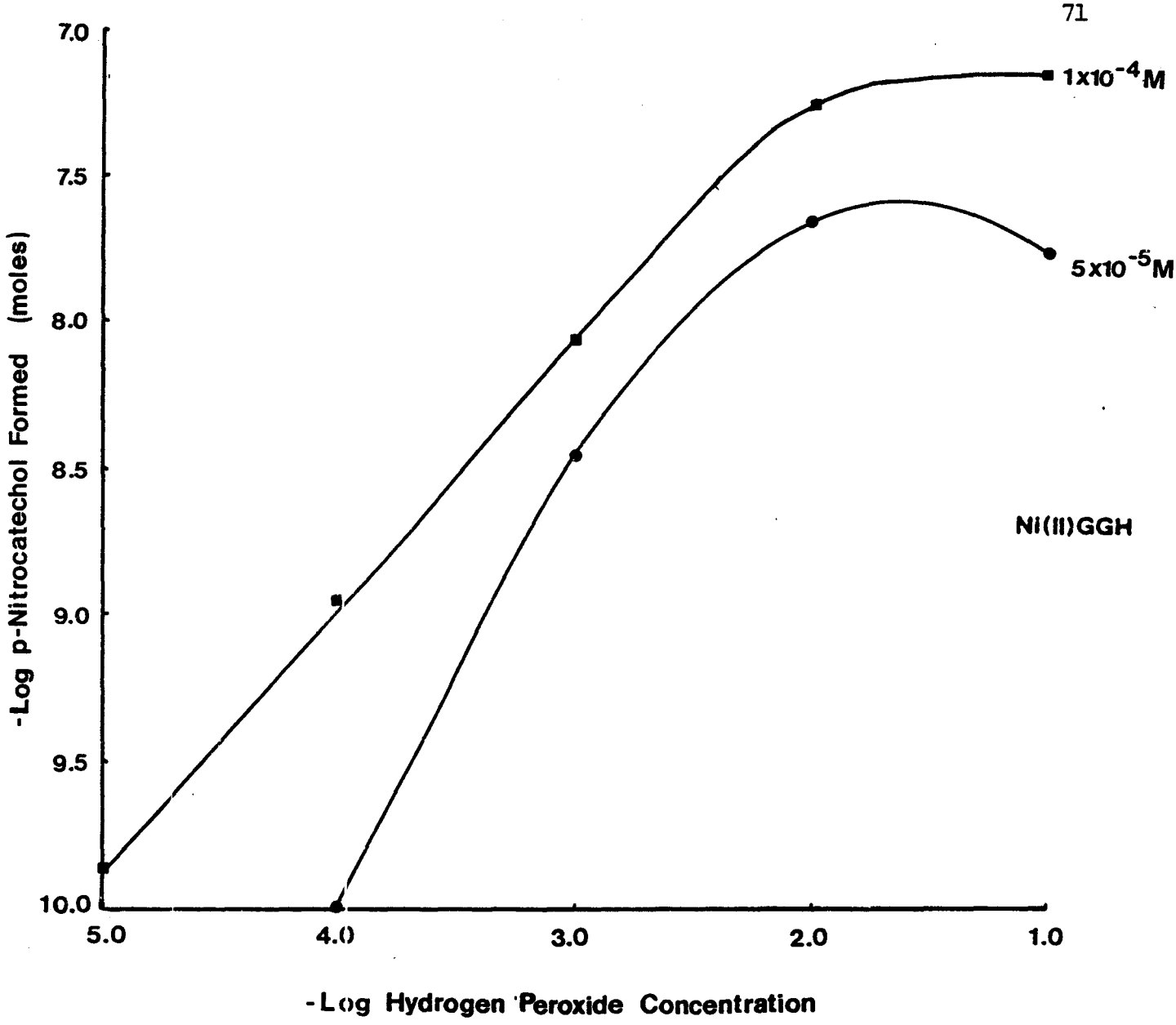

Figure 3.24: Effect of different concentrations of H_2O_2 and Ni(II)GGH on the yield of p-nitrocatechol. The reaction mixture consisted of: 1.5 mM p-nitrophenol and was carried out in 0.1 M KH_2PO_4 (pH=7.4).

presence of 10^{-4} M nickel(II)GGH. The other nickel complexes listed in Table 3.6 can catalyze this reaction as well, but the rates are much slower. Fe^{2+}/EDTA hydroxylation of p-nitrophenol is well characterized (Florence et al., 1985) and was used as the positive control in this experiment. It is clear that nickel(II)-peptide complexes are not as effective as this positive control.

Although both catalysts yield hydroxylation products with similar UV/VIS spectra (data not shown), (Fe^{2+}/EDTA)-mediated hydroxylation is significantly inhibited by mannitol (Florence et al., 1985), whereas this scavenger clearly has no inhibitory effect on the nickel(II)-peptide catalysts. Similarly, SOD does not have any suppressing effect, whereas catalase totally inhibits the reaction, again establishing hydrogen peroxide dependence. Although the yield of p-nitrocatechol was greater in the presence of SOD, the data in Table 3.6 indicate that this superoxide anion scavenger itself does not catalyze the hydroxylation of p-nitrophenol.

A quantitative assessment of the various species during Ni(II)GGH catalyzed disproportionation of H_2O_2 is shown in Figure 3.25. Calculations based on molar absorptivities, suggests that NBT^{2+} reduction and p-nitrocatechol formation occurs at an approximate 1:1 ratio; whereas the quantity of hydrogen peroxide decomposed is ten fold higher. It was not possible to quantify the release of molecular oxygen in this reaction since the solution concentration to which the electrode responds fails to take into account the O_2 lost into the ambient air.

Table 3.6: Hydroxylation of p-nitrophenol during Ni(II)-Oligopeptide Complex Catalyzed Disproportionation of Hydrogen Peroxide.

Additions to Reaction Mixture[a]	Quantity of p-nitrocatechol Formed (moles x 10^8)[b]
no addition	0.06
Ni^{2+}	0.06
GGH	0.07
8 µg/mL SOD	0.00
Heat-Treated (8 µg/mL) SOD	0.00
Ni(II)GGH	2.47
8 µg/mL SOD	2.57
Heat-Treated (8 µg/mL) SOD	2.47
0.3 µg/mL Catalase	0.07
0.03 M Mannitol	2.05
0.11 M Mannitol	2.68
0.39 M Mannitol	2.56
Ni(II)asp-ala-his-lys	0.09
Ni(II)GGHG	1.56
Air-Oxidized Ni(II)GGH (oxNi(II)GGH)	1.53
Fe^{2+}/EDTA	2.93

a: Initial reaction mixture contained: 1.5 mM p-nitrophenol, 10 mM hydrogen peroxide in 0.1 M KH_2PO_4 (pH=7.4); all additions were made at 1 x 10^{-4} M unless otherwise specified; reaction time was 30 minutes and the reaction was initiated by the addition of H_2O_2.

b: Values represent the average of triplicate experiments with a maximum range of $\pm$0.01 in all cases.

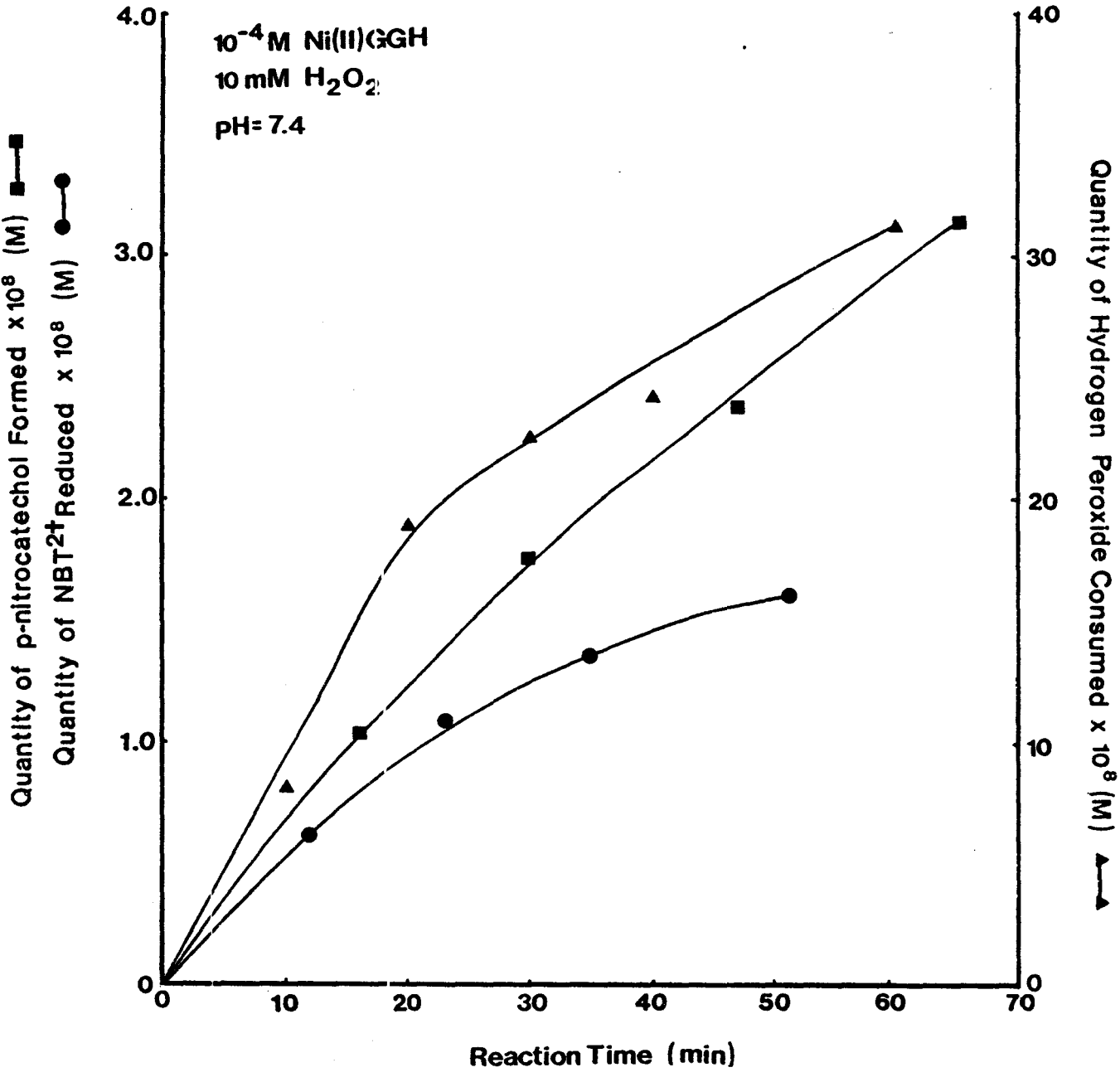

Figure 3.25: Quantitative summary of the various species formed during Ni(II)GGH-catalyzed disproportionation of H_2O_2 (c.f. Figs. 3.19, 3.22 and 3.23).

3.4. Nickel(II)-Peptide Catalyzed Degradation of Biomolecules.

3.4.1. Degradation of Uric Acid.

The formation of uric acid during xanthine oxidase catalyzed oxidation of hypoxanthine can be directly observed by following the absorbance at 292 nm. In the presence of Ni(II)GGH or oxNi(II)GGH, the decrease in absorbance following the conclusion of hypoxanthine oxidation suggests that uric acid degradation is occurring (Fig. 3.26), and this reaction is inhibited in the presence of catalase or SOD (data not shown). The nickel(II)-peptide complexes do not appear to inhibit the enzyme since the completion of uric acid formation, requires approximately the same time-span in both the control samples and in the presence of the nickel(II) complexes. By contrast, oxNi(II)GGH clearly inhibited the enzyme by about 50 % such that the absorbance at 292 nm continues to increase for an additional 3 min.

The ability of various nickel(II) complexes to catalyze the degradation of uric acid (in the presence of H_2O_2) is summarized in Figure 3.27. The reactivity sequence in Equation 3.6 is supported by this data. The glycine peptides did not catalyze this reaction at pH=7.4, but did so at pH values near 11.0 (Eqn. 3.7). Presumably, this indicates that the metal complex does not form in appreciable amount unless alkaline conditions exist. In all cases, uric acid was in 250 % excess of the nickel complex and 100 % destruction of the molecule was eventually observed.

$$\text{Ni(II)GGH} > \text{Ni(II)GGHG} > \text{Ni(II)asp-ala-his-lys} \quad \text{at pH=7.4} \qquad (3.6)$$

$$\text{Ni(II)GGGG} > \text{Ni(II)GGGa} > \text{Ni(II)GGG} \quad \text{at pH=11.0} \qquad (3.7)$$

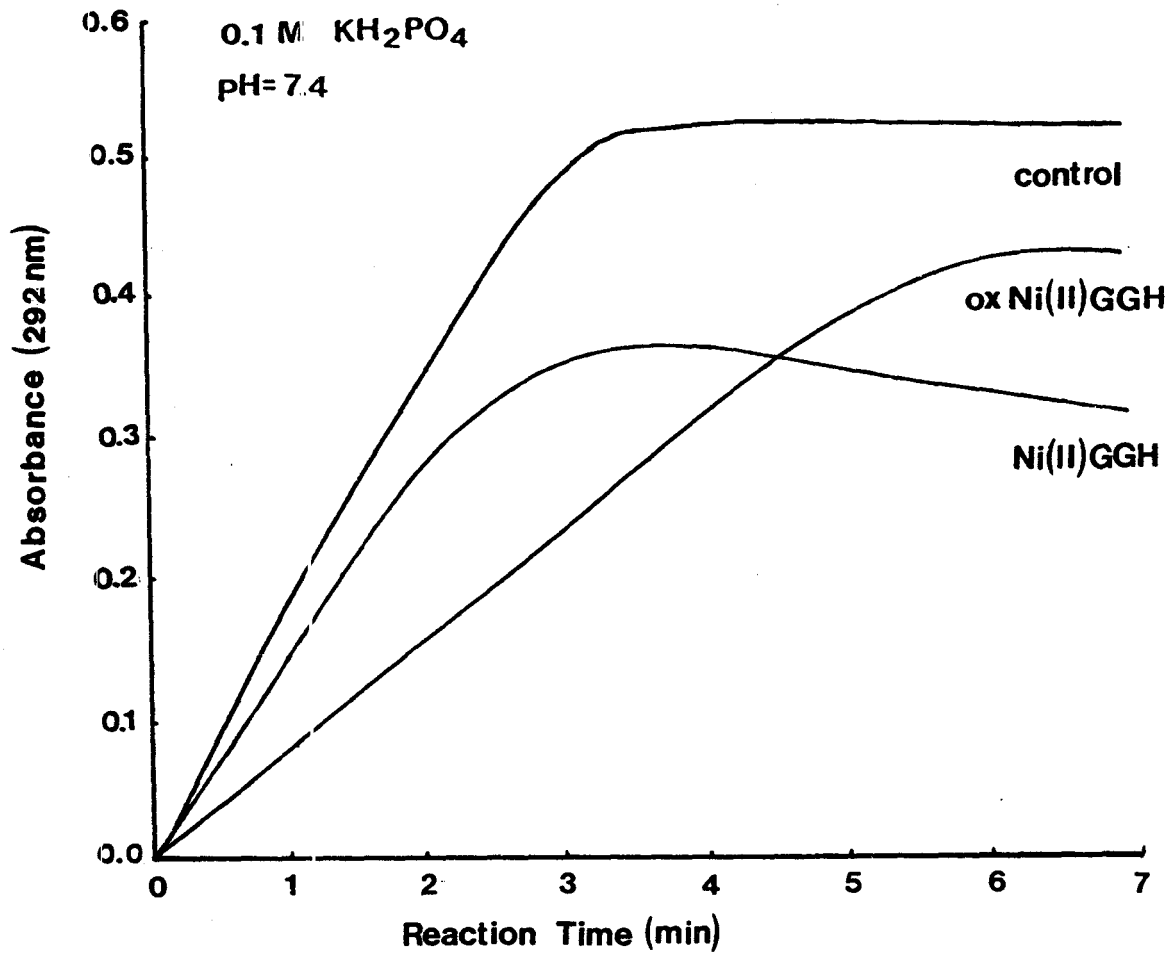

Figure 3.26: Effect of Ni(II)GGH and oxNi(II)GGH on uric acid production during xanthine oxidase catalyzed oxidation of hypoxanthine. Reaction mixture contained: 0.25 μM hypoxanthine, 10^{-7} M xanthine oxidase in 0.1 M KH_2PO_4 (pH=7.4).

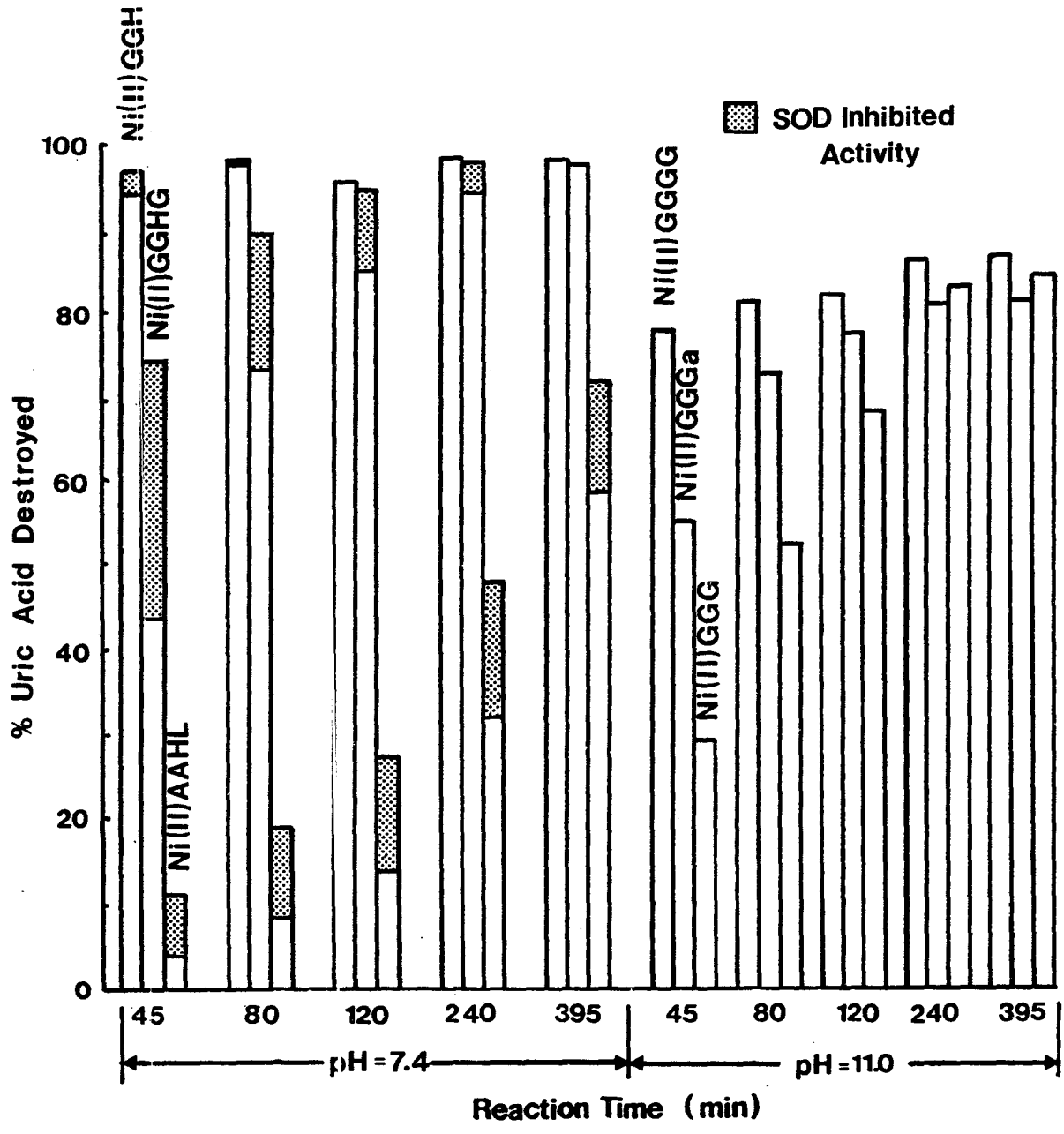

Figure 3.27: Degradation of uric acid catalyzed by various nickel(II)-peptide complexes in the presence of H_2O_2. Reactions were carried out in triplicate and were initiated by adding H_2O_2 (0.02 M) to samples containing 10^{-4} M nickel(II) complex and 0.27 mM uric acid in 0.1 M KH_2PO_4 (pH=7.4). 20 µg/mL SOD was added to corresponding samples to quantify its inhibitory effect.

Table 3.7: The Ability of Ni(II) Complexes to Catalyze the Degradation of Uric Acid.

Additions to Reaction Mixture[a]	% Uric Acid Destroyed after 60 minutes[b]
Ni(II)GGH	93.7 %
Ni(II)GGHG	88.2 %
Ni(II)asp-ala-his-lys	54.6 %
Ni(II)EDTA	0.0 %
Ni(II)Cysteine	0.0 %
Ni(II)Histidine	0.0 %
Ni(II)HSA[c]	0.0 %
Ni(II)Penicillamine[d]	0.0 %
Ni(II)Glutathione[d]	0.0 %
Cu(II)GGH[d]	0.0 %
Fe^{2+}/EDTA	0.0 %

a: The reaction mixture contained: 0.26 mM uric acid, 0.1 M hydrogen peroxide, in 0.1 M KH_2PO_4 (pH=7.4); all additions were made at 1 x 10^{-4} M, unless otherwise specified.

b: Results are expressed as the mean of duplicate experiments (Maximum SD $\pm$ 0.1 %).

c: 20 mM hydrogen peroxide was used; under these conditions, 96.6 % of the uric acid was destroyed after 45 min in the presence of Ni(II)GGH.

d: 10 mM hydrogen peroxide was used; under these conditions, 85.5 % of the uric acid was destroyed after 60 min in the presence of Ni(II)GGH.

Table 3.8: The Effect of Various Inhibitors on the Rate of Uric Acid Destruction Catalyzed by Ni(II)GGH in the Presence of Hydrogen Peroxide.

Additions to Reaction Mixture[a]	% Uric Acid Destroyed After 60 Minutes[b]
none	73.8 %
0.1 mM HSA	72.8 %
38.3 µg/mL SOD	16.2 %
27.2 µg/mL Catalase	2.2 %
18.0 mM Mannitol	73.0 %
73.0 mM Mannitol	71.7 %
1.0 mM Imidazole	73.1 %
43.0 mM Imidazole	64.1 %
76.0 mM Imidazole	53.8 %
1.0 mM $(NH_4)_2HPO_4$	66.5 %

a: The reaction mixture consisted of: 0.25 mM uric acid, 10 mM hydrogen peroxide, 0.1 mM Ni(II)GGH in 0.1 M KH_2PO_4 (pH=7.4)

b: The results are expressed as the mean of three replicates. The SD did not exceed $\pm$ 0.1 %.

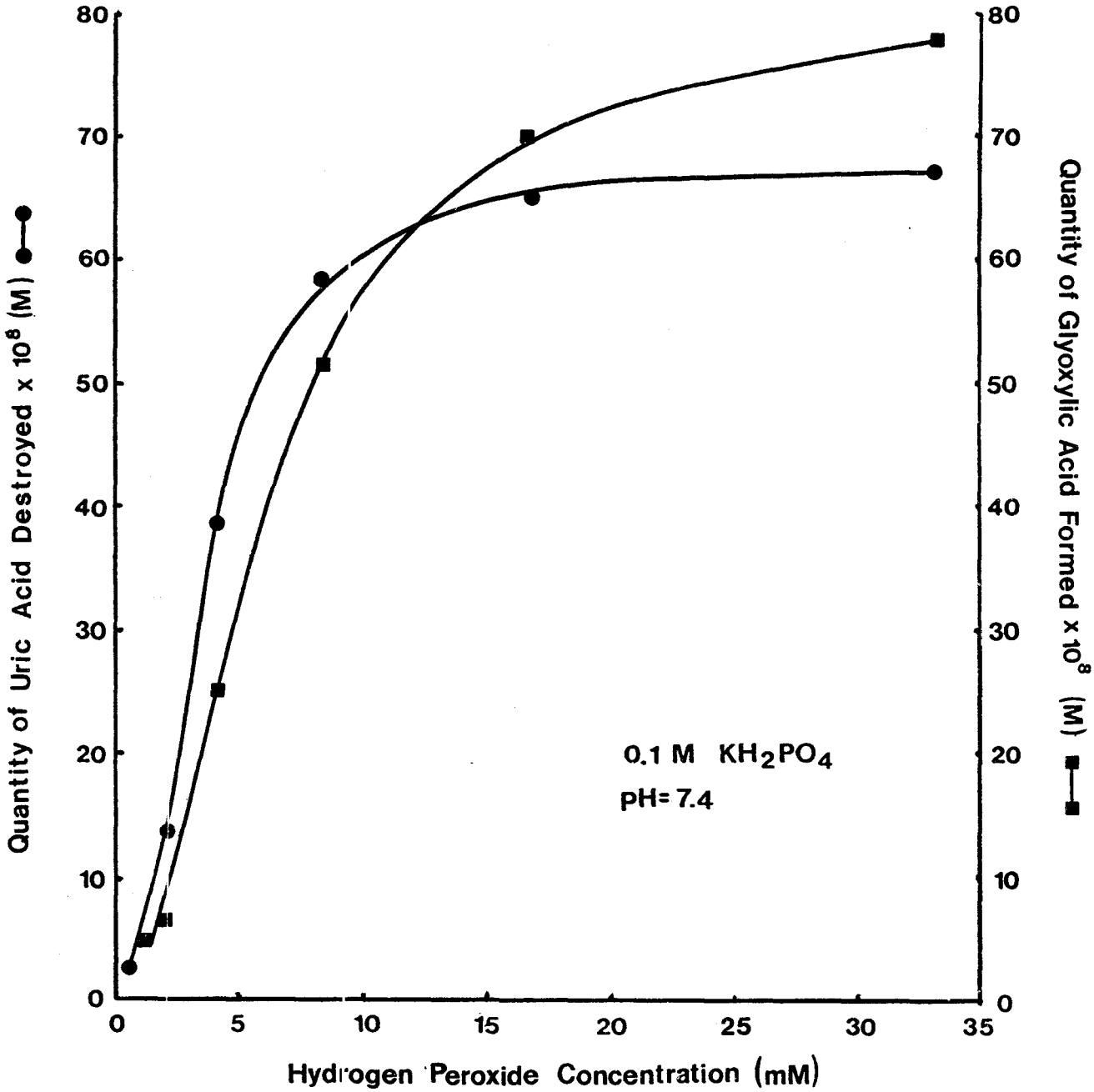

Figure 3.28: Mass balance (amount of uric acid consumed and glyoxylic acid produced) during H_2O_2-dependent Ni(II)GGH-catalyzed destruction of uric acid.

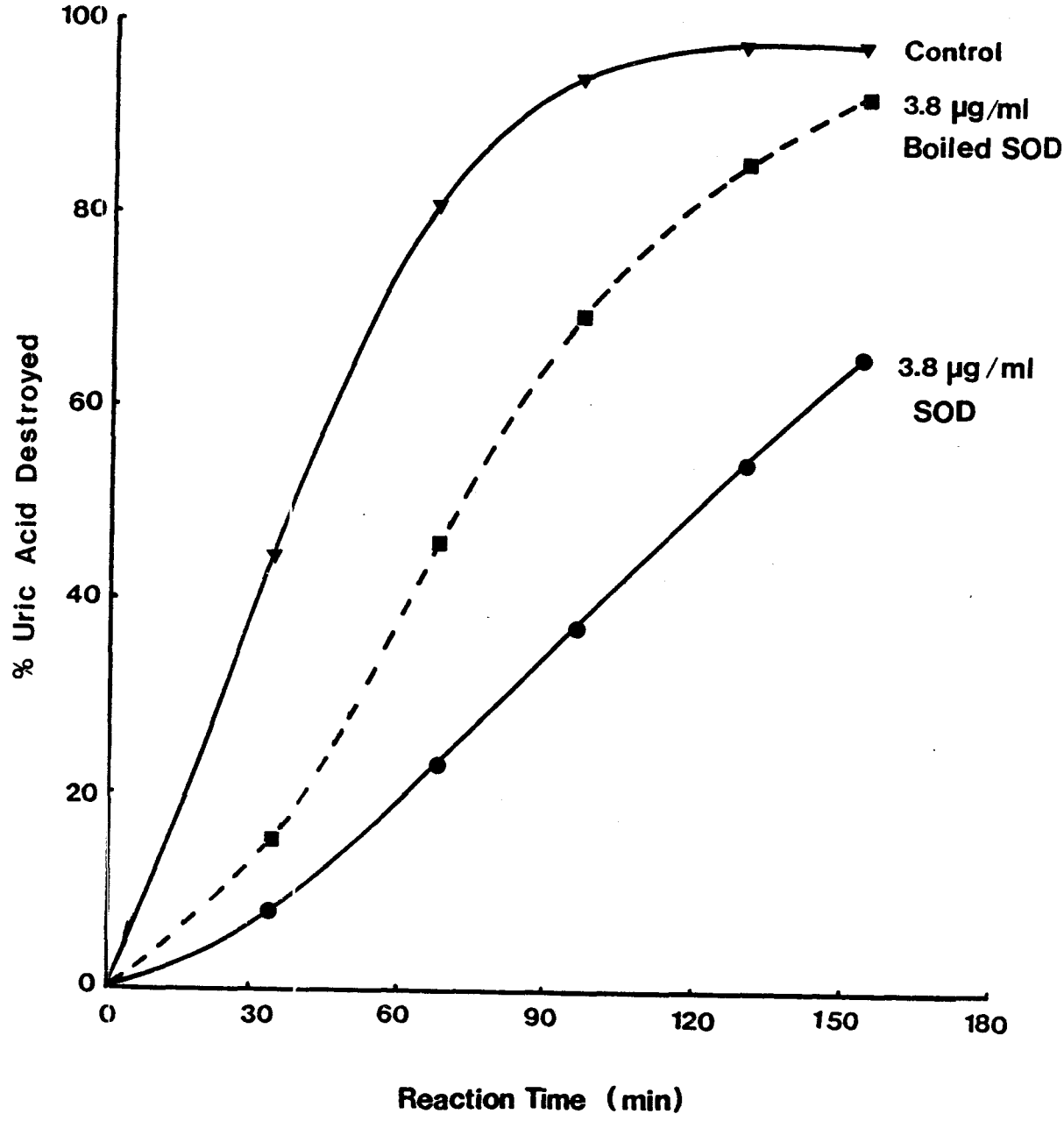

Figure 3.29: Effect of heat-treated and untreated SOD on the Ni(II)GGH-catalyzed destruction of uric acid. Reaction mixture consisted of: 30 mM H_2O_2, 10^{-4} M Ni(II)GGH and 0.26 mM uric acid in 0.1 M KH_2PO_4 (pH=7.4). Heat-treatment involved placement (of SOD) in a boiling water bath for 10 min.

Copper bound to GGH or Fe^{2+}/EDTA in the presence of H_2O_2 did not display this catalytic activity.

The amount of uric acid consumed was directly correlated with the quantity of glyoxylic acid formed (Fig. 3.28). The effect of various inhibitors on this reaction is summarized in Table 3.8. SOD alone inhibited the rate of uric acid destruction by about 65 % and inhibition by heat-treated SOD (boiled for 10 min) was reduced to 30 % (Fig. 3.29). Inhibition by catalase is virtually complete, and dose-dependent inhibition was observed at high concentrations of $(NH_4)_2HPO_4$ or imidazole. By contrast mannitol, like HSA, had no effect (Table 3.8) even at high concentrations (73 mM).

3.4.2. Formation of a Thiobarbituric Acid Reactive Substance from 2-Deoxy-D-Ribose.

Well-characterized hydroxyl radical generating catalysts such as Fe^{2+}/EDTA and Cu^{2+}/1,10-phenanthroline catalyze a "TBA detectable damage to 2-deoxy-D-ribose". This reaction is far more effective in the presence of hydrogen peroxide. As shown in Table 3.9, nickel complexed to any of the histidine-containing peptides, but neither the hydrated Ni^{2+} ion nor the peptides themselves, displays this catalytic activity. This reaction yields products with the same UV/VIS spectral characteristics observed in the Fe^{2+}/EDTA-catalyzed reaction (data not shown). The formation of the TBA chromogen catalyzed by the nickel complexes is inhibited by the presence of SOD, catalase, and high concentrations of glutathione, but not when the hydroxyl radical scavengers, mannitol or urea was added.

Table 3.9: Measurement of Thiobarbituric Acid Detectable Damage to Deoxyribose in the Presence of Hydrogen Peroxide and Various Nickel Complexes and the Effect of Oxygen Radical Scavengers.

Additions to Reaction Mixture[a]	Absorbance (535 nm)[b]	Absorbance Relative to Control
0.4 mM $FeSO_4$	0.430 ±0.006	> 100 %
0.4 mM $FeSO_4$ (minus H_2O_2)	0.279 ±0.006	> 100 %
Cu^{2+}-1-10 phen/1.9 mM Glut	0.455 ±0.011	> 100 %
Ni(II)GGH (control)	0.178 ±0.003	100 %
1.9 mM Glutathione	0.157 ±0.005	88.2 %
3.8 mM Glutathione	0.139 ±0.003	78.1 %
16 µg/mL SOD	0.088 ±0.003	49.6 %
140 µg/mL Catalase	0.032 ±0.001	17.4 %
0.14 M Urea	0.166 ±0.007	93.2 %
30 mM Mannitol	0.524 ±0.003	> 100 %
60 mM Mannitol	0.519 ±0.004	> 100 %
H_2O_2 (alone)	0.001 ±0.001	0.0 %
GGH (alone)	0.070 ±0.001	39.3 %
Ni^{2+} (alone)	0.083 ±0.002	46.6 %
2.0 mM Glutathione	0.000 ±0.001	0.0 %
Ni(II)GGHG	0.139 ±0.003	78.1 %
Ni(II)asp-ala-his-lys	0.106 ±0.001	59.6 %

a: The reaction mixture contained: 0.9 mM deoxyribose, 70 mM KCl and 50 mM H_2O_2 in 0.1 M KH_2PO_4 (pH=7.4); all additions made at 1 x 10^{-4} M unless otherwise specified.

b: The absorbance is expressed as the mean ±SD of three replicates.

3.5. Chemiluminescence in the Presence of Nickel(II) Peptide Complexes and Superoxide Anions.

Chemiluminescence was observed during xanthine oxidase oxidation of hypoxanthine only in the presence of Ni(II)GGH or Ni(II)GGHG (Fig. 3.30). Of the various scavengers added, only SOD reduced this chemiluminescence to background levels (Table 3.10). Direct mixing of H_2O_2 and Ni(II)GGH or Ni(II)GGHG yielded a powerful burst of chemiluminescence that was again diminished in the presence of SOD.

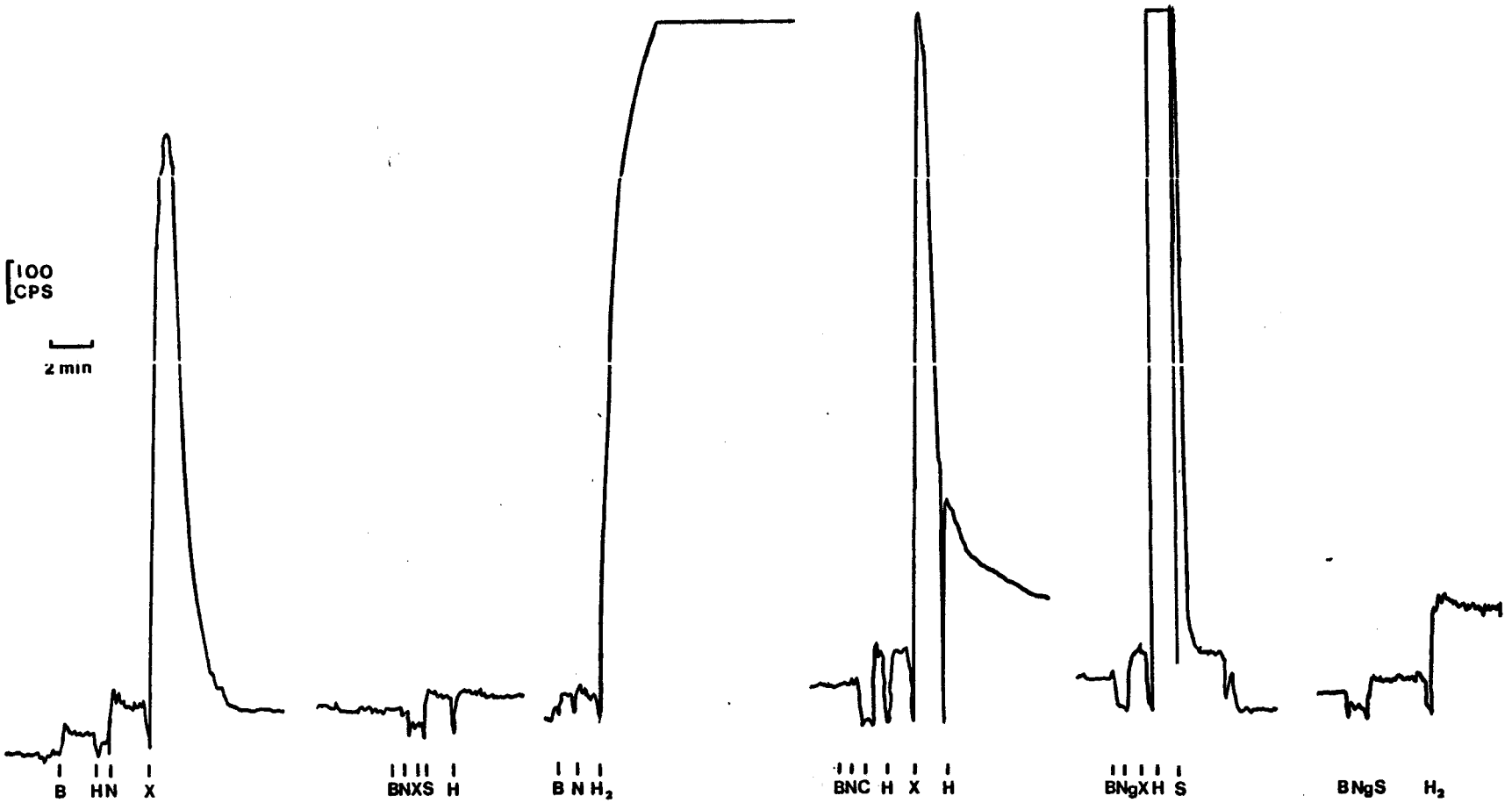

Figure 3.30: Chemiluminescence in the presence of Ni(II)GGH or Ni(II)GGHG and superoxide anions. Reactions were initiated by the addition in the order given of 53 μM hypoxanthine (H), 0.1 μM xanthine oxidase (X) or 50 mM hydrogen peroxide (H_2) to samples containing 2.5 x 10^{-4} M Ni(II)GGH (N) or Ni(II)GGHG (N_g) in 0.1 M KH_2PO_4 (B) with a total volume of 2 mL. The effect of 0.1 mg/mL catalase (C) and 12 μg/mL SOD (S) is also shown.

Table 3.10: Chemiluminescent Activity of Ni(II)-Peptide Complexes in the Superoxide-Anion Generating System.

Additions to Reaction Mixture	Corrected counts per second[a]
System 1[b]	1400
minus Ni(II)GGH	60
minus hypoxanthine	118
plus 12 µg/mL SOD	78
plus 0.1 mg/mL Catalase	1598
plus 0.2 mg/mL Catalase	1508
plus 23 mM 2,5 Dimethylfuran	1056
plus 50 mM Hydrogen Peroxide	40,000
System 2[c]	22,000
5×10^{-5} M Ni(II)GGHG	11,362
plus 23 mM 2,5 Dimethylfuran	24,800
System 3[d]	920
plus 12 µg/mL SOD	310

a: Corrected counts per second (CPS) is the CPS observed minus the background. Data represents single measurement, although the relative responses were reproducible from experiment to experiment.
b: The complete system consisted of: 0.53 mM hypoxanthine, 0.1 µM xanthine oxidase and 2.5×10^{-4} M Ni(II)GGH in 0.1 M KH_2PO_4 (pH=7.4); background counts for the buffer alone were 40 CPS.
c: Same as in b but Ni(II)GGHG was present instead; background counts for the buffer alone were 110 CPS.
d: 50 mM H_2O_2 was added to 5×10^{-5} M Ni(II)GGH in 0.1 M KH_2PO_4 (pH=7.4).

4: DISCUSSION:

4.1. Characterization and Properties of the Nickel(III) and Nickel(II) Peptide Complexes Studied:

4.1.1. UV/VIS Spectra.

Histidine-containing nickel(II)-peptide complexes used in this study and prepared under physiological conditions (of 0.1 M KH_2PO_4 or 0.1 M HEPES, pH=7.4) displayed UV/VIS spectral properties identical to those reported by other investigators using much more alkaline conditions (for example, at pH=11, Bryce et al., 1966; and at pH=8.2, Bossu and Margerum, 1977). A change in the UV/VIS absorption spectrum from the low intensity absorption band of the Ni(II) complexes (near 420 nm) to two intense charge-transfer bands centered at 340 nm and at 245 nm accompanies electrochemical oxidation (Bossu and Margerum, 1977; Subak et al., 1985). Although Bryce et al. (1966) reported seeing a second absorption shoulder centered between 450 nm and 480 nm for Ni(II)GGH, such a peak was not observed in this study. Bulk electrolysis is not 100 % efficient and hence the quantity of Ni(III) present must be assessed before molar absorptivities can be calculated. Using this approach, Bossu and Margerum (1977) and Kirvan and Margerum (1985) determined that characteristic absorption maxima extend anywhere between 325 to 355 nm with ranging from 4,000 and 6000 M^{-1} cm^{-1} for a series of electrochemically generated nickel(III)-peptide complexes.

Under the conditions used in the present study, although the immediate products of electrochemical oxidation are nickel(III) as judged by EPR evidence and the formation of a brown product, the exact

number of oxidizing equivalents (ie. Ni(III)) were not determined. Hence, the molar absorptivities given in Table 3.1 are really only a qualitative indication of the approximate yield and stability of the Ni(III) complex at the time of measurement. For Ni(III)GGGa, a molar absorptivity of 1000 ± 130 M^{-1} cm^{-1} at 315 nm was obtained which is only 20 % of the value reported by Bossu and Margerum (1977) under similar conditions (c.f., 5360 ± 150 M^{-1} cm^{-1} at 325 nm).

Similar comparisons cannot be made for the Ni(III)-histidine-containing oligopeptides because the UV/VIS spectral properties have not been reported. However, the Ni(III)/(II) redox potentials of the histidine containing peptide complexes are higher than of the other peptide complexes (Section 4.1.3.), suggesting that the nickel(II) complex is favoured. Hence, the efficiency of conversion and the corresponding molar absorptivities (as defined above), might be expected to be lower (Buttafava et al., 1986).

It is not clear at this point whether the decomposition of Ni(III) complexes involves reversion to the original nickel(II) complex, or rearrangement to form novel products. Although both pathways are presumed to occur, the latter appears to be favoured as judged by the persistence of the brown colour, and by previous reports demonstrating that the autoxidation of other nickel(II)-oligopeptide complexes resulted in the formation of novel products via a nickel(III) intermediate (Paniago et al., 1971; Bossu et al., 1978).

4.1.2. Air Oxidation of Ni(II)GGH.

Air-oxidized Ni(II)GGH, oxNi(II)GGH, is further characterized by a novel second intense absorption peak at 305 nm. To our knowledge, this

band has not been reported in the literature, although it has been observed by Dr. Margerum and his colleagues (private communication). Its intensity is buffer and pH-dependent and it will not form under anaerobic conditions (data not shown). The origin of this absorption peak is not known with certainty. Unpublished work, drawn from Dr. Margerum's laboratory, indicates that immediately after the formation of the "Ni(II)(H_{-2}(GGH))$^{-}$" complex (10^{-3} M) in 4.97 x 10^{-3} M borate buffer (pH=6.5) the complex undergoes an autoxidative reaction such that in the presence of 1.9-fold excess of Ni(II)GGH over dissolved molecular oxygen, there is complete oxygen consumption with a stoichiometric release of carbon dioxide. This reaction was shown to conclude after 2 to 3 hours, and the characteristic peak at 305 nm began to develop in an autocatalytic fashion (Gray and Margerum, unpublished data). During the initial phase of the autoxidative process, an oxidizing agent was shown to be present which was most abundant during the greatest rate of O_2 uptake and was no longer detectable when the peak at 305 nm had fully formed (t ~ 24 h). In a subsequent study using Ni(II)GGGG, similar reactions were observed and the oxidizing power was attributed to the presence of a nickel(III) intermediate (Bossu et al., 1978). Although it is suspected that the autoxidation of Ni(II)GGH occurs via a similar intermediate, there is no direct evidence as spectral changes attributable to Ni(III) are not observed. Support for the role of Ni(III) is provided in the present study. Specifically, it was found that the 2- to 3-h induction time required before initial evidence of the 305 nm peak was eliminated by first generating the Ni(III)GGH by electrochemical oxidation.

Immediately after electrolysis, spectral changes were apparent in the 305 nm range at a rate of 0.017 abs units/min (for a 10^{-3} M sample; Fig. 3.3).

Based on these results, a mechanism for the formation of the 305 nm peak may be proposed. It is postulated that molecular oxygen binds to the nickel complex facilitating the formation of the superoxide anion radical:

$$Ni(II)GGH\text{-}O_2 \rightleftharpoons Ni(III)GGH\text{-}O_2^- \qquad (4.1)$$

Thus an electron is transferred from the nickel center to the oxygen molecule resulting in the formation of a transient $Ni(III)\text{-}O_2^-$ species The activated O_2 and/or the tervalent nickel itself has the potential to oxidize the peptide, perhaps forming a ligand radical which then decarboxylates to yield CO_2. Subsequently, there is then some kind of peptide modification that yields the brownish-yellow complex characterized by the absorbance maximum at 305 nm.

It is clear that the final product that absorbs at 305 nm is not a Ni(III) complex since the oxidizing power is clearly absent at this point. EPR signals were not detectable during any stage of the autoxidation process; although it is possible that the absolute concentration of Ni(III) may have been beyond the detection limit of the EPR instrument (which is 10^{-6}-10^{-7} M; Willard et al., 1974). Furthermore, the complex with the "fully formed" 305 nm peak can be broken up by acidification (to pH=2). Upon readjustment to the original pH, this peak was observed again (data not shown). This suggests ligand modification, as Ni(III) would not be stable as the free ion in the

acidified solution. In macrocyclic systems where nickel-catalyzed activation of molecular oxygen has been observed, similar intermediates to those shown in Equation 4.1 have also been proposed (Kimura et al., 1981). These macrocyclic complexes have low redox potentials (-0.24 V versus SCE), are easily oxidized and the intermediates are able to catalyze the hydroxylation of benzene (Kimura et al., 1982; Kimura and Machida, 1984). Attempts to hydroxylate benzene during the autoxidative process using Ni(II)GGH were not successful (Nieboer et al., private communication).

4.1.3. Presence and Reversibility of the Ni(III)/(II) Redox.

Freshly prepared nickel(II) peptide complexes are low spin d^8 species which are EPR silent. Definitive evidence for the presence of the high spin (nickel(III)) d^7 species is given by the detection of EPR signals (Bossu and Margerum, 1977; Lappin et al., 1978). Although it is not known what percentage of the nickel complexes are oxidized (by electrochemical oxidation), Figures 3.5-3.8 confirm that nickel(III) is present and the position of the $g_{//}$ peak in the 2800-2900 G region indicates that it is the metal that is oxidized, and not the ligand itself (Barefield and Mocella, 1975; Bossu and Margerum, 1976; Lappin et al., 1978). If ligand oxidation had occurred, the paramagnetic product would be a nitrogen- or carbon-centered radical, and such species would have peaks in the 3200 G region. In other words, the complex would be rewritten as Ni(II)$\dot{G}$GH and the $g_{//}$ and $g_{\perp}$ peaks would be very close to each other (Lappin et al., 1978; Brodovitch et al., 1980).

Like the nickel(II)-macrocyclic polyamine complexes, the

nickel(II) oligopeptide complexes have strong in-plane donors which tend to stabilize the tervalent state of nickel relative to the solvated cation itself or to complexes with non-macrocyclic ligands (for example, nickel(II)histidine; Zeigerson et al., 1979; Bencini et al., 1981; Buttafava et al., 1986). The strength of the various equatorial donors has been shown to increase in the order N^-(peptide) ~ N^-(amide) > $-NH_2$ > imidazole ~ CO_2^- and this results in a corresponding increase in the equitorial g ($g_\perp$) value (Subak et al., 1985). A change from a truly square-planar complex to a tetragonally distorted octahedral geometry accompanies electrochemical oxidation of the nickel(II) oligopeptides. Specifically, Lappin et al. (1978) defined the tetragonally distorted octahedral complexes of nickel as those which give signals with $g_\perp$ greater than (i.e., to the left of) $g_{//}$ (c.f., Figs. 3.5-3.8). Based on molecular orbital considerations, the observed multiplicity is consistent with the residence of the free electron in the d_z^2 orbital or which may be thought of as pointing along the axial-plane of the nickel(III) complex (Subak et al., 1985). If the oxidized products were square planar, $g_\perp$ would be located to the low field side of $g_{//}$, and this is not observed. The tetragonally-distorted geometry is the most common for nickel(III) complexes (Sugiura and Mino, 1979), and this allows the use of the shape of the signals at $g_{//}$ to identify the axially coordinating species.

The EPR spectrum for Ni(III)GGH in 0.1 M KH_2PO_4 (pH=7.4, Fig. 3.5) suggests that two different nickel complexes are present. The data support the interpretation that a major species with axially coordinating oxygen donor atoms (^{16}O, I=0, singlet at $g_{//}$) coexists

with a minor species that contains one axially coordinating nitrogen donor atom (^{14}N, I=1, triplet at $g_{//}$). Presumably, water molecules occupy the axial coordination sites in the former case, and an attachment of a second GGH ligand (ie. Ni(II)-$(GGH)_2$) likely occurred in the latter case (Lappin et al., 1978; Sugiura and Mino, 1979; Kirvan and Margerum; 1985). Preparation of Ni(III)GGH in 0.1 M $NaClO_4$ at progressively decreasing pH values results in a corresponding decrease in the minor species, such that at pH=6.5 only the major species (observed in phosphate buffer) exists (Fig. 3.8). That is, at pH=6.5 the excess GGH present (~ 10 %) is protonated, effectively inhibiting its axial coordination to the Ni(III)GGH complex.

Both asp-ala-his-lys and GGHG can also stabilize the tervalent nickel in 0.1 M KH_2PO_4 at pH=7.4 (Fig. 3.6 and 3.7). However, in contrast to Ni(II)GGH, the axially coordinating atom is provided by the ligand itself. For asp-ala-his-lys, information based on NMR data suggests that the carboxylate oxygen from the side chain of aspartic acid appears to axially coordinate in the nickel(II) complex (Laussac and Sarkar, 1984). The corresponding Ni(III) species appears to maintain this structure, resulting in a singlet at $g_{//}$. For GGHG , the triplet at $g_{//}$ suggests that a nitrogen donor atom is coordinated at one of the axial positions. The exact nature of the nitrogen donor atom is unknown but likely involves either the deprotonated amide function between histidine and the carboxy-terminal glycine residues or the nitrogen of the imidazole ring of histidine (Dr. Margerum, personal communication).

The reversibility of the change in oxidation state can be assessed using cyclic voltammetry. A linear relationship between $E_{cathode}$-

E_{anode}) as a function of the square root of the scan rate suggests that a metal complex has reversible redox properties (Willard et al., 1974). For Ni(II)GGH in phosphate buffer (0.1 M, pH=7.0 or 7.7), this criterion is fulfilled as shown in Figure 3.10. By contrast to controlled-potential electrochemical oxidation in which the generated Ni(III) complexes decompose to form new Ni(II) products, the immediate reduction of the freshly-formed Ni(III) intermediate to the starting nickel(II) complex occurs in cyclic voltammetry. That is, upon forming the Ni(III) species, it is quickly reduced back to Ni(II) before any geometric rearrangement (e.g., square-planar arrangement to a tetragonally-distorted octahedral) and the accompanying acid base equilibration is allowed to reach completion (Bossu and Margerum, 1977).

The reversible electrochemical behaviour allows the midpoint between the oxidation and reduction peaks to be a reasonable estimate of the Ni(III)/(II)-peptide redox couple. The redox potential of the nickel-histidine containing oligopeptides prepared under the conditions used in this study were all around 0.732 V (versus SCE), which are values similar (maximum deviation ± 8 mV) to those reported by Bossu and Margerum (1977) at pH=8.2. The redox potentials for the other Ni(II) tri- and higher order peptides that lack histidine are slightly lower (e.g., 0.50-0.66 V versus SCE; Bossu and Margerum, 1977); however strong alkaline conditions (e.g., pH=9.6) are required as the nickel will not complex to the oligopeptides at pH values near 7.4.

4.2. Superoxide Dismutase Activity of Nickel(II)-Peptide Complexes.

4.2.1. The SOD assay: Background.

Nickel(II)-peptide complex scavenging of superoxide radical anions was determined by its inhibition of cytochrome c reduction (Eqn 4.2). But a correction(s) has to be made for this reagent's sensitivity to other oxidizing and reducing agents (for example, H_2O_2 and ß-

$$\text{Ferricytochrome c} + O_2^- \longrightarrow \text{Ferrocytochrome c} + O_2 \qquad (4.2)$$

mercaptoethanol; Forman and Boveris, 1982). The addition of SOD (an enzyme that efficiently removes O_2^-) to the reference sample assures that any further reduction in the sample (without SOD) is mediated by O_2^-. Hence the reduction of cytochrome c by other reducing agents will occur in both the sample and the reference and reduction of the cytochrome c by the superoxide anion will only be observed in the sample. Catalase was added to both the reference and the sample to remove H_2O_2 which can oxidize cytochrome c causing an under estimation of the O_2^- flux.

The hypoxanthine/xanthine oxidase (HX/XO) and acetaldehyde/xanthine oxidase (ACET/XO) systems are known sources of O_2^- (Eqns. 4.3 and 4.5), H_2O_2 (Eqn. 4.4 and 4.6) and $^{\bullet}OH$ (Halliwell and Gutteridge, 1981; Richmond et al., 1981; Fridovich, 1985a). The predominant species depends on the pO_2, pH and on the substrate concentration. Air-equilibrated solutions produce approximately 15 % O_2^- at pH=7.8 and this value increases to 100 % when the pH is 10.0 and the pO_2 is 1.0 atmosphere (Fridovich, 1985a).

Hypoxanthine (HX) is a "double substrate" for xanthine oxidase

releasing uric acid as the final product, which has an absorbance maximum at 292 nm.

$$HX + 2\,O_2 + H_2O \longrightarrow HXO + 2\,O_2^- + 2\,H^+ \quad (4.3)$$

$$HX + O_2 + H_2O \longrightarrow HXO + H_2O_2 \quad (4.4)$$

$$HXO + 2\,O_2 + H_2O \longrightarrow HXO_2 + 2\,O_2^- + 2\,H+ \quad (4.5)$$

$$HXO + O_2 + H_2O \longrightarrow HXO_2 + H_2O_2 \quad (4.6)$$

The product of reactions 4.5 and 4.6, uric acid (HXO_2) has been shown to be an effective nonspecific, free-radical scavenger (Ames et al., 1981). Consequently, acetaldehyde which is oxidized more slowly by XO was also used as a substrate (Eqn. 4.7 and 4.8).

$$CH_3C(O)H + 2\,O_2 + H_2O \longrightarrow CH_3COO^- + 2\,O_2^- + 3\,H^+ \quad (4.7)$$

$$CH_3C(O)H + O_2 + H_2O \longrightarrow CH_3COO^- + H_2O_2 + H^+ \quad (4.8)$$

4.2.2. Superoxide Dismutase Activity.

Earlier studies with a series of nickel(II) complexes of macrocyclic polyamine derivatives (possessing partial oligopeptide structures), demonstrated reversible redox properties. These complexes were found to inhibit (xanthine/xanthine oxidase)-mediated reduction of nitroblue tetrazolium ion (Kimura et al., 1981, Kimura et al., 1983). This activity appeared more dependent on the substituents attached to these macrocyclic rings than on their individual redox potentials. These complexes involved non-biological ligands and the experiments were done at high pH, thus making it difficult to assess the biological relevance of these reactions.

In the present study, similar SOD-type activity was observed when

three specific histidine-containing oligopeptides and human serum albumin were bound to nickel(II) in aqueous media (e.g., phosphate buffer) at physiological pH values (i.e., 7.4). Inhibition of cytochrome c reduction does not occur in the absence of the ligand and was very dependent on the nickel(II) complex concentration (Figs. 3.12-3.14). The ranking of SOD activity (Eqn. 3.4) shows that Ni(II)GGH is the most active, displaying a two to three-fold greater reactivity than Ni(II)GGHG and Ni(II)asp-ala-his-lys, respectively. Similar trends in reactivity were observed when the same experiments were performed at pH=8.2, suggesting that the difference in reactivity of the nickel(II) complex is not based on the fraction complexed (data not shown). Since all three nickel(II) histidine containing oligopeptide complexes have virtually the same redox potentials (E° ~ 0.73 versus SCE), the basis for the difference in reactivity must be the presence of axially coordinating atoms (ie. substituent effects) on both Ni(II)asp-ala-his-lys and Ni(II)GGHG and not on Ni(II)GGH. The approximate doubling of reactivity for Ni(II)GGH possibly involves both an increase in the potential number of dismutation sites and perhaps some characteristic(s) of the ligand field itself which promotes the dismutation process. Specifically, if the decrease in cytochrome c reduction observed is due to the consumption of O_2^- by the nickel(II) oligopeptide complexes, Ni(II)GGH is square planar with two open axially-symmetrical sites which allows a greater probability of attachment (by O_2^-) and subsequent dismutation. Consistent with this model is the decrease in the catalytic activity observed for Ni(II)asp-ala-his-lys in all reactions, since one of the axial sites is known to

be blocked by an oxygen atom of the carboxylate group extending from the side chain of aspartic acid (Laussac and Sarkar, 1984).

Attempts to demonstrate increased levels of molecular oxygen in the presence of Ni(II)GGH yielded ambivalent results due to the lack of sensitivity of the oxygen electrode, oxygen consumption by the enzyme and the metal complex itself, and the complicated interplay between the various reduced oxygen radical species in the HX/XO system.

The effect of Ni(II)GGH and oxNi(II)GGH on a more biologically relevant source of oxygen radicals was assessed. Human polymorphonuclear leukocytes release a burst of oxygen radicals known as the "Respiratory Burst" when an appropriate stimulus is applied. This results in the release of powerful oxidative species, which when triggered *in vivo* (e.g., after endocytosis) is used to kill offending organisms (DeChatelet *et al.*, 1976; Babior, 1978; Klebanoff, 1980; Weiss and LoBuglio, 1980). A decrease in the superoxide-anion radical flux generated by cells stimulated with phorbol ester (Fig. 3.16) was observed in the presence of both nickel complexes. Attempts to detect an increase in the hydrogen peroxide flux yielded mixed results due to the inherent toxicity of the reagents (o-dianisidine) used and a possible release of catalase from some of these cells.

A decrease in cytochrome c reduction may also be mediated by an inhibition of the enzyme catalyzing the production of superoxide anions (i.e., xanthine oxidase). However, the present study confirms that at the level at which the nickel(II) complexes were shown to almost completely inhibit cytochrome c reduction, minimal inhibition of uric acid production was observed (Fig. 3.15). However, this does not hold

for oxNi(II)GGH as this complex clearly inhibits xanthine oxidase, slowing down its activity by 40-50 % (Fig. 3.26). Furthermore, a parallel increase in the hydrogen peroxide flux associated with an increase in the amount of Ni(II)GGH added occurs simultaneously with the decrease in cytochrome c reduction. Similarly, there is an increase in the rate of catalase-inhibited cytochrome c reoxidation in HEPES buffer in the presence of increased concentration of Ni(II)GGH indicating that a greater level of hydrogen peroxide is present (data not shown). Although an increase in the level of oxygen could not be shown unequivocally, the data so far suggests that superoxide dismutation occurs.

The exact mechanism by which the nickel(II)-peptide complexes mediate the SOD-type activity is unknown, but one possibility will now be presented. CuZn-SOD catalyzes the reaction eliminating O_2^- radicals (Eqns. 4.9-4.11; Fee, 1981).

$$E\text{-}Cu^{2+} + O_2^- \longrightarrow E\text{-}Cu^{+} + O_2 \qquad (4.9)$$

$$E\text{-}Cu^{+} + O_2^- + 2\,H^+ \longrightarrow E\text{-}Cu^{2+} + H_2O_2 \qquad (4.10)$$

$$2\,H^+ + O_2^- + O_2^- \longrightarrow H_2O_2 + O_2 \qquad (4.11)$$

The decrease in O_2^- and the increase in H_2O_2 produced in the presence of the nickel(II)-peptide complexes is consistent with the following mechanism:

$$Ni(II) + O_2^- + 2\,H^+ \longrightarrow Ni(III) + H_2O_2 \qquad (4.12)$$

$$Ni(III) + O_2^- \longrightarrow Ni(II) + O_2 \qquad (4.13)$$

$$2\ H^+ + O_2^- + O_2^- \longrightarrow H_2O_2 + O_2 \qquad (4.14)$$

Hence, the nickel(II) complexes are initially oxidized by O_2^-, perhaps by initial axial coordination to the metal center, followed by electron transfer to the superoxide anion with subsequent release of H_2O_2. A second O_2^- reduces the Ni(III) intermediate, allowing for the regeneration of the original Ni(II) complex. Although reaction 4.13 has not been observed directly in the present study, the one electron reduction potentials for the nickel-histidine-containing-peptide complexes (~ + 0.96 V versus SHE) and for O_2 (~ - 0.15 V versus SHE; Macartney, 1986) suggests that the O_2^- should be able to reduce the intermediate Ni(III) complexes. Furthermore, reduction of Ni(III) by O_2^- has been proposed previously. Specifically, Macartney (1986) suggested that O_2^- mediates the reduction of Ni(III)tris(2,2'-bipyridine) complexes during the catalytic cycle involved in the decomposition of H_2O_2.

Other metal ions were tested for potential superoxide dismutation activity in the presence of GGH. Although the degree of binding to GGH in HEPES buffer (pH=7.4) by each of the individual metals tested is not known, it is clear in Table 3.3, that only nickel and copper and manganese confer this activity. It is known that for Mn^{2+}, Zn^{2+}, and Cd^{2+}, complex formation involving the deprotonated peptide linkage does not occur (Dolovich et al., 1984). This specificity suggests that a nickel centered square-planar complex is a prerequisite for superoxide dismutase activity. Both nickel and copper can form square-planar complexes under the appropriate conditions. Interestingly, copper ion's inherent SOD activity was significantly diminished upon binding to GGH.

Although Kimura et al. (1981) states clearly that Cu(II)GGH has no SOD activity, the current study observed approximately 51 % inhibition of cytochrome c reduction at 0.3 mM Cu(II)GGH; however, very different experimental conditions were used.

If the dismutation of O_2^- by the nickel(II)-histidine containing oligopeptides does proceed as described in Equations 4.12-4.14, other oligopeptide combinations that can lower substantially the redox potential of the nickel complex may well be better catalysts. Unfortunately, the redox potentials of only a limited number of oligopeptides involving few amino acids (including leucine, phenylalanine, histidine, glycine, valine and isoleucine) have been reported. In addition to lowering the redox potential, clearly, the choice of amino acids may also confer certain favourable structural properties (e.g., open axial positions and substituent effects) which can further enhance the catalytic reactivity of the nickel(II) complex.

4.3. Activation of Hydrogen Peroxide by Nickel(II)-peptide Complexes.

Many metal ions and their corresponding complexes have been shown to promote the disproportionation of hydrogen peroxide in aqueous media (Macartney, 1986). However, only few reports demonstrating a similar role for nickel have ever been presented (Wells and Fox, 1977; Siegel et al., 1979; Macartney, 1986). H_2O_2 usually is an oxidant, but can itself be oxidized by aquo-metal ions such as Ce^{4+}_{aq}, Mn^{3+}_{aq}, Ag^{3+}_{aq}, Co^{3+}_{aq} and Ti^{3+}_{aq}. The electron transfer process is believed to involve an inner-sphere mechanism in which the H_2O_2 molecule would coordinate directly with the metal forming a $MOOH^{(n-1)+}$ intermediate prior to electron transfer. By contrast, oxidation of H_2O_2 by nickel appears to

be favoured by an outer-sphere process in which a ligand must be present to support the metal in the higher oxidation state; and the electron transfer to the metal center seems to occur without direct association of the two species (McCartney, 1986).

The overall stoichiometry for the two-electron oxidation of H_2O_2 to molecular oxygen likely involves the reduction of metal-ion intermediates in the higher oxidation state (Brodovitch et al., 1980, 1982; Macartney, 1986). By contrast, certain metals can promote the disproportionation of H_2O_2 in a catalytic fashion (Eqns. 4.15-4.17; Florence, 1984).

$$M^{n+} + H_2O_2 \longrightarrow M^{(n-1)+} + O_2^- + 2\,H^+ \qquad (4.15)$$

$$2\,H^+ + M^{(n-1)+} + O_2^- \longrightarrow M^{n+} + \tfrac{1}{2}\,O_2 + H_2O \qquad (4.16)$$

$$H_2O_2 \longrightarrow \tfrac{1}{2}\,O_2 + H_2O \qquad (4.17)$$

Hence, reaction 4.15 would generate the O_2^- which in turn oxidizes the lower oxidation state complex with the generation of molecular oxygen (Eqn. 4.16). By contrast, H_2O_2 disproportionation catalyzed by catalase is very efficient and proceeds as described in the following equations (Hay, 1984).

$$Fe^{3+} + H_2O_2 \longleftrightarrow Fe^{3+}\text{-}HO_2^- + H^+ \qquad (4.18)$$

$$H^+ + Fe^{3+}\text{-}HO_2^- \longrightarrow H_2O + \underset{\text{Compound I}}{FeO^{3+}} \qquad (4.19)$$

$$FeO^{3+} + H_2O_2 \longrightarrow Fe^{3+} + O_2 + H_2O \qquad (4.20)$$

$$2\,H_2O_2 \longrightarrow 2\,H_2O + O_2 \qquad (4.21)$$

In this mechanism, H_2O_2 binds to catalase to form Compound I, which is then able to oxidize another H_2O_2 molecule. Although not shown, Compound 1 may exists as iron(IV) or even iron(V) (Eqn. 4.22; Halliwell and Gutteridge, 1984; Ullrich, 1983; Fridovich, 1986).

$$Fe(III)O \longleftrightarrow Fe(IV)O^{-} \longleftrightarrow Fe(V)O^{2-} \qquad (4.22)$$

In the present study, similar reaction(s) may be postulated to occur with many of the Ni(II)-oligopeptide complexes. Specifically, it was found that the addition of an excess of H_2O_2 to physiological solutions (0.1 M phosphate buffer, pH=7.4) containing the nickel(II)-deprotonated-peptide complex, but not to solutions containing the hydrated nickel ion or the peptide itself, resulted in the rapid disproportionation of hydrogen peroxide. The products that form include oxygen (Table 3.4, Fig. 3.20), superoxide anions (Table 3.5, Fig. 3.21), and an intermediate capable of mediating monoxygenase-type reactions (Table 3.6, Fig. 3.23). Except for Ni(III)asp-ala-his-lys, the divalent form consistently displayed enhanced activity over the corresponding tervalent form.

There is no reason to exclude complexes of nickel(II) from catalyzing the disproportionation of H_2O_2 by mechanisms similar to those

$$Ni(III) + H_2O_2 \longrightarrow Ni(II) + O_2^{-} + 2\,H^{+} \qquad (4.23)$$

$$2\,H^{+} + Ni(II) + O_2^{-} \longrightarrow Ni(III) + \tfrac{1}{2}\,O_2 + H_2O \qquad (4.24)$$

$$H_2O_2 \longrightarrow \tfrac{1}{2}\,O_2 + H_2O \qquad (4.25)$$

$$Ni(II) + H_2O_2 \longleftrightarrow [NiO]^{2+} + H_2O \quad (4.26)$$

$$[NiO]^{2+} + H_2O_2 \longrightarrow Ni(II) + O_2 + H_2O \quad (4.27)$$

$$2\ H_2O_2 \longrightarrow O_2 + 2\ H_2O \quad (4.28)$$

By contrast to the iron in catalase, the activated oxygen atom in the nickel complex would be more exposed and this may allow other reactions to occur that would otherwise be unlikely if this site were buried inside a protein.

$$[NiO]^{2+} \longleftrightarrow Ni(III)O^- \longleftrightarrow Ni(III) + {}^{\bullet}O^- \text{ (or } {}^{\bullet}OH) \quad (4.29)$$

$$[NiO]^{2+} \cdots RH \longrightarrow ROH + Ni^{2+} \quad (4.30)$$

$$[NiO]^{2+} + 2\ H_2O_2 \longrightarrow Ni^{2+} + H_2O + 2\ O_2^- + 2\ H^+ \quad (4.31)$$

$$[NiO]^{2+} \equiv Ni(III)O] \rightleftharpoons Ni(III)O^- \rightleftharpoons Ni(IV)O^{2-} \quad (4.32)$$

The postulated $[NiO]^{2+}$ species is a potentially very powerful oxidizing agent due to its electron deficient nature and because it is a potential source of hydroxyl radicals. The exact nature of this species is not known but by analogy to some iron systems, the intermediate may be represented in several ways as shown in Equation 4.32 (Ulrich, 1983). Although rare, complexes of tetravalent nickel have been observed and have been well characterized (Nag and Chakravorty, 1980; Cooper et al., 1983). In many of these complexes, the higher oxidation state is stabilized by the appropriate coordination of highly electronegative elements; however, such compounds are generally of the mixed-valence (Ni^{II} and Ni^{IV}) type (Cooper et al., 1983). In the case of the iron-centered cytochrome P_{450} enzymes, such intermediates are capable of radical abstraction at C-H

bonds and/or additions to double bonds and this is commonly used to explain the hydroxylating and epoxidating properties of these enzymes.

In the hydroxylation assay, the results indicate an almost 1:1 ratio between the quantity of p-nitrocatechol formed and superoxide anion detected. This suggests that reactions such as 4.23, 4.30 and 4.31 may be relevant. By contrast, the inability of the hydroxyl radical scavenger, mannitol, or even SOD to inhibit p-nitrocatechol formation suggests that perhaps reaction 4.29 is not important and that free $^{\bullet}OH$ are not formed. Specifically, Fe^{2+}/EDTA in the presence of H_2O_2 is a known source of $^{\bullet}OH$ radicals and its hydroxylation of p-nitrophenol is significantly inhibited (82 %) by the presence of mannitol (Florence, 1984). Hence the formation of p-nitrocatechol is likely mediated by the postulated $[NiO]^{2+}$ species. Although a detailed analysis was not carried out, $[NiO]^{2+}$ should be capable of oxidizing similar aromatic substrates like benzene, salicylic acid, phenol, benzoic acid, etc. It is also postulated to be involved in the degradation of uric acid and deoxyribose (and hence DNA; Section 4.4).

It was found that nickel(II)HSA was able to catalyze the formation of O_2^- anions in the presence of H_2O_2. This represents the first piece of evidence that HSA may support the redox activity of nickel. Unfortunately, hydroxylation of p-nitrophenol could not be demonstrated; however, this does not mean that a reactive intermediate did not form. Perhaps the activated oxygen molecule preferentially attacked the large protein molecule that is in very close proximity. Interestingly, although the addition of H_2O_2 has no effect on the UV/VIS spectra of any of the freshly prepared nickel(II) oligopeptide

complexes, its addition to oxNi(II)GGH and to Ni(II)HSA resulted in the formation of a peak centered at 378 nm suggesting that the two complexes may have structural similarities.

Equations 4.33 and 4.34 represent alternative mechanisms describing nickel(II)-oligopeptide complex catalyzed disproportionation of H_2O_2 based upon work with model iron(II) complexes in acetonitrile (Sawyer and Sugimoto, 1985).

$$Ni(II) + 2\ H_2O_2 \longleftrightarrow [Ni(II)(H_2O_2)_2] \qquad (4.33)$$

$$[Ni(II)(H_2O_2)_2] \longrightarrow Ni(II) + O_2 + 2\ H_2O \qquad (4.34)$$

$$2\ H_2O_2 \longrightarrow O_2 + 2\ H_2O$$

This mechanism has been referred to as the catalase or the dioxygenase model (Sawyer and Sugimoto, 1985). In these types of complexes, the metal center is believed to be directly involved in the electron transfer process and therefore must have redox properties (Siegel, 1979).

In both mechanisms presented, there is a potential need to have a change in the oxidation state. This is consistent with the fact that only nickel(II) complexes which support a change in the oxidation state and not the isolated Ni^{2+} itself, will catalyze the disproportionation of H_2O_2. Furthermore, transition metal ions with filled atomic orbitals (e.g., Zn^{2+} and Cd^{2+}) are redox inactive and are without significance in oxygen chemistry. By contrast, copper, iron, manganese, cobalt, molybdenum and vanadium are especially important in the biological handling of molecular oxygen (Siegel, 1979; Ullrich, 1983). Any

structural disturbance of the biologically defined ligands may result in the liberation of toxic oxygen intermediates which can damage their environment. Iron and copper are especially important in biology and their levels are rigorously controlled. Production of extremely damaging radicals have been observed with simple complexes of copper (Florence, 1984, Florence et al., 1985), iron and titanium (Halliwell and Gutteridge, 1984; Grootveld and Halliwell, 1986; Halliwelll and Gutteridge, 1986) and cobalt (Fridovich, 1986). The results of the present study using simple oligopeptide ligands, suggests that nickel can also potentiate oxygen damage.

It has been speculated that the histidine imidazole ring near the active site of catalase facilitates the deprotonation of H_2O_2 (Hay, 1984). It is interesting to speculate whether the imidazole ring in Ni(II)GGH might have a similar role since Ni(II)GGH is seven-fold more active than Ni(II)GGG or Ni(II)GGGG at pH=11 even though the latter have much lower redox potentials (Bossu and Margerum, 1977). Although facilitated-proton transfer is probably not likely in the Ni(II)GGH since the imidazole moiety is bound to the nickel. Nevertheless, this moiety may be involved in the stabilization of the oxygen radicals generated at the nickel through its considerable π-electron density.

Similar reactions as to those described above have been observed for some iron complexes. $Fe(II)(MeCN)_4(ClO_4)_2$ and $Fe(III)Cl_3$ in acetonitrile have been shown to potentiate monoxygenase, oxidase, dioxygenase, as well as catalase-type reactions in the presence of H_2O_2 and the appropriate substrate (Sawyer and Sugimoto, 1985).

4.4. Degradation of Uric Acid and 2-Deoxy-D-Ribose by Ni(II) Peptide Complexes.

Several biological enzymes such as myeloperoxidase, horse radish peroxidase, verdoperoxidase and lactoperoxidase can catalyze the degradation of uric acid in the presence of H_2O_2. In addition, various hemoproteins (e.g., hematin) are themselves able to degrade uric acid; although the reaction is much faster in the presence of H_2O_2, (Howell and Wyngaarden, (1960). Allantoin was identified as the main product using thin layer chromatography (Howell and Wyngaarden, 1960). Although it is known that the active component common to each of these proteins is a trivalent iron-porphyrin prosthetic group, the exact mechanism of uric acid degradation remains somewhat speculative (Howell and Wyngaarden, 1960; Ames et al., 1981).

Xanthine oxidase catalyzes the oxidation of hypoxanthine to uric acid (Fig. 4.1). In experiments with xanthine oxidase, it was observed that Ni(II)GGH and oxNi(II)GGH can also catalyze the degradation of uric acid; this process was inhibited by the presence of both catalase and SOD. Subsequent experiments using Ni(II)GGH clearly established that only H_2O_2 was required to initiate this reaction. Attempts to detect allantoin using thin layer chromatography revealed a product that co-migrated with pure allantoin, but the spots were generally faint against a high background. Further evidence for the formation of allantoin was obtained by initially breaking down the molecule to glyoxylate, and subsequently forming a chromophoric product.

It was observed that a 2-3 fold excess of uric acid (over Ni(II)GGH) can be completely degraded (99 %) in the presence of excess H_2O_2 suggesting that a catalytic reaction may be taking place. The

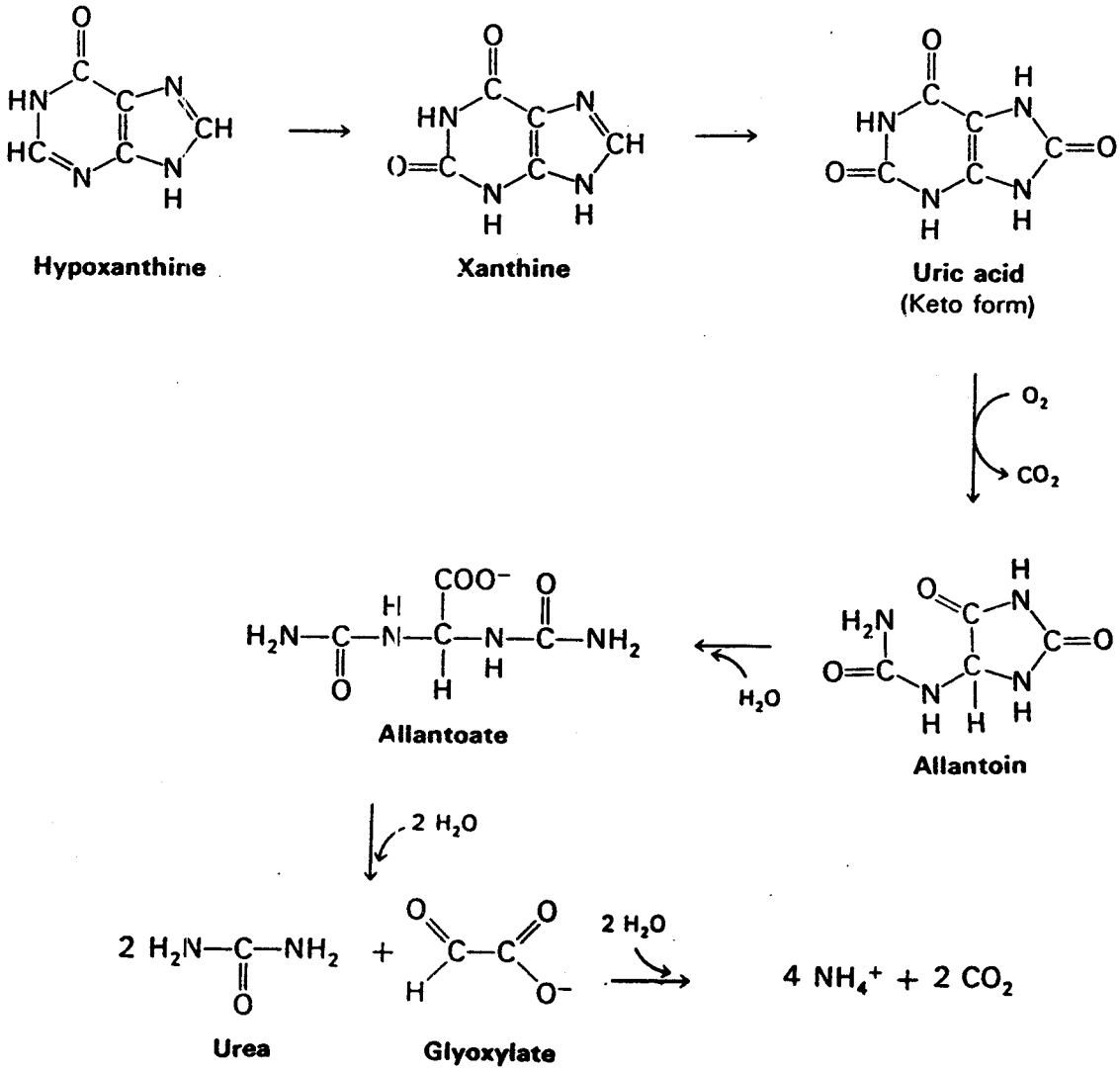

Figure 4.1: Pathway for the degradation of hypoxanthine to glyoxylate, ammonia and carbon dioxide. Adopted from Stryer (1981).

reaction results in an almost stoichiometric formation of allantoin (detected as glyoxylate). All nickel(II) oligopeptide complexes were capable of catalyzing this reaction under appropriate conditions; however, only the histidine-containing peptides catalyzed the same reaction at physiological pH. It is clear that hydroxyl radicals are not involved, since the presence of Fe^{2+}/EDTA (a known source of $^{\bullet}OH$) did not promote the degradation of uric acid; Furthermore, mannitol had no modulating effect in the above reactions. Anionic and neutral molecules like azide, imidazole, phosphate, sulphate and ammonia have been shown by ESR to stabilize nickel(III) square-planar complexes by coordinating to the axial positions (Brodovitch et al., 1982; Murray and Margerum, 1982). Hence the suppressing effect of imidazole and ammonia on the rate of uric acid degradation may involve either the stabilization of the higher oxidation state or the competitive inhibition for the H_2O_2 "binding site" on the nickel(II) square-planar complex.

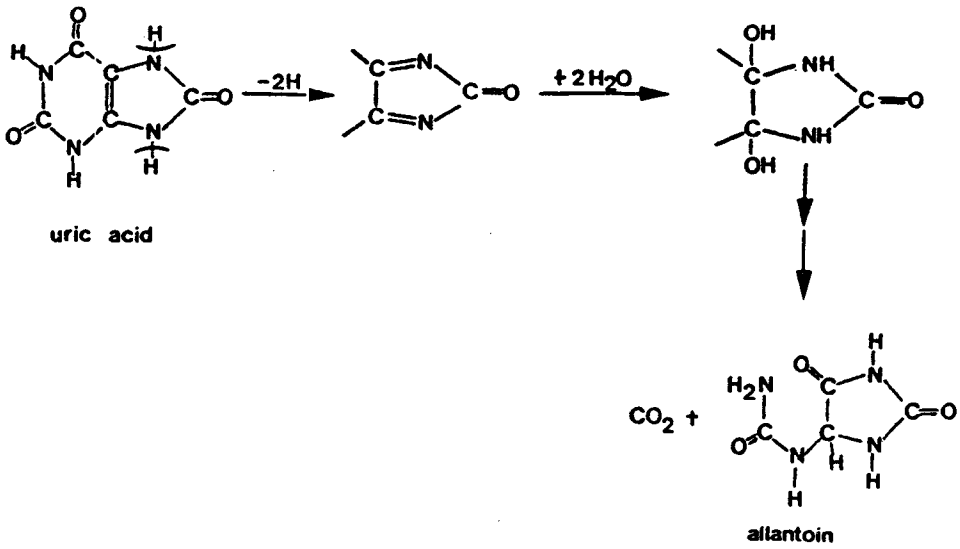

(4.34)

Two different mechanisms describing the degradation of uric acid have been proposed. Paul and Avi-Dor (1954) presented a 2-step dehydrogenation mechanism yielding a glycol intermediate before breaking down to allantoin (Eqn. 4.34).

Alternatively, Howell and Wyngaarden (1960) proposed a detailed mechanism which involves a methemoglobin-peroxide (ie., iron-peroxide) catalyzed dehydrogenation of uric acid followed by an attack of a hydroxyl radical. Whatever the details are at the molecular level, Ames et al. (1981) concludes that the ferryl moiety $[FeO]^{2+}$ is likely involved, and the reaction is not initiated by the hydroxyl radical. Similarly, it is clear that hydroxyl radicals are not directly involved for the nickel(II) peptide catalysts. The simplest mechanism that can be postulated involves the oxidizing power of $[NiO]^{2+}$; it may act by abstracting a hydrogen atom by analogy to the ferryl ion (Eqn 4.35).

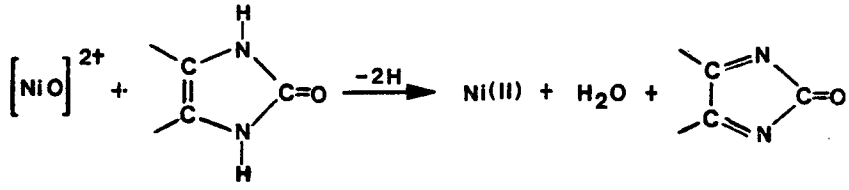

(4.35)

Subsequent reactions would be as described in Equation 4.34. The strong inhibitory effect of SOD demonstrates that superoxide anions are involved.

The simplest interpretation is that the degradation involves peroxidase-type reactions which can be represented as follows:

$$UAH_2 + H_2O_2 \xrightarrow{\text{Ni(II) complex}} UA \xrightarrow{2\ H_2O} \text{allantoin} + CO_2 \qquad (4.36)$$

Hence, the uric acid (UAH_2) gets dehydrogenated to form dehydrouric acid (UA), and upon the addition of water, the molecule rearranges and decarboxylates to form allantoin. Although many large proteins (e.g., peroxidases) can mediate the oxidation of uric acid, this is the first indication that simple peptide chelates of nickel(II), involving three amino acids can catalyze a similar reaction.

The degradation of 2-deoxy-D-ribose is far more complicated. Although the mechanism is unknown, a substance that reacts with thiobarbituric acid (TBA) is generated. Hydroxyl radicals are believed to be involved in its formation, since SOD, catalase and mannitol are known to diminish the quantity of chromophoric product formed (Halliwell and Gutteridge, 1981). Hence the addition of reagents known to stimulate the production of $^{\bullet}OH$ radicals like $FeSO_4$ and Cu(II)/1,10-phenanthroline in the presence of reducing agents results in extensive deoxyribose damage (Halliwell and Gutteridge, 1981). In the present study, only the Nickel(II)-oligopeptide complex, and not the nickel(II) ion or the peptide alone stimulated deoxyribose damage; and this effect was modified by the presence of SOD and catalase, but not mannitol or urea. Thus it is clear that hydroxyl radicals are not likely involved, but as with the degradation of uric acid, the $[NiO]^{2+}$ moiety might be involved, such as in hydrogen atom abstraction.

4.5. Chemiluminescence.

Chemiluminescence (CL) has frequently been used in oxygen-radical research to detect the formation of excited species and cellular damage. CL in these systems has often been attributed to the presence of singlet oxygen.

$$^1O_2 \quad O_2(^1\Delta g) \longrightarrow {}^3O_2 + hv \qquad (4.37)$$

$$2\ ^1O_2 \longrightarrow 2\ ^3O_2 + hv \qquad (4.38)$$

The spontaneous or monomolecular decay of singlet oxygen ($^1O_2$) to its triplet electronic ground state ($^3O_2$) results in the emmision of light detectable at 1270 nm (Eqn. 4.37); whereas in bimolecular transitions (ie., bimolecular decay) as depicted in reaction 4.38, the emissions take place at 634 and 703 nm (Cadenas and Sies, 1985). Biologically relevant sources of singlet oxygen are summarized in Equations 4.39 to 4.45 (Paine, 1978; Krinsky, 1984):

$$OCl^- + H_2O_2 \dashrightarrow {}^1O_2 + Cl^- + H_2O \qquad (4.39)$$

$$H_2O_2 + {}^-O_2 \dashrightarrow OH^- + {}^\bullet OH + {}^1O_2 \qquad (4.40)$$

$$O_2^{\cdot-} + {}^\bullet OH \dashrightarrow {}^\bullet OH + {}^1O_2 \qquad (4.41)$$

$$O_2^- \dashrightarrow e^- + {}^1O_2 \qquad (4.42)$$

$$2\ H^+ + O_2^- + O_2^- \dashrightarrow H_2O_2 + {}^1O_2 \qquad (4.43)$$

$$H^+ + RCOO^\bullet + RCOO^\bullet \dashrightarrow RC{=}O + RCOH + {}^1O_2 \qquad (4.44)$$

Although metal ions can catalyze many of these reactions, there is still much controversy assigning an associated emission of light specifically to the presence of singlet oxygen. Other reactions (which may involve metals) such as the decay of excited (triplet) carbonyl moiety ($-\overset{O^*}{C}-$) will emit photons (Cadenas and Sies, 1985).

Emission of chemiluminescence was observed during copper-2,9-dimethyl-1,10-phenanthroline catalyzed oxidation of H_2O_2 (Florence et al., 1985). This activity was attributed to the presence of $^1O_2$ based on the effects of singlet oxygen scavengers. However, CL was maximal 40

min after the initiation of the reaction. This makes interpretation difficult, since the strongest burst of CL is usually observed early in the reaction.

In the present study, CL was observed when Ni(II)GGH or Ni(II)GGHG were present in the hypoxanthine/xanthine oxidase reaction mixture or when directly added to a solution of H_2O_2. This light emission was only observed when the nickel(II) complexes were added before the initiation of the reactions. This burst was found to last as long as the supply of substrate (hypoxanthine) lasted (approximately 3.5 min), and could be lengthened by the addition of greater concentrations of hypoxanthine or by repetitive addition of this reagent. However, the counts were invariably lower in this instance, possibly due to inhibition of enzyme by high concentrations of the substrate (Fridovich, 1985a). Once the reaction had gone to completion, chemiluminescence could not be re-established by adding fresh hypoxanthine or xanthine oxidase. The only oxygen scavenger capable of quenching this Ni(II)-complex induced chemiluminescence was SOD; and since both nickel(II)-peptides are known to generate O_2^- in the presence of H_2O_2, this suggests that this radical is somehow involved. One interpretation might be that Reactions 4.13, 4.24 or 4.27 may be generating a small amount of singlet oxygen. However, the singlet oxygen trap, 2,5-dimethylfuran did not have any significant effect on CL activity. Specifically, although the presence of 10^{-4} M 2,5-dimethylfuran decreased the number of photons detected to about 1,056 CPS from 1400 (see Table 3.10), the addition of higher concentrations (up to 30 mM) did not lead to a corresponding decrease. Even though light emission could be detected, the specific involvement

of singlet oxygen remains to be proven.

4.5. Concluding Remarks.

Until recently, it was believed that nickel(II) had little biological relevance and that in aqueous solutions it is relatively inert to changes in oxidation state. However, several bacterial systems and several enzymes have been shown to exhibit absolute nickel dependence and the basis for its activity involves changes in oxidation state. Initially, macrocyclic polyamine complexes, and subsequently oligopeptide complexes of nickel(II) were used to study the redox properties of nickel(II) in solution. The presence of nickel(III) has been clearly established by electron paramagnetic resonance spectroscopy and cyclic voltammetry and the effect of equatorial and axial substituents in these largely square-planar complexes are in the early stages of investigation.

Results of the current study establishes that nickel can form strong complexes with specific oligopeptides, creating chelates with reversible redox properties under physiological conditions. The deleterious effects of acute or chronic exposure to nickel and its compounds in humans are well known. Animal and cell-culture studies have shown that nickel compounds have a number of biochemical effects and that cellular bioavailability of nickel(II) may be a predisposing factor. The exact factors governing the potency of carcinogenic nickel compounds remains to be determined. Few detailed studies on the activation of dioxygen species by nickel(II) complexes have been reported and have mostly been limited to reactions with molecular

oxygen. The results of the present study demonstrate that reactions between nickel(II)-oligopeptide complexes and the partial reduction products of molecular oxygen do occur. Such reactions are capable of generating strongly oxidizing intermediate(s) capable of mediating biologically-damaging reactions. Under physiological conditions, simple tripeptide complexes of nickel(II) were capable of catalyzing the hydroxylation of p-nitrophenol, oxidizing uric acid, damaging 2-deoxy-d-ribose and generating chemiluminescence.

It is known that uric acid has strong antioxidant properties. Because of its high concentration in human plasma (2.6-6.0 mg/dl), it has been hypothesized that it has a protective role against oxidant- and free radical damage (Ames et al., 1981; Smith and Lawing, 1983). It is possible that a local or general decrease in uric acid levels may compromise the ability to deal with oxidative insults, thus facilitating damage by, for example, activated oxygen species (e.g., lipid peroxidation and inflammation). Similar degradation of other endogenous antioxidants may be postulated. Oxidative damage of DNA mediated by the hydroxyl radical, $^{\bullet}OH$, results in the release of the ribose sugar. Clearly, any species capable of cleaving the ribose sugar has a strong potential to damage and mutate DNA. Although chemiluminescence could not be attributed to the presence of singlet oxygen, it is clear that high energy species can be generated when appropriate complexes of nickel(II) and hydrogen peroxide occur together. Their generation in vivo could potentially mediate some form of tissue damage.

In workers with occupational exposure to nickel, there are life-

long insults of nickel containing fumes and aerosols and deposition of particulates containing nickel in the respiratory tract is known to occur. After prolonged exposure, accumulation of nickel compounds within the lungs are known to reach an uncomfortable high level (Nieboer et al., 1984c). In such tissue, an equilibrium likely exists between the free hydrated nickel(II) species and nickel bound to biological ligands. Deposition of foreign matter in the lungs, such as particulates of nickel, results in cellular infiltration by phagocytes (Katsnelson and Privalova, 1984; Lynn, 1984). Phagocytotic processes induce the release of oxygen-derived radicals. Potentiation of such oxidative species by nickel(II) complexes may be hypothesized to cause local depletion of antioxidants like uric acid and glutathione. This would make that area susceptible to oxidative damage such as lipid peroxidation and inflammatory-type reactions. A significant quantity of these oxidative species (e.g., hydrogen peroxide) may enter a cell containing an abnormally high concentration of complexed nickel(II). The intracellular interaction and activation of these species may potentiate damaging effects which may include mutagenesis, or altered gene expression and cell growth. The likelihood of such toxicological events occurring in vivo is unknown, although lipid peroxidation in liver, kidneys and lungs in vivo induced by injection of nickel(II) salts in rodents has recently been demonstrated (Sunderman, 1986). It is conceivable that if exposure to nickel compounds is of long duration such as experienced by nickel-refinery workers, a number of activated species may be formed which could escape the natural protective barriers in exposed organs. It is clear that if any of these reactions

are biologically relevant, they may well constitute a crucial mechanistic component of nickel carcinogenesis. From this perspective, the findings of this thesis open up a promising new area of research.

REFERENCES

Abbracchio, M. P., Evans, R. M., Heck, J. D., Cantoni, O. and Costa, M. (1982a). The regulation of ionic nickel uptake and cytotoxicity by specific amino acids and serum components. Biol. Trace Elem. Res., 4, 289-301.

Abbracchio, M. P., Hack, J. D. and Costa, M. (1982b). The phagocytosis and transforming activity of crystalline metal sulfide particles are related to their negative surface charge. Carcinogenesis, 3, 175-180.

Ames, B. N., Cathcart, R., Schwiers, E. and Hochstein, P. (1981). Uric acid provides an antioxidant defense in humans against oxidant- and radical-caused aging and cancer: A hypothesis. Proc. Natl. Acad. Sci., 78, 6858-6862.

Anke, M., Groppel, B., Kronemann, H. and Grün, M. (1984). Nickel-An Essential Element. In: Sunderman F. W. Jr., ed., IARC Scientific Publication No. 53, Nickel in the Human Environment., Lyon France, pp. 339-365.

Auclair, C. and Voisin, E. (1985). Nitro Blue Tetrazolium Reduction. In: Greenwald, R. A., ed., CRC Handbook of Methods for Oxygen Radical Research, CRC Press, Inc, pp. 123-132.

Babior, B. M. (1978). Oxygen-dependent microbial killing by phagocytes (first of two parts). N. Engl. J. Med., 298, 659-667.

Barefield, E. K. and Mocella, M. T. (1975). Mechanism of Base promoted nickel(III) complexes of macrocyclic amines. A coordinated ligand intermediate. J. Am. Chem. Soc., 97. 15-18.

Bencini A., Fabbrizzi L. and Poggi, A. (1981). Formation of nickel(III) complexes with n-dentate amine macrocycles (n=4,5,6). ESR and electrochemical studies. Inorg. Chem., 20, 2544-2549.

Benson, J. M., Henderson, R. F. and McClellan, R. O. (1986). Comparative cytotoxicity of four nickel compounds to canine and rodent alveolar macrophages in vitro. J. Toxicol. Environ. Health., 19, 105-110.

Berry, J. P., Galle, P., Poupon, M. F., Pot-Deprun, J., Chouroulinkov, I., Judde., J. G., Dewally, D. (1984). Electron Microprobe In Vito Study of Interactions of Carcinogenic Nickel Compounds with Tumour Cells. In: Sunderman, F. W., Jr., ed., IARC Scientific Publication No. 53, Nickel in the Human Environment., Lyon, France, pp. 153-164.

Biggart, N. W. and Costa, M. (1986). Assessment of the uptake and mutagenicity of nickel chloride in salmonella tester strains. MRLett., 209-215.

Birnboim, H. C. (1982). DNA strand breakage in human leukocytes exposed to a tumor promoter, phorbol myristate acetate. Science, 215, 1247-1249.

Blakeley, R. L. and Zerner, B. (1984). Jack bean urease: The first nickel enzyme. J. Molecular Catalysis., 23, 263-292.

Bohning, D. E. (1983). Particle Deposition and Pulmonary Defense Mechanisms. In: Rom, W. N., ed., Environmental and Occupational Medicine., Little, Brown and Company, Boston, pp. 85-98.

Borchers, R. (1977). Allantoin determination. Anal. Biochem., 79, 612-613.

Bossu, F. P. and Margerum, D. W. (1976). The stabilization of trivalent Nickel in deprotonated-peptide complexes. J. Am. Chem. Soc., 98, 4003-4004.

Bossu, F. P. and Margerum, D. W. (1977). Electrode potential of nickel(III,II)-peptide complexes. Inorg. Chem., 16, 1210-1214.

Bossu, F. P., Paniago, E. B., Margerum, D. W., Kirksey, S. T. Jr. and Kurtz, J. L. (1978). Trivalent nickel catalysis of the autoxidation of nickel(II) tetraglycine. Inorg. Chem., 17, 1034-1042.

Boysen, M., Waksvik, H., Solberg, L. A., Reith, A. and Hogetveit, A. C. (1980). Histopathological Follow-Up Studies and Chromosome Analysis in Nickel Workers. In: Brown, S. S. and Sunderman, F. W. Jr., eds., Nickel Toxicology., London, Academic Press, pp.35-38.

Boyum, A. (1968). Isolation of leukocytes from human blood. Scand. J. Clin. Lab. Invest. (Suppl. 97), 9-11.

Brawn, K and Fridovich, I (1980). Superoxide radical and superoxide Dismutases: threat and defense. Acta Physiol. Scand., 492(suppl), 9-18.

Brodovitch, J. C., Haines, R. I. and McAuley, A. (1980). Nickel(III)-tris(di-imine) complexes: a series of strong one-electron oxidants. Can. J. Chem., 59, 1610-1614.

Brodovitch, J. C., McAuley, A. and Oswald, T. (1982). Kinetics and mechanism of the oxidation of hydroquinone and catechol by $[Ni^{III}cyclam]^{3+}$ in aqueous perchlorate media. Inorg. Chem., 21, 3442-3447.

Bryce, G. F., Roeske, R. W. and Gurd, F. R. N. (1966). L-histidine-containing peptides as models for the interaction of copper(II) and nickel(II) ions with sperm whale apomyoglobin. J. Biol. Chem., 241, 1072-1080.

Buttafava, A., Fabbrizzi, L., Perotti, A., Poggi, A., Poli, G. and Seghi, B. (1986). Trivalent nickel bis(triaza macrocyclic) complex.

Ligand ring size and medium effects on the nickel(III)/nickel(II) redox couple potential. Inog. Chem., 25, 1456-1461.

Cadenas, E. and Sies, H. (1985). Detecting Singlet Oxygen by Low-Level Chemiluminescence. In: Greenwald, R. A., ed. CRC Handbook of Methods for Oxygen Radical Research. CRC Press, Inc, Florida, pp. 191-195.

Cecutti, A. and Nieboer, E. (1981). Nickel Metabolism and Biochemistry., In: NRCC Document 18568, Effect of Nickel in the Canadian Environment., Ottawa, pp. 193-216.

Clark, B. R. and Evans, D. H. (1976). Infrared studies of quinone radical anions and dianions generated by flow-cell electrolysis. J. Electroanal. Chem. 69, 181-194.

Cooper, D. A., Higgins, S. J. and Levason, W. (1983). Co-ordination chemistry of higher oxidation states. Part 7. Nickel(III) and nickel(II)-nickel(IV) complexes of ethylenediamine and related ligands. A clarification. J. Chem. Soc. Dalton Trans., 2131-2133.

Costa, M. and Mollenhauer, H. H. (1980). Carcinogenic activity of particulate nickel compounds is proportional to their cellular uptake. Science, 209, 515-517.

Costa, M., Heck, D. and Robison, S. H. (1982). Selective phagocytosis of crystalline metal sulfide particles and DNA strand breaks as a mechanism for the induction of cellular transformation. Cancer Res., 42, 2757-2763.

Costa, M. and Heck, J. D. (1984). Perspectives on the Mechanism of Nickel Carcinogenesis., In: Eichhorm, G. L. and Marzill, L. G., eds., Adv. Inorg. Biochem., 6, 285-308.

Day, N. E. and Brown, C. C. (1980). Multistage model and primary prevention of cancer. JNCI., 64, 977-989.

DeChatelet, L. R., Shirley, P. S. and Johnson, R. B. Jr. (1976). Effect of phorbol myristate acetate on the oxidative metabolism of human polymorphonuclear leukocytes. Blood, 47, 545-554.

Del Maestro, R. F., (1980). An approach to free radicals in medicine and biology. Acta Physiol. Scand., 492(suppl), 153-168.

Doll, R., Morgan, L. G. and Speizer, F. E. (1970). Cancer of the lung and nose in nickel workers. Br. J. Cancer., 34, 102-105.

Doll, R. (1984). Nickel exposure: A Human Health Hazard., In: Sunderman, F. W., Jr., eds., IARC Scientific Publication No. 53, Nickel in the Human Environment., Lyon, France, pp. 3-21.

Dolovich, J., Evans, S. L. and Nieboer, E. (1984). Occupational asthma from nickel sensitivity: I Human serum albumin in the antigen

determinant. Br. J. Ind. Med., 41, 51-55.

Donskoy, E., Forouhar, F., Gillies, C. G., Marzouk, A., Reid, M. C., Zaharia, O., and Sunderman, F. W. Jr. (1986). Hepatic Toxicity of nickel chloride in rats. Ann. Clin. Lab. Sci., 16, 108-117.

Dorinsky, P. M. and Davis, W. B. (1986). Chronic bronchitis. Chest., 89, 321-323.

Drake, H. L. (1982). Occurrence of nickel in carbon monoxide dehydrogenase from Clostridium pasteurianum and Clostridium thermoaceticum. J. Bacteriol., 149, 561-566.

EPA Document. (1986). Health Assessment Document for Nickel and Nickel Compounds, EPA/600/8-83/012FF, September 1986, Final Report, U. S. Enviromental Protection Agency. Washington D. C.

Fantone, J. C. and Ward, P. A. (1985). Polymorhonuclear leukocyte-mediated cell and tissue injury. Human Path., 16(10), 973-978.

Fee, J. A. (1981). The Copper/zinc Superoxide Dismutase. In: Sigel, H., eds., Metal ions in biological systems,. Marcel Dekker, Inc, pp. 259-298.

Florence, T. M. (1984). The production of hydroxyl radical from hydrogen peroxide. J. Inorg. Biochem., 22, 221-230.

Florence, T. M., Stauber, J. L. and Mann, K. J. (1985). The reaction of copper-2,9-dimethyl-1,10-phenanthroline with hydrogen peroxide. J. Inorg. Biochem., 24, 243-254.

Forman, H. J. and Boveris, A. (1982). Superoxide Radical and Hydrogen Peroxide in Mitochondria. In: Pryor, W. A., eds., Free radical in biology, Academic Press, pp. 65-90.

Formicka-Kozlowska, G., Bezer, M. and Pettit, L. D. (1983). Coordination ability of the thyrotropin releasing factor, L-pyroglutamyl-L-histidyl-L-prolinamide (TRF).III> Cu(II) and Ni(II) complexes with TRF and its di- and tripeptide analogues. J. Inorg. Biochem., 18, 335-347.

Frank, L. and Massaro, D. (1980). Oxygen toxicity. Am. J. Med., 69, 116-126.

Fridovich, I. (1985a). Xanthine Oxidase. In: Greenwald, R. A., ed., CRC Handbook of Methods for Oxygen Radical Research., CRC Press, pp. 51-53.

Fridovich, I. (1985b). Cytochrome c. In: Greenwald, R. A., ed., CRC Handbook of Methods for Oxygen Radical Research, CRC Press, pp. 121-122 and 213-216.

Fridovich, I. (1986). Biological effects of the superoxide radical. Arch. Biochem. Biophys., 247, 1-11.

Fullerton, A., Andersen, J. R., Hoelgaard, A. and Menne, T. (1986). Permeation of nickel salts through human skin in vitro. Contact Dermatitis., 15, 173-177.

Furst, A. and Radding, S. B., (1980). An Update on Nickel Carcinogenesis., In: Nriagu, J. O., ed., Nickel in the Environment., New York, John Wiley & Sons, pp. 585-600.

Gardner, D. E. (1980). Dysfunction in Host Defence Following Nickel Inhalation. In: Brown, S. S. and Sunderman, F. W. Jr., eds., Nickel Toxicology., Toronto, Academic Press, pp. 120-124.

Glennon, J. D. and Sarkar, B. (1982). Nickel(II) transport in human blood serum. Biochem. J., 203, 15-23.

Glennon, J. D., Hughes, D. W. and Sarkar, B. (1983). Nickel(II) binding to glycylglycyl-l-tyrosine-N-methyl amide, a peptide mimicking the NH_2-terminal nickel(II)-binding site of dog serum albumin: A ^{1}H and ^{13}C-nuclear magnetic resonance investigation. J. Inorg. Biochem., 19, 281-289.

Goddard, J. G., Basford, D. and Sweeney, G. D. (1986). Lipid peroxidation stimulated by iron nitrilotriacetate in rate liver. Biochem. Pharmac., 35, 2381-2387.

Grandjean, P. Selikoff, I. P., Shen, S. K. and Sunderman, F. W. Jr. (1980). Nickel concentrations in plasma and urine and shipyard workers. Am. J. Ind. Med., 1, 181-189.

Grandjean, P. (1984). Human Exposure to Nickel. In: Sunderman, F. W., Jr. ed., IARC Scientific Publication No. 53, Nickel in the Human Environment., Lyon, France. 469-485.

Grandjean, P. (1986). Health Effects Document on Nickel. Submitted as a Special Document to the Ontario Ministry of Labour. 204 pp.

Grootveld, M. and Halliwell, B. (1986). An aromatic hydroxylation assay for hydroxyl radicals utilizing high-performance liquid chromatography (HPLC). Use to investigate the effect of EDTA on the Fenton reaction. Free Rad. Res. Comms., 1, 243-250.

Halliwell, B. and Gutteridge, J. (1981). Formation of thiobarbituric-acid-reactive substance from deoxyribose in the presence of iron salts. FEBS Letters., 128, 347-351.

Halliwell, B. and Gutteridge, J. M. C. (1984). Oxygen toxicity, oxygen radicals, transition metals and disease. Biochem. J., 219, 1-14.

Halliwell, B. and Gutteridge, J. (1986). Oxygen Free Radicals and iron in relation to biology and medicine: some problems and concepts. Arch. Biochem. Biophys. 246, 501-514.

Hansen, K. and Stern, R. M. (1983). Env. Health Perspect., 51, 223.

Hansen, K. and Stern, R. M. (1984). Toxicity and Transformation Potency of Nickel Compounds in BHK Cells in vitro. In: Sunderman, F. W. Jr. ed., IARC Scientific Publication No. 53. Nickel in the Human Environment. Lyon, France, pp. 193-200.

Harris, W. R. (1986). Estimation of the ferrous-transferrin binding constant based on thermodynamic studies of nickel(II)-transferrin. J. Inorg. Biochem., 27, 41-52.

Hay, R. W. (1984). Bio-inorganic chemistry. Toronto, Halsted Press, chapter 6.

Heikkila, R. E. (1985). Inactivation of superoxide dismutase by diethyldithiocarbamate. In: Greenwald, R. A., ed., CRC Handbook of Methods for Oxygen Radical Research., CRC Press, pp. 387-390.

Herlant-Peers, M. C., Hildebrand, H. F. and Kerckaert, J. P. (1983). In vitro and in vivo incorporation of ^{63}Ni[II] into lung and liver subcellular fractions of Balb/C mice. Carcinogenesis., 4, 387-392.

Ho, W. and Furst, A. (1973). Nickel excretion by rats following a single treatment., Proc. West. Pharmacol. Soc., 16, 245-248.

Horak, E. and Sunderman, F. W. Jr. (1973). Fecal nickel excretion by healthy adults. Clin. Chem. 19, 429-430.

Horecker, B. L. and Heppel, L. A. (1948). The reduction of cytochrome c by xanthine oxidase. J. Biol. Chem., 178, 683-690.

Howell, R. R. and Wyngaarden, J. B. (1960). On the mechanism of peroxidation of uric acid by hemoproteins. J. Biol. Chem., 235, 3544-3550.

Jacobs, S. A. and Margerum, D. W. (1984). Solution properties of Bis(dipeptide) nickelate(III) complexes and kinetics of their decomposition in acid. Inorg. Chem., 23, 1195-1201.

Kaldor, J., Peto, J., Easton, D., Doll, R., Hermon, C. and Morgan, L. (1986). Model for respiratory cancer in nickel refinery workers. JNCI., 77, 841-848.

Katsnelson, B. A. and Privalova, L. I. (1984). Recruitment of phagocytizing cells into the respiratory tract as a response to the cytotoxic action of deposited particles. Environ. Health. Perspect., 55, 313-325.

Kimura, E., Sakonaka, A. and Nakamoto, M. (1981). Superoxide dismutase activity of macrocyclic polyamine complexes. Biochim. Biophys. Acta, 678, 172-179.

Kimura, E., Sakonaka, A., and Machida, R. (1982). Novel nickel(II) complexes with doubly dioxopentaamine macrocyclic ligands for uptake and activation of molecular oxygen. J. Am. Chem. Soc. 104, 4255-4257.

Kimura, E., Yatsunami, A., Watanabe, A., Machida, R., Koike, T., Fugioka, H., Kuramoto, Y., Sumomogi, M., Kunimitsu, K. and Yamashita, A. (1983). Further studies on superoxide dismutase activities of macrocyclic polyamine complexes of copper(II). Biochim. Biophys. Acta, 745, 37-43.

Kimura, E., Machida, R. and Kodama, M. (1984). Macrocyclic dioxopentaamines: novel ligands for 1:1 Ni(II)-O_2 adduct formation. J. Am. Chem. Soc., 106, 5497-5505.

Kimura, E. and Machida, R. (1984). A mono-oxygenase model for selective aromatic hydroxylation with nickel(II)-macrocyclic polyamines. J. Chem. Soc. Chem. Commun., 499-500.

Kirchgessner, M. and Schnegg, A. (1980). Biochemical and Physiological Effects of Nickel Deficiency., In: Nriagu, J. O., ed., Nickel in the Human Environment., New York, John Wiley & Sons, pp. 635-652.

Kirvan, G. E. and Margerum, D. W. (1985). Characterization of bis(tripeptido)nickelate(III) complexes in aqueous solution. Inorg. Chem., 24(20), 3245-3253.

Klebanoff, S. J. (1980). Oxygen metabolism and the toxic properties of phagocytes. Ann. Int. Med., 93, 480-489.

Knight, J. A., Hopfer, S.M., Reid, M. C., Wong, S. H-Y. and Sunderman, F. W. Jr. (1986). Ethene (ethylene) and ethane exhalation in Ni[II]-treated rats, using and improved rebreathing apparatus. Ann. Clin. Lab. Sci., 16, 386-394.

Kreyberg, L. (1978). Lung cancer in workers in a nickel refinery. Brit. J. Ind. Med., 35, 109-116.

Krinsky, N. I. (1984). Biology and Photobiology os Singlet Oxygen. In: Bors, W., Saran, M. and Tait. D., eds., Oxygen Radicals in Chemistry and Biology., Berlin, Walter de Gruyter & Co., pp.453-464.

Kurokawa, Y., Matsushima, T., Imazawa, T., Takamura, N., Takahashi, M. and Hayashi, Y. (1985). Promoting effect of metal compounds on rat renal tumorigenesis. J. Am. Col. Toxicol., 4, 321-330.

Lappin, A. G., Murray, C. K. and Margerum, D. W. (1978). Electron paramagnetic resonance studies of nickel(III)-oligopeptide complexes. Inorg. Chem., 17, 1630-1634.

Laussac, J. P. and Sarkar, B. (1984). Characterization of the copper(II)-and nickel(II)-transport site of human serum albumin. Studies of copper(II) and nickel(II) binding to peptide 1-24 of human serum albumin by ^{13}C and ^{1}H NMR spectroscopy. J. Am. Chem. Soc., 23, 2832-2838.

Léonard, A. and Jacquet, P. (1984). Embryotoxicity and Genotoxicity of Nickel. In: Sunderman, F. W. Jr., ed., IARC Scientific Publication No. 53. Nickel in the Human Environment., Lyon, France, pp. 277-291.

Linden, J. V., Hopfer, S. M., Grossling, H. R. and Sunderman, F. W. Jr. (1985). Blood Nickel Concentrations in Patients with Stainless-Steel Hip Protheses. Ann. Clin. Lab. Sci., 15, 459-464.

Lucassen, M. and Sarkar, B. (1979). Nickel(II)-binding constituents of human blood serum. J. Toxicol. Environ. Health. 5, 897-905.

Lynn, W. S. (1984). Control of the cellular influx in lung and its role in pulmonary toxicology. Environ. Health. Perspect., 55, 307-311.

Macartney, D. H. (1986). The oxidation of hydrogen peroxide by tris(polypyridine) complexes of osmium(III), iron(III), ruthenium(III) and nickel(III) in aqueous media. Can. J. Chem., 64, 1936-1942.

Maines, M. D. (1980). Nickel Alterations of Heme Biosynthesis and Degradation: Implications for the Oxidative Metabolism of Drugs and Carcinogens. In: Nriagu, J. O., ed., Nickel in the Environment., New York, John Wiley & Sons, pp. 547-568.

Margoliash, E. and Frohwirt, N. (1959). Spectrum of horse-heart cytochrome c. Biochem. J., 71, 570-572.

Markert, M., Andrews, P. C. and Babior, B. M. (1984). Measurement of O_2^-Production by Human Neutrophils. The Preparation and Assay of NADPH Oxidase-Containing Particles From Human Neutrophils., In: Packer, L., ed., Methods in Enzymology, No. 105. Oxygen Radicals in Biological Systems, London, Academic Press, pp.358-365.

Marklund, S. L. (1985). Pyrogallol autoxidation. In: Greenwald, R. A., ed., CRC Handbook of Methods for Oxygen Radical Research, CRC Press, pp. 243-247.

Marx, J. L. (1983). Do tumor promoters affect DNA after all. Science, 219, 158-159.

Marzouk, A. and Sunderman, F. W. Jr. (1985). Biliary Excretion in rats. Toxicol. Lett. 27, 65-71.

McCord, J. M. and Fridovich, I. (1968). The reduction of cytochrome c by milk xanthine oxidase. J. Biol. Chem. 243, 5753-5760.

Monteiro, H. P., Abdalla, D. S. P., Faljoni-Alario, A. and Bechara, E. J. H. (1986). Generation of active oxygen species during coupled autoxidation of oxyhemoglobin and õ-aminolevulinic acid. Biochim Biophys. Acta., 881, 100-106.

Murray, C. K. and Margerum, D. W. (1982). Axial coordination of monodentate ligands with nickel(III) peptide complexes. Inorg Chem. 21, 3501-3506.

Mushak, P. (1980). Metabolism and Systemic Toxicity of Nickel., In: Nriagu, J. O., ed., Nickel in the Environment., New York, John Wiley & Sons, pp.491-523.

Nag, K. and Chakravorty, A. (1980). Monovalent, trivalent and tetravalent nickel. Coord. Chem. Rev. 33, 87-147.

Nieboer, E., Evans, S. L. and Dolovich, J. (1984a). Occupational asthma from nickel sensitivity: II factors influencing the interaction of Ni^{2+}, HSA. and serum antibodies with nickel related specificity. Br. J. Ind. Med., 41, 56-63.

Nieboer, E., Maxwell, R. I. and Stafford, A. R. (1984b). Chemical and Biological Reactivity of Insoluble Nickel Compounds and the Bioinorganic Chemistry of Nickel. In: Sunderman, F. W. Jr., ed., IARC Scientific Publication No. 53. Nickel in the Human Environment., Lyon, France, pp. 439-458.

Nieboer, E., Yassi, A., Jusys, A. A. and Muir, D. C. F. (1984c). The Technical Feasibility and Usefulness of Biological Monitoring in the Nickel Producing Industry., Special Document, McMaster University, Hamilton, Ontario, 286 pp.

Nieboer, E., Maxwell, R. I., Rossetto, F. E., Stafford, A. R., Stetsko, P. I. and Tom. R. T. (1987). Physicochemical, metabolic and molecular aspects of nickel carcinogenesis. In preparation.

Nielsen, G. D. and Flyvholm, M. (1984). Risk of High Nickel Intake with Diet. In: Sunderman, F. W., Jr. ed., IARC Scientific Publication No. 53, Nickel in the Human Environment., Lyon, France, pp. 333-338.

Nomoto, S., McNeely, M. D., and Sunderman, F. W. Jr. (1971). Isolation of a α_2-macroglobulin from rabbit serum. Biochem. Med., 8, 171-181.

Nomoto, S. (1980). Fractionation and Quantitative Determination of Alpha-2 Macroglobulin-Combined Nickel in Serum by Affinity Column Chromatography. In: Brown, S. S. and Sunderman, F. W. Jr., eds., Nickel Toxicology., London, Academic Press, pp.89-90.

Oskarsson, A. and Tjälve, H. (1979a). Binding of ^{63}Ni by cellular constituents in some tissues of mice after the administration of $^{63}NiCl_2$ and $^{63}Ni(CO)_4$. Acta Pharmacol. Toxicol., 45, 306-314.

Oskarsson, A. and Tjälve, H. (1979b). An autoradiographic study on the distribution of $^{63}NiCl_2$ in mice. Ann. Clin. Lab. Sci., 9, 47-59.

Oskarsson, A. and Tjälve, H. (1979c). The distribution and metabolism of nickel carbonyl in mice. Br. J. Ind. Med., 36, 326-335.

Paine, A. J. (1978). Excited states of oxygen in biology: their possible involvement in cytochrome P_{450} linked oxidations as well as in the induction of the P_{450} system by many diverse compounds. Biochem Pharmac., 27, 1805-1813.

Paniago, E. B., Weatherburn, D. C. and Margerum, D. W. (1971). The reaction of nickel(II) peptide complexes with molecular oxygen. Chem. Commun., 1427-1428.

Patierno, S. R. and Costa, M. (1985). DNA-protein cross-links induced by nickel compounds in intact cultured mammalian cells. Chem. Biol. Interactions., 55, 75-91.

Paul, K. G. and Avi-Dor, Y. (1954). The oxidation of uric acid with horse radish peroxidase. Acta Chem Scand., 8(4), 637-649.

Richmond, R., Halliwell, B., Chauhan, J. and Darbre, A. (1981). Superoxide-dependent formation of hydroxyl radicals: Detection of hydroxyl radicals by the hydroxyl of aromatic compound. Anal. Biochem., 118, 328-335.

Rieth, A., and Brogger, A. (1984). Carcinogenicity and Mutagenicity of Nickel and Nickel Compounds. In: Sunderman, F. W., Jr. ed., IARC Scientific Publication No. 53, Nickel in the Human Environment., Lyon, France, pp. 175-192.

Rivadel, E. and Sanner, T. (1980). Metal salts as promoters of in vitro morphological transformation of hamster embryo cells initiated by benzo(a)pyrene. Cancer Lett., 8, 203-208.

Roberts, R. S., Julian, J. A., Muir, D. C. F. and Shannon, H. S. (1984). Cancer Mortality Associated with the High-Temperature Oxidation of Nickel Subsulfide. In: Sunderman, F. W. Jr., ed. IARC Scientific Publication No. 53. Nickel in the Human Environment., Lyon, France, pp. 23-35.

Sawyer, D. T. and Sugimoto, H. (1985). Activation of Hydrogen Peroxide by $Fe(II)(MeCN)_4(ClO_4)_2$ and $Fe(III)Cl_3$ in Acetonitrile: Model Systems for the Active Sites of Peroxidases, Catalase, and Monoxygenase. In: Xavier, A. V., eds., Proceedings of the Second International Conference on Bioinorganic Chemistry., V. C. H. Publishers., 236-245.

Seefelt, L. C. and Arp, D. J. (1986). Purification to homogeneity of Azotobacter vinelandii hydrogenase: a nickel and iron containing αß dimer. Biochimie., 68, 25-34.

Sellers, R. M. (1980). Spectrometric determination of hydrogen peroxide using potassium titanium(VI) Oxalate. Analyst, 105, 950-954.

Sen, P. and Costa, M. (1986). Pathway of nickel uptake influences its interaction with heterochromatic DNA. Toxicol. Appl. Pharmocol., 84, 278-285.

Shelnutt, J. A., Alston, K., Ho, J. Y., Yu, N. T., Yamamoto, T. and Rifkind, J. M. (1986). Four- and five-coordinate species in nickel-reconstitutes hemoglobin and myoglobin: Raman identification of the nickel-histidine stretching mode. Biochem., 25, 620-627.

Shelnutt, J. A. (1987). Axial Ligation in nickel porphyrins and nickel corphins related to coenzyme-F430 of methyl reductase. Biophys. J., 51, A405.

Siegel, H., Wyss, K., Fischer, B. E. and Prijs, B. (1979). Metal ions and hydrogen peroxide. Catalase-like activity of Cu^{2+} in aqueous solution and its promotion by the coordination of 2,2-bipyridyl. Inorg. Chem., 18, 1354-1357.

Smith, R. C. and Lawing, L. (1983). Antioxidant activity of uric acid and 3-N-ribosyluric acid with unsaturated fatty acids and erythrocyte membranes. Arch. Biochem Biophy., 223, 166-172.

Spears, J. W., Harvey, R. W. and Samsell, L. J. (1986). Effects of dietary nickel and protein on growth, nitrogen metabolism and tissue concentrations of nickel, iron, zinc, manganese and copper in calves. J. Nutr., 116, 1873-1882.

Stryer, L. (1981). Biochemistry, W. H. Freeman and Company, San Francisco.

Subak, E. J. Jr., Loyola, V. M. and Margerum, D. W. (1985). Substitution and rearrangement reaction of nickel(III) peptide complexes in acid. Inorg. Chem., 24, 4350-4356.

Sugimoto, H. and Sawyer, D. T. (1984). Iron(III)-induced activation of hydrogen peroxide to ferryl ion (FeO^{2+}) and singlet oxygen ($^1O_2$) in acetonitrile: Monooxygenations, dehydrogenations, and dioxygenations of organic substrates. J. Am. Chem. Soc., 106, 4283-4285.

Sugiura, Y. and Mino, Y. (1979). Nickel(III) complexes of histidine-containing tripeptides and bleomycin. Electron spin resonance characteristics and effect of axial nitrogen donors. Inorg. Chem., 18, 1336-1339.

Sunderman, F. W. (1977). A review of the metabolism and toxicology of nickel. Ann. Clin. Lab. Sci., 7, 377-398.

Sunderman, F. W. Jr., (1981). Recent research on nickel carcinogenesis. Environ. Health Perspect., 40, 131-141.

Sunderman, F. W., Jr., Costa, E. R., Fraser, C., Hui, G., Levine, J. J., and Tse, T. P. H. (1981). ^{63}Nickel-Constituents in renal cytosol of rats after injection of ^{63}nickel chloride. Ann. Clin. Lab. Sci., 11, 488-496.

Sunderman, F. W. Jr., (1983). Potential toxicity from nickel contamination of intravenous fluids. Ann. Clin. Lab. Sci., 13, 1-4.

Sunderman. F. W. (1984a). Recent advances in metal carcinogenesis. Ann. Clin. Lab. Sci., 14, 93-122.

Sunderman, F. W., Jr. (1984b). Carcinogenicity of nickel compounds in animals. In: Sunderman, F. W., Jr., ed., IARC Scientific Publication No. 53, Nickel in the Human Environment., Lyon, France, pp.127-142.

Sunderman, F. W. Jr., Crisostomo, M. C., Reid, M. C., Hopfer, S. M. and Nomoto, S. (1984b). Rapid analysis of nickel in serum and whole blood by electrothermal atomic absorption spectrometry. Ann. Clin. Lab. Sci., 14, 232-241.

Sunderman, F. W. Jr., Marzouk, A., Zaharia, O. and Reid, M. C. (1985). Increased lipid peroxidation in tissues of nickel chloride-treated rats. Ann. Clin. Lab. Sci., 15, 229-236.

Sunderman, F. W. Jr., Hopfer, S. M., Crisostomo, M. C. and Stoeppler, M. (1986). Rapid analysis of nickel in urine by electrothermal atomic absorption spectrometry. Ann. Clin. Lab. Sci., 16, 219-230.

Sunderman, F. W. Jr. (1986). Metals and Lipid Peroxidation. Acta Pharmacol. Toxicol., 59, 248-255.

Templeton, D. M. and Sarkar, B. (1985). Peptide and carbohydrate complexes of nickel in human kidney. Biochem. J., 230, 35-42.

Thomson, A. J. (1982). Proteins containing nickel. Nature, 298, 602-603.

Troll, W. and Wiesner, R. (1985). The role of oxygen radicals as a possible mechanism of tumor promotion. Ann. Rev. Pharmacol. Toxicol., 25, 509-528.

Ullrich, V. (1983). The Role of Metal Ions in the Chemistry and Biology of Oxygen., In: Bors, W., Saran, M. and Tait, D., eds., Oxygen Radicals in Chemistry and Biology. pp. 391-404.

Uziel, M., Owen, B. and Butler, A. (1986). Toxic response of hamster embryo cells exposure to mixtures of Ni^{2+} and benzo(a)pyrene. J. Appl. Toxicol., 6, 167-170.

Vercellotti, G. M., Sweder van Asbeck, B. and Jacob, H. S. (1985). Oxygen radical-induced erythrocyte hemolysis by neutrophils J. Clin. Invest., 76, 956-962.

Waksvik, H., Boysen, M. and Hogetveit, A. C. (1984). Increased incidence of chromosomal abberations in peripheral lymphocytes of retired nickel workers. Carcinogenesis, 5, 1525-1527.

Weiss, S. J. and LoBuglio, A. F. (1980). An oxygen-dependent mechanism of neutrophil-mediated cytotoxicity. Blood, 55, 1020-1024.

Weitberg, A. B., Weitzman, S. A., Destrempes, M., Latt, S. A. and Stossel, T. P. (1983). Stimulated human phagocytes produce cytogenetic changes in cultured mammalian cells. N. Engl. J. Med., 308, 26-30.

Wells, C. F. and Fox, D. (1977). Kinetics of the oxidation of hydrogen peroxide by tris(2,2'-bipyridine)-nickel(III) ions in aqueous perchlorate media: Comparison with oxidation by aqua-cations. J. C. S. Dalton, 1498-1501.

Willard, H. H., Merritt, L. L. Jr. and Dean, J. A. (1974). Instrumental Methods of Analysis., New York, Litton Educational Publishing, Inc.

Witschi, H. P. and Hakkinen, P. J. (1984). The role of toxicological interactions in lung injury. Environ. Health Perspect., 55, 139-148.

Zeigerson, E., Ginzburg, G., Schwartz, N., Luz, Z. and Meyerstein, D. (1979). Electrochemical preparation of stable nickel(III) complexes with tetradentate macrocyclic ligands in aqueous solutions. J. Chem. Soc., 6, 241-243.